NEW BONDED PHASE MATERIALS FOR SEPARATiONS

by

SIRANTHA PERERA

Presented to the Faculty of the Graduate School of

The University of Texas at Arlington in Partial Fulfillment

of the Requirements

for the Degree of

DOCTOR OF PHILOSOPHY

THE UNIVERSITY OF TEXAS AT ARLINGTON

DECEMBER 2012

This dissertation is dedicated to my beloved wife, Sriyani Liyanage and my loving daughter,

Anudi Perera.

ACKNOWLEDGEMENTS

I would like to offer my profound gratitude to my research supervisor, Professor Daniel W. Armstrong for his support and guidance throughout my research career here at UTA. If not for his continuous guidance, suggestions and patience I would not have been able to complete this Ph.D. He is a great mentor and one of the best teachers I have had the opportunity to learn from. I consider myself to be fortunate to be able to pursue my Ph. D under his supervision.

I make this an opportunity to thank my committee members, Professor Frederick MacDonnell and Professor Richard Guan for their valuable suggestions and comments. I am especially thankful to Professor. MacDonnell for letting me synthesize ruthenium complexes in his lab and valuable advice in numerous ways. Also, I am thankful to Professor Saiful Chowdhury for being in my final defense committee. I appreciate their precious time spent on my behalf.

I am grateful to my former and current lab mates: Junmin, Jeff, Boe Ye, Renee, Molly, Xinxin,Ping, Chunlie, Koko, Violet, Ben, Pritesh, Xiaotong, Eranda, Dilani, Aruna, Qing, Sophie, Zack, Yun-Cheol, Yasith, Tharanga, Nilusha, Milan, Edra, Eva, Jonathan, Ross, Jason, Choyce, Lili, Tran, Sara, and Victor for helping me one way or the other.

It is my pleasure to acknowledge the faculty and staff of the department of Chemistry and Biochemistry for helping me in numerous ways. I thank Mrs. Barbara Smith for being very helpful in placing orders and being friendly, always with a warm smile. I also remember with great pleasure, Dr. Brian Edwards for helping me with reviving otherwise malfunctioning instrumentation and running the MALDI at all times

without any hesitation. I wish to thank Debbie, Jill, Jim, Nancy and Helen for helping me in one way or the other.

I am grateful to Professor. Dias and Professor. Rajapakshe for giving me the opportunity to pursue my Ph.D. here at UTA. Also I take this opportunity to thank Professor. Namal Priyantha and Professor Ayanthi at University of Peradeniya, whose words changed my entire life. I also make this opportunity to thank the free education system of Sri Lanka which enables me to come thus far in education.

I humbly thank my loving parents for their love, support and encouragement. I thank my brother and sister for their love and always being there for me. I wish to thank my wife's family for their love, support and encouragement.

At last but not least, I am grateful to my beloved wife Sriyani who stood by me, encouraged and backed me up whenever I needed help in my life. It was your dream to see me graduate with a Ph.D. You made me do it. It was not easy, but together we did it. Also, I thank my loving daughter, Anudi for her patience and always being there for me with smile. Your love gave me a sense of relief at times when I was busy with work and writing.

<div align="right">November 12, 2012</div>

<div align="center">v</div>

ABSTRACT

NEW BONDED PHASE MATERIALS FOR SEPARATIONS

SIRANTHA PERERA, PhD

The University of Texas at Arlington, 2012

Supervising Professor: Daniel W. Armstrong

Separations play an important role in day to day life as well as in science and technology. This dissertation focuses on novel and versatile techniques involving synthesizing new bonded chiral stationary phases (CSPs) and using existing CSPs for the separation of target chiral analytes in HPLC. It also includes development of new ionic liquid (IL) based silica bonded polymeric coatings for solid phase microextraction gas chromatography (SPME-GC) in headspace and direct immersion for polar analytes and finally, coupling new MALDI matrix bonded SPME fibers and laser desorption for rapid identification of biological materials.

Enantiomerically pure Ru complexes were introduced as novel bonded chiral stationary phases. Among the three binding chemistries to the silica gel studied, reductive animation of aldehyde-functionlized silica worked best. The Ru complex-bonded CSP provided enantioselectivity in the polar organic mode toward compounds with acidic groups and binaphthyl type compounds in the normal phase mode. Next the two best aromatic-functionalized cyclofructan-based CSPs, R-napthylethyl-carbamatecyclofructan (RN-CF6) and dimethylphenyl-carbamate cyclofructan 7 (DMP-

CF7) were synthesized and evaluated with different classes of chiral analytes. These two CSPs showed enantioselectivity toward a broad range of compounds such as chiral acids, amines, metal complexes and neutral compounds.

In another study, twelve types of commercial CSPs (cyclodextrin types and cyclofructan types) were evaluated by separating newly synthesized seventeen racemic tetrahydrobenzimidazole analytes. Among the twelve different CSPs, enantiomeric recognition was most frequently observed with Cyclobond RN and LARIHC CF6-P while the Cyclobond DMP yielded the greatest number of baseline separations in HPLC.

Four new ionic liquids (ILs) were prepared and bonded onto 5 μm silica particles for use as adsorbents in SPME. The two polymeric IL fibers were effective in headspace SPME for short chain alcohols. Immersion SPME can be used with the polymeric IL fibers for short chain alcohols and for polar and basic amines. Their efficacy compares favorably to that of commercial fibers for polar analytes in both modes. The mechanical strength and durability of the polymeric fibers were excellent.

Finally, 3-hydroxy-2-naphthoic acid (HNA) and 2-hydroxy-1-(2-hydroxy-4-sulfo-1-naphthylazo)-3-naphtoic acid (HHSNNA) were tested as MALDI matrices for peptides and proteins and compared to two classical matrices: α-cyano-4-hydroxycinnamic acid (CHCA) and 2,5-dihydrobenzoic acid (DHB). HNA was found to be a good MALDI matrix comparing well with DHB and CHCA. The proton-donor compounds were covalently bound to silica particles of different pore diameters. Only the wide pore silica material gave observable MALDI spectra. The wide pore bonded silica materials were then attached in a thin layer onto wires to be used as fiber tips in SPME peptide extractions. The peptide adsorbed to the SPME fibers were introduced into the mass spectrometer for fiber laser desorption ionization (FILDI) spectrum recording.

TABLE OF CONTENTS

LIST OF ILLUSTRATIONS

xi

LIST OF TABLES

CHAPTER 1

GENERAL OVERVIEW

1.1 Introduction to separations

Separation science is an extremely broad and diverse field that has profound impact on many areas of science and technology.[1-4] In its simplest manifestation, a separation is defined as the process in which a mixture is separated into at least two components having different compositions. The separation process definition can not only have a chemical connotation but also a physical one. Taking a small metal ball from a beaker of water using a scoop is simple case of a separation. The same separation can be accomplished by remove the metal ball by filtering the liquid through using some piece of cloth or filter paper. This simple separation method does not remove any microscopic contamination from the water. To remove microscopic contamination one needs to use special filters or other methods.

In real life most separations are not simple and straightforward because particles may be invisible to the naked eye and the materials may be more complicated and need advance techniques to achieve separation. The distillation of alcohol in the beverage industry is a simple separation process. The artificial kidney is a prominent example of a separation of biomedical importance. Also the isotope separation of ^{235}U from ^{238}U is important in nuclear energy. Chemical separations are broadly employed in chemical and process industries as these examples show, to remove contaminations from raw materials, refining products, protecting the environment, etc.[5] The most commonly used

chemical separation methods include extraction, distillation, crystallization, chromatography, ion exchange, membranes, filtrations, etc.

The focus of this thesis is on synthesizing new bonded phase materials for separation of: (a) non-chiral polar analytes, (b) peptides and proteins by solid phase microextraction coupled with gas chromatography and MALDI, and (c) chiral analytes using chiral high performance liquid chromatography.

1.2 Enatiomeric separations in HPLC
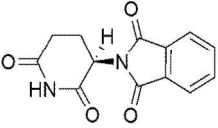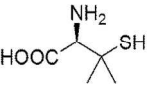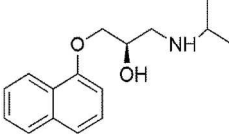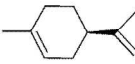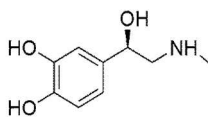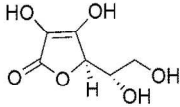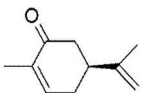
Traditionally, the separation of enantiomers has been one of the more problematic areas separation science. Enantiomers have same physical and chemical properties in an isotropic environment apart from the rotation of the plane of polarized light. A mixture having equal amounts of enantiomers is known s a racemic mixture. In 1848, Pasteur reported the first separation of enantiomers from a racemic mixture.[6] Enantiomeric separations have become essential not only research but also in many industries, such as the pharmaceutical, food, agrochemical and petrochemical industries.

Living entities consist of D-sugars and L-amino acids. Two enantiomers can have different pharmacological effects in biological systems, and therefore enantiomeric separations are important for the drug development industry. Some examples of enantiomers which show different pharmacological effects are in Table 1.1.[7-11] Guidelines for the development of new stereoisomeric drugs were released by the Food and Drug Administration (FDA) in 1992.[12] The new guidelines require pharmaceutical companies to analyze the racemates and all the enantiomers of stereoisomeric drugs.

There are numerous techniques for the separation of enantiomers. However, enantiomeric separations done by chromatographic methods have become very popular.

2

The ease of operation and scalability of high efficiency chromatographic methods have made them more attractive. The development of novel, highly selective stationary phases has been one of the more challenging areas of research in chromatographic separation science.

Table 1.1 The effect of chirality of some of the enantiomers

Compound	Structure	Isomer	Effect
Thalidomide		(R) -	Anti-nausea
		(S) -	Teratogenic
Penicilamine		(R) -	Highly toxic
		(S) -	Anti-arthritic
Propranolol		(R) -	Active contraceptive
		(S) -	?-Adrenergic blocker
Limonene		(R) -	Odor of orange
		(S) -	Odor of lemon
Epinephrine		(R) -	10 times less effective than (S)-enantiomer
		(S) -	Active vasoconstrictor
Ascorbic acid		L-Threoascorbic acid	Vitamin C, antiscorbutic
		D-Threoascorbic acid	No antiscobutic properties
Carvone		(R) -	Odor of spearmint
		(S) -	Odor of caraway

1.3 Bonded phase material for chiral liquid chromatography

In the middle of Twentieth Century, analytical separations mostly depended on crystallization, precipitation, extraction, and distillation techniques. Since then chromoatography has become the dominant analytical method in both research and industry.[13,14] In early 1900s Russian botanist Michael S. Tswett reported the separation of plant pigments by column liquid chromatography.[15] The first enantiomeric separation was Louis Paster's work on crystallization and hand-picking the mirror-image, individual tiny crystals of ammonium sodium tartrate.[16] Until the early 1980s, enantiomeric separations were still considered to be very challenging processes.[17] Since then numerous techniques, such as gas chromatography (GC), liquid chromatography (LC), supercritical fluid chromatography (SFC), and capillary electrophoresis (CE) have been developed and used to separate enantiomers and as a result, this area of separations has become quite popular. Among these techniques, HPLC with chiral stationary phases (CSPs) has dominated due to its broad selectivity, good reproducibility and capability of both analytical and preparative scale separations. Generally the desired CSPs are obtained either by chemically bonding or physically coating a chiral selector onto a solid support.

Advantages of the immobilized chiral stationary phases are that less chiral selector is needed for preparative separations and immobilized chiral selectors do not interfere with the detection method. Chiral selectors can be categorized as π-π association types, polymeric types, macrocyclic types, and ligand exchange types.[18] At least three points of interaction between a chiral selector and an enantiomer are needed to achieve enantiorecognition.[19,20] The selection of the desired chiral selector or chiral stationary phase is dependant on the structure of the chiral analyte that is to be separated. Even though large numbers of CSPs have been commercialized, researchers

are still making efforts to develop new, more effective and universal chiral stationary phases. Polysaccharide stationary phases, macrocyclic glycopeptide stationary phases, and to a smaller extent, cyclodextrin and π-complex stationary phases are currently the most dominant in chiral liquid chromatography.

1.3.1 π-complex CSPs

The π-complex CSPs were first introduced by Mikes and co-workers in 1970's.[21,22] Subsequently Pirkle et al synthesized various analogous CSPs and some of them have been commercialized.[23-26] These CSPs have been synthesized by chemically binding either a chiral π-acidic or π-basic moiety to the solid support, usually silica gel. Some π-complex CSPs contain both chiral π-acidic or π-basic moieties which extend their separation window to both chiral π-basic and π-acidic analytes. Usually, π-π acceptor-donor interactions are important for enantiomeric separations on the π-complex stationary phases. The CSPs, which have π-basic groups are frequently used to separate the π-acidic analytes and vice versa. In addition, hydrogen bonding, steric and dipole-dipole interactions also play important role in chiral recognition on this CSPs. Usually, the π-complex CSPs are used in the normal phase mode, because π-π, dipolar and hydrogen bonding interaction are more prominent in nonpolar solvents such as heptane and hexane.

1.3.2 Polymeric CSPs

Polymeric chiral stationary phases are the most popular and widely used HPLC CSPs in industry. Polymeric CSPs can be further categorized into two sub classes based on natural chiral polymers such as proteins and polysaccharides and synthetic chiral polymers.

1.3.2.1 CSPs based on natural polymers

1.3.2.1.1 Protein based CSPs

Proteins are natural chiral polymers consisting of L-amino acids. Due to the broad enantioselectivity of this class of CSP, protein based CSPs were popular chiral selectors for HPLC in the 1980's.[27-29] The reversed phase mode is used exclusively for protein based CSPs. Usually protein based CSPs are not used in preparative scale separations due to the low molar loading of the high molecular weight chiral proteins (40,000-70,000 Daltons) on the support. Also only a small part of the protein is responsible for the enantiomeric separation. Therefore these CSPs are easily overloaded and have limited capacity. The protein-based CSPs are the most labile of all CSPs. Temperature, pH, and the mobile phase composition can deteriorate the enatioselectivity of the CSPs by causing irreversible changes in the structures of the proteins.

1.3.2.1.2 Polysaccharide based CSPs

Cellulose and amylose are the most abundant naturally occurring chiral polysaccharides redundant. Both are linear polymers consisting of D-glucose, but with different linkages between the glucose units. The glucose units are linked by β-1,4-glycosidic linkages in cellulose and in amylose, through α-1,4- glycosidic linkages. Native cellulose and amylose are themselves not effective chiral selectors.[18] These CSPs showed enhanced enantiomeric separations for wide groups of analytes after derivatizing their hydroxyl groups.[30, 31]

Okamoto et al. further advanced the polysaccharide based CSPs by coating ester or carbamate derivatives of polysaccharides onto 3-aminopropyl silanized silica gel. These CSPs had good efficiencies, high mechanical strength, and broad enantioselectivity.[32,33] Among the different derivatizes of cellulose and amylose CSPs, the

3,5-dimethylphenylcarbamate derivatives (Chiralcel OD and Chiralpak AD) are the most broadly applicable.

Generally cellulose and amylose based CSPs are used in the normal phase mode. A few polysaccharide based CSPs can be used in the reverse phase mode. However, selecting the mobile phases and sample solvents need to be considered before screening chiral analytes using these CSPs. The CSPs used in the reverse mode cannot be used in the normal phase mode.[34] Usually CSPs used in normal phase mode cannot be used in the reversed phase mode due to irreversible changes in the three dimensional structure of the chiral selectors.[34] Recently immobilization of the chiral selectors on the support, drastically improved the durability and robustness of the polysaccharide based CSPs .Recently, the immobilized form of AD (IA) and OD (IB) columns were commercialized and the immobilized CSPs have enhanced the solvent compatibility compared to the coated type CSPs.[35,36]

1.3.2.2 CSPs based on synthetic polymers

Synthetic polymers CSPs have several interesting features compared to other CSPs. Not only polymerizing different types of chiral monomers via different methods can obtain various types chiral polymers but also CSPs with the opposite configurations also can be synthesized. These synthetic polymeric CSPs have higher sample loading capacities compared to other CSPs and the covalent bonding of chiral selectors on to the silica support show higher robustness for these CSPs.[37,38]

The synthetic polymer CSPs can be categorized into two classes. They are CSPs synthesized from reacting with achiral monomers in the presence of chiral catalysts[39] or reacting with enantiomeric monomers. In the first method the stereochemistry of the chiral catalyst gives the chirality of the entire polymer, either left-hand or right-hand helical coils. In the second method two opposite configuration of the

synthetic polymeric CSPs can be synthesized and therefore elution order of the analyte can be easily reversed. Generally these type CSPs are widely used in preparative scale due to the higher loading capacity on the solid supports. Nevertheless to achieve good selectivity and efficiency, the degree of polymerization and chiral selector density must be carefully controlled to obtain a thin and uniform layer on the porous support without changing the morphology.[38]

1.3.3 Macrocyclic CSPs

Macrocyclic CSPs consist of three types of chiral selectors. They are chiral crown ethers, cyclodextrin derivatives, and macrocyclic glycopeptides. Among the macrocyclic chiral selectors, cyclodextrins are dominated in enantiomeric separations in GC and in CE.[17,40] Cyclodextrin-based CSPs are also one of the significant HPLC chiral stationary phases, mostly in the reverse phase and polar organic modes.[17,40]

1.3.3.1 Chiral crown ether based CSPs

Cram and co-workers synthesized the chiral crown ether based CSPs for HPLC.[41-43] The cavity of 18-crown-6 ether skeleton is an ideal size for complexation of potassium and ammonium ions. The inclusion complexation of ammonium ions with the 18-crown-6 ether skeleton is the main reason for the retention and chiral separation of analytes on this CSP. For this reason, crown ether based CSPs separate racemic analytes containing primary amine functional groups. Acidic mobile phase additives such as perchloric acid are required for complete protonation of the primary amine chiral analytes.[44,45]

1.3.3.2 Cyclodextrins based CSPs

Cyclodextrins (CDs) are cyclic oligomers of α-(1,4)-linked glucose and the most common cyclodextrins have 6, 7 or 8 (α, β, γ-CD) glucose units. The first bonded β-cyclodextrin CSP was developed by Armstrong and coworkers in 1983-84.[46,47]

Subsequently, other cyclodextrins, containing native α-cyclodextrin, γ-cyclodextrin, and different derivatives of β-cyclodextrin, have been synthesized as chiral stationary phases in HPLC.[48,49] The cyclodextrin is a "cup" shape macrocyclic molecule. The cavity size of CDs increase with the number of glucose units. The internal cavity diameters of α, β, γ-CDs are 0.57 nm, 0.78 nm, and 0.95 nm, respectively.[46,47] Secondary hydroxyl groups are at the 2- and 3- carbon positions located on one rim of the cyclodextrin molecule. The primary 6-hydroxyl groups are located on the opposite side. The inside cavity of CDs molecules are hydrophobic in nature owing to the hydrophobic methylene hydrogens.

Cyclodextrins can be chemically bonded to the silica gel via isocyanate, diisocyanate or ether linkage reagents. Most commercially available cyclodextrin CSPs have developed using an ether linkage which is free of nitrogen atoms.[46,47] The cyclodextrin stationary phases are known to be multimodal chiral stationary phases and the separation mechanisms diverge in different modes.[46,47-50] The inclusion complexation between the hydrophobic portion of analytes and the hydrophobic CD cavity is the main interaction which effects enantio-recognition. Other secondary interactions such as hydrogen bonding and steric interactions also play an important role in chiral recognition. In the polar organic mode, the CD cavity is mainly occupied by the mobile phase such as acetonitrile and faster adsorption/desorption kinetics that occur at the surface of the cyclodextrin. Aromatic derivative groups such as dimethylphenyl, R,S-naphthylethyl play an key role in the normal phase mode due to π-π interactions.

1.3.3.3 Macrocyclic glycopeptides based CSPs

Macrocyclic glycopeptides stationary phases were developed by Armstrong in 1994 as chiral selectors for HPLC.[51-58] Vancomycin (Chirobiotic V and V2), teicoplanin (Chirobiotic T and T2), teicoplanin aglycone (Chirobiotic TAG), and ristocetin A

(Chirobiotic R) are six commercially available glycopeptide based CSPs. The teicoplanin aglycone chiral selector is synthesized by removing the sugar moieties from teicoplanin and the rest of other selectors are formed by fermentation. All the glycopeptides have fairly similar structures and have a typical aglycon "basket", which contains three or four fused macrocyclic rings. Among the four glycopeptides, vancomycin has the most open basket, whereas teicoplanin and teicoplanin aglycon have the most closed baskets.[59] All the glycopeptides chiral selectors have ample functional groups, such as amino groups, hydroxyl groups, carboxylic acid groups, aromatic moieties, and amide linkages. The ionizable groups, amine, and carboxylic acid on the chiral selectors play a major role in the separation of enantiomers that also are ionizable. Amino acids have been resolved most effectively on the glycopeptides CSPs, particularly on teicoplanin. One distinctive feature of the glycopeptide–based CSPs are their complementary selectivity and these CSPs can be used in all three operational modes.

1.3.3.4 Cyclofructan CSPs

Cyclofructans (CFs) are one of the comparatively small groups of macrocyclic cyclic oligosaccharides.[60,61] Cyclofructans consist of six or more β-(2-1) linked D-fructofuranose units. (see Figure 1.1) In 1989, cyclofructans were first reported by Kuwamura and Uchiyama.[61] They were produced by fermentation of inulin by *Bacillus circulans.* Cyclofructans with degree of polymerization six, seven and eight have been isolated and the abbreviation for these compounds are CF6, CF7 and CF8 to indicate the number of D-fructofuranose units present in the macrocyclic ring. The cyclodextrins (CDs) are the one of best known members of the macrocyclic molecule in HPLC; however cyclofructans (CFs) are considerably different in both their structure and performance. CFs have been mostly used as food additivies,[62-64] ink formulation agents,[65] lubricants [30] etc.

10
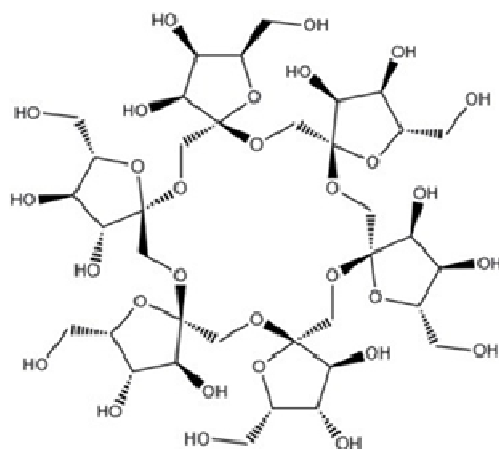
Figure 1.1 Molecular structure of native cyclofructan 6 (CF6)

Native cyclofructan 6 showed only limited enantioselectivity to a few types of compounds in HPLC, however derivatized cyclofructans seem to be outstanding chiral selectors which can separate enantiomers of various types of molecules. Aliphatic derivatized cyclofructans are effective in the polar organic mode and afford remarkable enantiorecognition for chiral primary amines.[66] Aryl derivatized cyclofructans are less effective for amine compounds, however they have a broad enantiorecognition for chiral acids, secondary, tertiary amines, alcohols, and metal complexes.[66,67] Derivatization groups can offer extra interaction sites and by adding aromatic groups to CF6, can increase π-π interactions which are important for many effective chiral selectors.

The development and screening of new chiral stationary phases (CSPs) will be discussed in Chapter 2 and Chapter 3. The enantiomeric separation of newly synthesized tetrahydrobenzimidazole intermediates by HPLC and CE will be discussed in Chapter 4.

1.4 Bonded phase material for SPME

1.4.1 Introduction to SPME

Solid phase microextraction (SPME) is a simple method in which sample extraction and sample introduction are combined into a one step technique. It was introduced by Pawliszyn and coworkers more than 15 years ago.[68] SPME has turned into an easy and popular technique for the study of different volatile and semi-volatile compounds, owing to its simple, fast, solvent-less, and consistent properties.

The SPME technique consists of two processes: analyte extraction and desorption. First, the desired extracting phase is either physically coated or chemically bonded on a solid support (usually fused silica or stainless steel). The coating is contacted with the sample for a specific time and the desired analytes are extracted from the sample into the extraction phase by partition or adsorption. The extraction step either can be headspace (for gaseous or volatile analytes) or by direct immersion. (for liquid analytes) Thermally stable analytes can be desorbed by using a heated injector in gas chromatography. Less volatile or thermally labile analytes can be desorbed from the extraction phases by an appropriate mobile phase or solvent used in high performance liquid chromatography. Once the other experimental conditions such as extraction temperature, extraction time, salt effect, and agitation, are kept constant, the amount of extracted analyte is merely proportional to its initial concentration. SPME is a multiphase equilibrium process with the sample matrix, fiber coating, and the headspace above the sample in headspace analysis, involves three phase equilibrium. In direct immersion SPME the two phase equilibrium involves aqueous and fiber coating. The three equilibria in headspace SPME is shown in Figure 1.2.
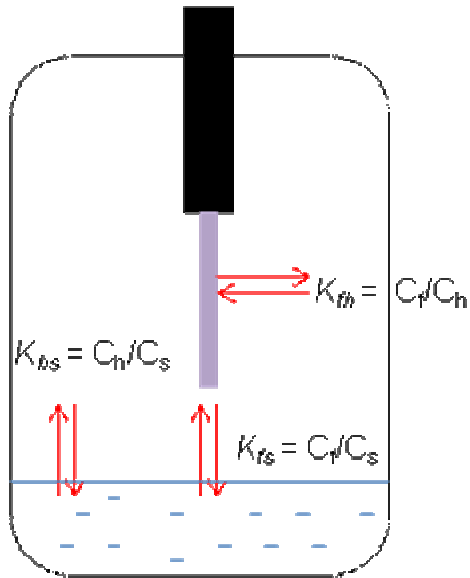
Figure 1.2 Three equilibria in headspace SPME

In a three phase system (headspace analysis) the equilibrium conditions can be expressed

as:

$$n = \frac{Kfh \cdot Khs \cdot Vf \cdot Co \cdot Vs}{KfhKhsVf + KhsVh + Vs} \quad \ldots \ldots \ldots \ldots (1)$$

where,

n = amount of analyte absorbed or adsorbed by the coating

C_o = initial concentration of analyte in the sample

K_{fh} = distribution constant of the analyte between fiber and headspace

K_{hs} = distribution constant of the analyte between headspace and sample

K_{fs} = distribution constant of the analyte between coating and sample

V_f = volume of the coating

V_s = volume of the sample

$$Kfs = Kfh.Khs \quad \ldots\ldots\ldots (2)$$

When the headspace volume is negligible, the $K_{hs}V_h$ term is zero. Hence equation 1 can be written as:

$$n = \frac{Kfs.Vf.Co.Vs}{KfsVf + Vs} \quad \ldots\ldots\ldots (3)$$

When the aqueous sample volume, V_s is much greater than the volume of the extracting coating phase V_f, then the $V_s \gg K_{fs}V_f$. So the equation 3 can be written as:

$$n = Kfs.Vf.Co \quad \ldots\ldots\ldots (4)$$

As a result, once the extraction sample volume is much larger than the volume of the extracting coating phase, the amount of extraction does not depend on the volume of the sample. Characteristic components in SPME device and direct immersion extraction and desorption using a heated injector in gas chromatography are shown in Figure 1.3 and Figure 1.4.
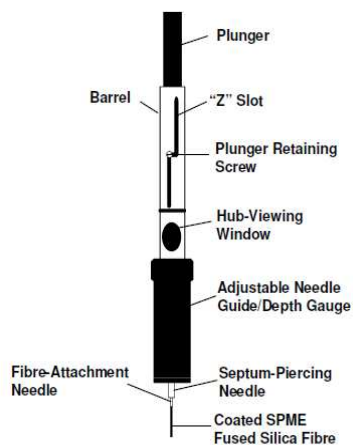
Figure 1.3 Components of a commercialized SPME device
(Source:http://www.sigmaaldrich.com/etc/medialib/docs/Supelco/General_Information/1/t
101928.Par.0001.File.tmp/t101928.pdf, Accessed: 09-24-2012)
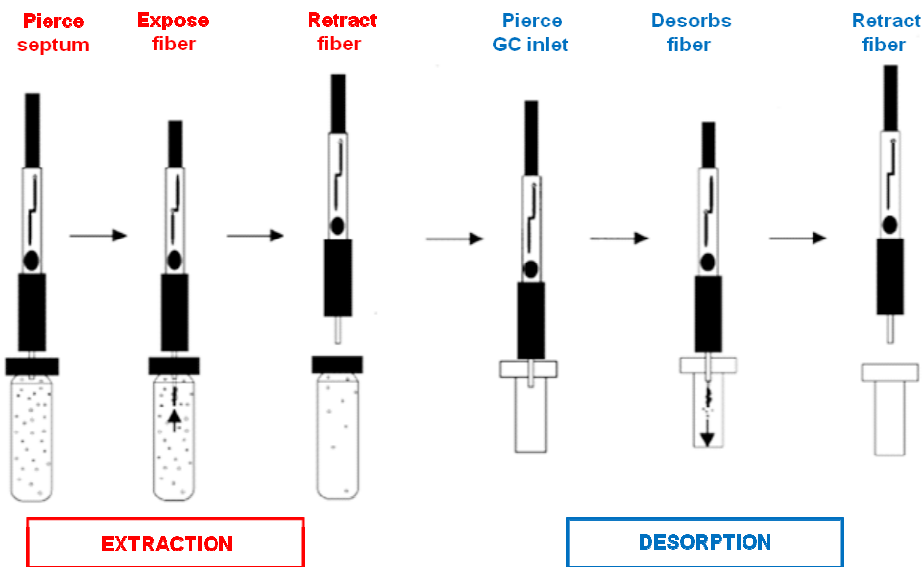
Figure 1.4 Direct immersion extraction and desorption method for a SPME-GC
(Source:http://www.sigmaaldrich.com/etc/medialib/docs/Supelco/General_Information/1/t
101928.Par.0001.File.tmp/t101928.pdf, Accessed: 09-24-2012)

15

1.4.2 Coating materials in solid phase micro extraction

The process of SPME consists of two main steps which are extraction and desorption. However both extraction and desorption happens on the same coating material (usually an organic polymer material) and therefore the properties of the coatings control the efficiency of SPME.[69] The different types of coated SPME fibers are commercially available. These coatings can be categorized into absorbent types and adsorbent types according to the nature of the coating material on the SPME fiber. Polydimethylsiloxane (PDMS) and polyacrylate (PA) coatings consist of highly viscous organic liquids, which extract analytes through absorption and consequently are considered absorbent–type fibers. The other type of coatings with PDMS-DVB (divinybenzene), Carbowax-DVB, Carboxen, and Templated resin are blended coating materials and so are considered as adsorbent-type fibers. In adsorbent-type coatings, the primary extraction phase is a porous solid. Adsorbent type coating, extract the analytes via adsorption rather than the absorption mechanisms.[70] Therefore, the fiber coating is a main component in SPME techniques and the development of a highly selective extracting coating material is the major challenging task in SPME. Hence, selecting the proper coating material is totally governed by the chemical properties of the analyte to be extracted.

The coating thickness of commercially available fibers vary from 7-100μm.[71] The commercially available polydimethylsiloxane (PDMS) fiber has three different coating thicknesses which are 7, 30 and 100μm and are often used to extract non polar and aromatic analytes. Polyacrylate (PA) and polyetheleneglycol (PEG) fibers are polar fibers and commonly used to extract polar analytes in both headspace and direct immersion analylsis. The fiber coating contains of both PDMS and divinylbenzene (PDMS-DVB) or

16

Carboxen are the blended SPME fibers used to extract amine, ester, and alcohol containing analytes.

1.4.2.1 Ionic liquid based coating material for SPME

Most of the ionic liquids (ILs) possess unique properties such as high thermal stabilities, negligible vapor pressure, high viscosities and the ability to undergo multiple solvation interactions. Owing to these outstanding properties, ILs are ideal alternatives to traditional absorbent type coating materials for SPME. In 2004, Liu and coworkers used 1-octyl-3-methyl imidazolium PF_6 monocationic ionic liquids as a disposable coating material and extracted benzene, toluene, ethylbenzene, and zylene (BTEX) in paints by headspace SPME.[72] Later Anderson and coworkers used more thermally stable dicationic polymeric IL-based materials as coatings and extracted esters in headspace.[73] They showed good analyte recoveries comparable to commercially available polydimethylsiloxane fibers. The application of these fibers are limited to headspace analysis due to the physical coating of the polymeric IL material on the fused silica.

We have developed two new monomeric and polymeric IL coating materials which are covalently bonded to silica. These new covalently bonded fibers are used in both headspace and direct immersion to extract small alcohols, amines, and polar analytes with higher reproducibility. The development new polymeric ILs fibers will be discussed in Chapter 4.

1.5 Bonded phase material for MALDI-MS

1.5.1 Introduction to MALDI-MS

MALDI is a soft ionization technique introduced by Karas and Hillenkamp[74] as a substitute matrix approach for LDMS (laser desorption mass spectrometry) in 1988. Subsequently, MALDI has been become the most widely used ionization method for the analysis of thermally labile, larger molecular weight non-volatile analytes, such as

oligosaccharides, oligonucleotides, peptide, proteins, and synthetic polymers. However, the fundamentals of this ionization mechanism and the exact role of the matrix are not yet fully clear and several research groups have offered different explanations. The most common and simple explanation is first, the large excess of matrix molecule absorbs UV or IR laser energy, then the matrix become ionized and dissociates and charge is transfer to the analyte molecule in gas phase chemical ionization by intermolecular interactions. Finally, the ionized analyte can be analyzed by the mass spectrometer. The schematic diagram of MALDI mechanism is shown in Figure 1.5
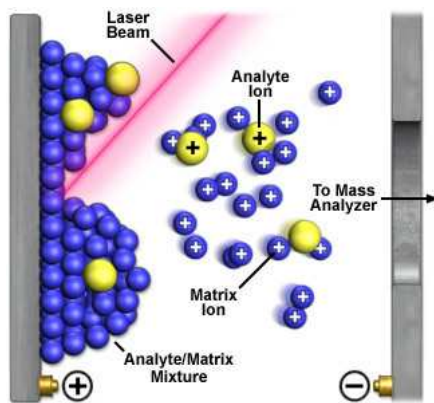
Figure 1.5 Schematic of the MALDI process
(Source:http://www.magnet.fsu.edu/education/tutorials/tools/ionization_maldi.html,
Accessed:09-26-2012)

1.5.2 Common MALDI matrices

The most commonly used UV-MALDI matrices are small organic molecules which absorb the energy in the range of the 266-355 nm. Classic matrices are organic molecules consisting of hydroxyl- groups (-OH) in ortho- or para- position and acidic groups or carbonyl functions (carboxyl group, ketones). The frequently used MALDI matrices are shown in Figure 1.6.

18

However most of the matrix molecules are only suitable for the analysis of specific types of analytes. Derivatives of benzoic acid, 2,5-dihydroxybenzoic acid (2,5-DHB) are the most frequently used MALDI matrices for the analysis of low molecular weight compounds, proteins and glycoproteins.[75] Derivaties of cinnamic acid such as α-cyano-4-hydroxycinnamic acid (CHCA), ferulic acid (FA) or sinapinic acid (SA)[76] are frequently used for the analysis of proteins; CHCA and FA are the most often used matrices for the analysis of peptides. Nitrogen-containing derivatives, like nicotinic acid and 3-hydroxypicolinic acid (3HPA), are also used as matrices for the analysis of oligonucleotides.[77]
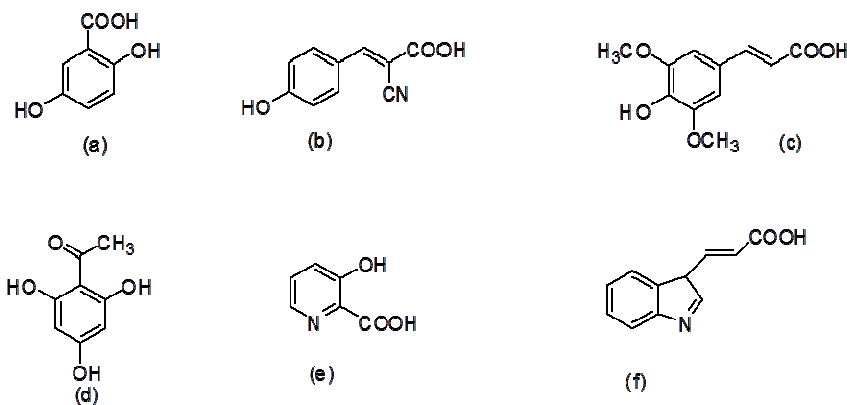
Figure 1.6 Commonly used solid matrices.
a) 2,5-dihydroxybenzoic acid (2,5-DHB), b) α-cyano-4-hydroxy-cinnamic acid (CHCA), c) sinapanic acid (SA), d) 2,4,6-trihydroxyacetophenone (THAP), e) 3-hydroxy-picolinic acid (3-HPA) and f) indoleacrylic acid (InAA)

1.5.3 Ionic liquid Matrices (ILMs)

Ionic liquids (ILs) are salts melting at temperatures below 100 °C. They have unique properties such as negligible vapor pressure, non-explosive, non-flammable, high viscosities, and ability to undergo multiple solvation interactions.[78] The properties of ionic liquids can be tuned by using different cationic and anionic moieties and therefore countless combinations with different physiochemical properties are possible. The most

frequently used cationic moieties are pyridinium, imidazolium, ammonium or phosphonium ions. Inorganic or organic anions such as chloride, bromide, tetrafluoroborate, bis(trifluoromethylsulfonyl)imide, and triflate often are used as anionic moieties.

Owing to the multiple solvation interactions, high viscosities and high thermal stability, these ionic liquids have been widely used in analytical techniques especially as stationary phase coatings in gas chromatography.[79] The ability to dissolve wide range of substances and negligible vapor pressure and high vacum stabilities are some of the key factors for the MALDI matrices. Armstrong et al. first introduced ILs as MALDI matrices[80] but it turned out the classical ILs (pyridinium and phosphonium ILs) were not functional as MALDI matrices. However, equimolar mixes of classical solid MALDI matrices, like DHB, CHCA or SA with organic bases, like, tributylamine, triethylamine, di-isopropyl amine were able to promote the ionization of the analyte.[80] These new class of ionic liquids are called as ionic liquid matrices (ILMs). Compared to traditional solid MALDI matrices, ILMs provide uniform, homogeneous distribution of the sample, does not required co-crystallization, nor searching for hot-spots. In addition it allows MALDI to be used as a quantitative method. Recently Armstrong and coworkers introduced a second generation ionic liquids matrices which provide good sensitivity and a wider mass range for synthetic polymers, oligosaccharide, peptides, and proteins.[81,82]

1.5.4 Alternate surface preparation techniques for LDI-MS

MALDI is a well-known soft ionization technique and is used in the analysis of different types of compounds including polymers, peptides and proteins. However, the main drawback of this technique is the difficultly to detect low molecular weight compounds, especially < 1000 m/z due, to the interference of matrix background in this low mass range.[83] Therefore several research groups introduced alternative methods to

analyze low molecular weight compounds using a laser desorption/ionization (LDI) mass spectrometry. The alternative methods are laser desorption/ionization on silicon (DIOS), surface enhanced laser desorption ionization (SELDI), nano-assisted laser desorption/ionization (NALDI), and sol-gels. Some of these alternative matrix free methods do not require co-crystallization.

1.5.4.1 DIOS

The desorption ionization on porous silicon (DIOS) was the first technique to apply a true matrix-free desorption/ionization in mass spectrometry.[84] In this matrix free method, the properties of porous silicon are very useful in analysis of the analyte. The nanocrystalline surface of porous silicon is produced by an etching procedure, which is an important parameter in the analysis of an analyte in MALDI.[85] The characteristic features of nanocrystalline surface morphology such as pore diameter and shape are dependant on preparation conditions like dopant type, ethching solution and etching time of the DIOS.[83] The surface of the porous silicon can absorb UV light without incorporating the classic MALDI matrices. DIOS is ideal for the detection of low molecular weight compounds such as choline (m/z 104) and acetylcholine (m/z 146).[86]

1.5.4.2 SELDI

Surface-enhanced laser desorption/ionization (SELDI) was introduced by Hutchens and Yip as a new desorption strategy for the mass spectrometric analysis of macromolecules.[87] The SELDI principle is quite simple. The solid phase protein chip chromatographic platforms in SELDI is composed of a chemically or biochemically modified surfaces. The chemically modified surfaces involve anionic exchange, cationic exchange, metal ion, hydrophobic or hydrophilic molecules where as biochemically modified surfaces involve antibody, receptor or enzyme as active platforms. Proteins are captured on the chromatographic surface by electrostatic interaction, partition, adsorption

or affinity. After adding a proper matrix onto the surface, the target protein can be ionized with a laser and the molecular mass can be determined by TOF-MS. Protein chips consisting of chemically treated platforms are commercially available and biochemically modified platforms are custom made. SELDI-TOF MS has been used to discover a potential disease diagnostic biomarker for bladder[88], breast[89], and ovarian cancers[89], and Alzheimer disease[90] SELDI-MS is a high-throughput method that permits the rapid screening for disease biomarker recognition in a reasonably short time.

1.5.4.3 NALDI

There are various methods that use nanostructures as a matrix-free LDI-MS but the carbon nanotube was the first approach, introduced by Xu and coworkers in 2003.[91] This technique is considered as Nano-Assisted Laser Desorption/Ionization (NALDI). The characteristic features of the nanotubes, such as capability of trapping analytes on the surface and transferring the energy to the analyte, show them to be an ideal candidate as a matrix free LDI-MS. Not only did the carbon nanotubes require less laser power to desorb/ionize the analyte but also showed less background noise compared to the commercial matrices. Silicon nanowires are another alternative for nanostructured material and have been used for matrix-free LDI –MS by Go et. al in 2005.[92] This technique has a higher detection sensitivity and is able to detect 500 amol of des-Arg^9 – bradykinin.[92]

1.5.4.4 Sol-gels

Sol-gels are another alternative technique for the matrix-free LDI-MS. Sol-gels are polymeric structures containing a siloxane backbone. The initial use of sol-gels for matrix-free LDI-MS was introduced by Lin & Chen, who embedded a matrix molecule into the sol-gel structure.[93] The common method to immobilize matrix molecules into the sol-gel structure is by condensation reaction of hydroxyl groups of matrix molecules (eg. 2,5-

22

dihydroxybenzoic acid) with TEOS (tetraethoxy silane) to form matrix attached sol-gel network. The surface of the matrix attached sol-gel network is able to absorb the laser light and let the analyte desorb without or with minimal background signal. These sol-gels have been used to detect biological proteins such as bradykinin, cytochrome C and insulin[93,94] and also these materials can also be use to extract benzo[a]pyrene from solution.[95]

1.6 Dissertation Organization

This dissertation presents research on bonded phase materials for separations in three areas: 1) development and screening of new chiral stationary phase (CSPs) and enantiomeric separation of newly synthesized tetrahydrobenzimidazole intermediates by HPLC and CE (Chapter 2 - 4); 2) bonded ionic liquid polymeric material for solid phase microextraction (Chapter 5); 3) coupling solid phase microextraction and laser desorption ionization for rapid identification of biological materials (Chapter 6).

CHAPTER 2

DEVELOPMENT OF NEW LC CHIRAL STATIONARY PHASES BASED ON

RUTHENIUM *TRIS*(DIIMINE) COMPLEXES

2.1 Abstract

Enantiopure ruthenium(II) *tris*(diimine) complexes have been covalently bonded to silica and evaluated as chiral stationary phases for LC. Three binding chemistries were tested and the CSP synthesized by reductive amination of the aldehyde-functionalized silica provided the largest enantioselectivity. The Ru complex-bonded CSP showed selectivity toward a variety of racemic compounds. Circular dichroism (CD) detection was used to confirm the enantiomeric separations. This CSP worked especially well for the enantiomeric separation of binaphthyl type compounds in the normal phase mode and appeared to be selective for acidic compounds in the polar organic mode. Effects of mobile phase composition on the enantioseparations were also studied.

2.2 Introduction

Enantiomeric separation has been an important topic for several decades. Among various chiral separation methods, LC with chiral stationary phases (CSPs) has been dominant due to its good reproducibility, wide selectivity, easy operation, and ability to do preparative and semipreparative separations.[31,46-48,51,96-98] CSPs are produced by immobilizing pure enantiomers (chiral selectors) to solid support (silica) via chemical bonding or physical absorption. Although a large number of papers related to the development of CSPs have been published, only a few types of CSPs dominate the field of LC enantiomeric separations. However, researchers continue to investigate new types of chiral stationary phases, in hopes of finding a more universal stationary phase or a

24

more specific stationary phase, which is especially powerful for selected groups of compounds.

One type of chiral selector that has not received much attention in LC is that of transition metal complexes.[99-103] The helical chirality of the enantiomers of ruthenium *tris*(diimine) complexes is shown schematically in Figure 2.1. The earliest study involving a metal-ligand complex as a stationary phase showed that the Δ- and Λ-enantiomers of a metal complex were absorbed on a clay support in stereoregular manners and similar behavior was observed between "enantiomers" of different types, such as Δ-[Ni(phen)$_3$]$^{2+}$ and Λ-[Ru(phen)$_3$]$^{2+}$[99] Yamagishi[101] reported that a column of Λ-[Ru(phen)$_3$]$^{2+}$ absorbed onto montmorillonite gave "optical resolution" of tris(chelated) and bis(chelated) metal complexes. Later, the same group extended the applicability of this column to chiral aromatic compounds, by showing separation of 2,3-diphenylpyrazine and binaphthyl enantiomers.[102] Also, they used spherically shaped synthetic hectorite instead of montmorillonite in order to improve the column efficiency.[103] However, all the reported columns were prepared by simply absorbing the metal complexes onto the clay and some mobile phases had to be avoided so as to prevent desorbtion of the chiral selectors from the clay.
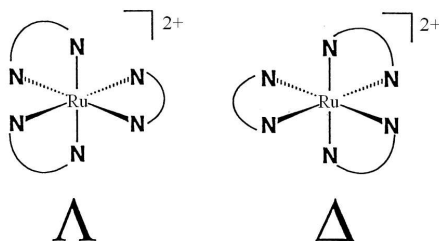
Figure 2.1 Mirror image relationship of Ru(II) *tris*(diimine) enantiomers

To our knowledge, the CSPs based on Ru complexes which are covalently linked to the support have not been reported. In the present work, we have attached chiral, non-

25

racemic Ru tris(diimine) complexes to high surface area silica gel in an attempt to improve the performance of this class of CSPs. Three different chemistries linking the Ru complex to 5-µm spherical silica gel were studied in order to improve the chiral selector loading. The CSP prepared via an amination reaction between aldehyde-functionalized silica and the peripheral amino group of Ru tris(phenanthroline) complex gave the best performance. The column was then evaluated as a chiral stationary phase for HPLC by injecting 155 racemic analytes. Three operation modes (normal phase mode, polar organic mode, and reversed phase mode) were tested. Effects of mobile phases composition on the separations were studied.

2.3 Experiment

2.3.1 Chemicals

Anhydrous N, N-dimethylformamide (DMF), anhydrous toluene, 3-(triethoxysilyl)propyl isocyanate, 1,6-diisocyanatohexane, sodium periodate, sodium cyanoborohydride, sodium monophosphate, phosphoric acid, ammonium nitrate, ammonium chloride, and most racemic analytes used in this study were purchased from Sigma-Aldrich (Milwaukee, WI, USA). Acetonitrile, 2-propanol, n-heptane, ethanol, and methanol of HPLC grade were obtained from EMD (Gibbstown, NJ). Tetramethylammonium nitrate (TMAN), ammonium trifluoroacetate, ammonium nitrate, ammonium chloride, and ammonium acetate were purchased from Sigma-Aldrich (St. Louis, MO). Water was obtained from Millipore (Billerica, MA). Kromasil silica (5µm spherical diameter, 100 Å and 200 Å pore size) was obtained from Supelco (Bellefonte, PA).

2.3.2 Synthesis of [Ru(phen)$_2$aminophen](PF$_6$)$_2$ and [Ru(phen)$_2$phendiamine](PF$_6$)$_2$

The compounds: 5-nitro-1,10-phenanthroline,[104] Ru(phen)$_2$Cl$_2$,[105] [Ru(phen)$_2$phendione]Cl$_2$ (phendione =1,10-phenanthroline-5,6-dione),[106] and

26

[Ru(phen)$_2$nitrophen](PF$_6$)$_2$ were prepared as previously reported.[107] Racemates of [Ru(phen)$_2$nitrophen](PF$_6$)$_2$ and [Ru(phen)$_2$phendione](PF$_6$)$_2$ were converted to chloride salts by metatheses, and resolved as reported.[107] Ru(phen)$_2$nitrophen]Cl$_2$ was reduced to [Ru(phen)$_2$(aminophen)]Cl$_2$ (aminophen=5-amino-1,10-phenanthroline), described in Ref.[107] [Ru(phen)$_2$(phendiamine)]Cl$_2$ (phendiamine=5,6-diamino-1,10-phenanthroline) was prepared according to Ref.[108]

2.3.3 Preparation of Ru complex-bonded chiral stationary phases

Three different linkage strategies for chemically attaching Ru tris(diimine) complex to 5μm-diameter silica gel were conducted and the synthetic schemes of three binding methods are shown in Figure 2.2.

27
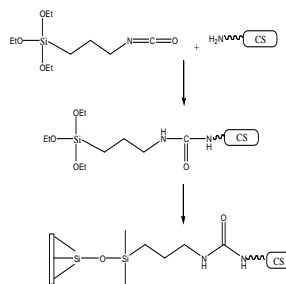
Binding method 1

Binding method 2
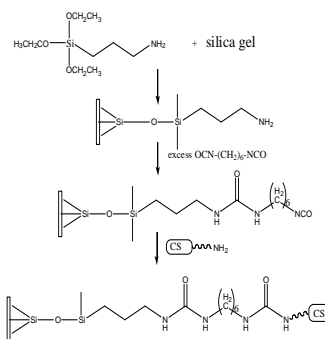
Binding method 3
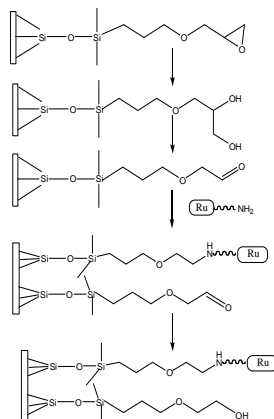
Figure 2.2 Syntheis schemes for three Ru complex-based CSPs

The first binding method[46,51] involved reacting Ru complex with excess 3-(triethoxysilyl)propyl isocyanate in anhydrous DMF at 90 ˚C for five hours. Then the product was added to dry silica gel and heated at 105 ˚C overnight. The mixture was

cooled, filtered and washed as indicated previously. The second approach involved three steps and was analogous to those reported previously for antibiotic stationary phases.[51] 3-Aminopropyl-triethoxysilane was added to silica-toluene slurry dropwise after the silica was dewatered using Dean-Stack trap. The mixture was refluxed for 4h and then cooled, filtered, and washed with toluene, methanol, and acetone. 1,6-Diisocyanatohexane was added to dry amino-silica toluene slurry while kept in an ice bath. Then the slurry mixture was heated to 70°C for 4h. The excess reactant was removed by vacuum filtration and the solid product was washed with anhydrous toluene. Then the Ru-complex in pyridine was added and the mixture was heated to 70°C and allowed to react for overnight. Finally the product was filtered, washed and dried. In the third linkage chemistry, the diol-silica was prepared according the literature.[110] The diol groups were oxidized in 60 mM sodium periodate in water/methanol (4:1) at room temperature. Then the aldehyde-silica was filtered and dried. Ru complex was added to the resulting aldehyde-silica in anhydrous methanol and refluxed overnight. Finally, the remaining aldehyde moieties were reduced by sodium cyanoborohydride (NaCNBH$_3$) in phosphate buffer (pH=3).[111] The elemental analysis results are shown in Table 2.1. Then the CSP was slurry packed into 25cm×0.46cm (i.d.) stainless steel column.

2.3.4 Column evaluation

The first chromatographic system was an HP (Agilent Technologies, Palo Alto, CA, USA) 1050 system, which consists of a UV VWD detector, an autosampler, a quaternary pump and Chemstation software. The second HPLC system was composed of a pump (Shimadzu, LC-6A) and a circular dichroism detector (Jasco, CD-2095 plus). For the LC analysis, the injection volume, the flow rate, and the detection wavelength are 5 μL, 1mL/min, and 254 nm, respectively. Separations were carried out at room temperature (~22 °C) if not specified. The mobile phase was degassed by ultrasonication

under vacuum for 5 min. The analytes were dissolved in ethanol, or the appropriate mobile phases. Each sample was analyzed in duplicate. In the normal phase mode, heptane/ethanol was used as the mobile phase. The mobile phase of the polar organic mode was composed of acetonitrile/methanol and a small amount of salt. Water/acetonitrile was used as the mobile phase in the reversed phase mode.

2.3.5 Calculations

The retention factor (k') was calculated using the equation $k' = (t_r-t_0)/t_r$, where t_r is the retention time, and t_0 is the dead time which is determined by the peak of the refractive index change due to the sample solvent. Selectivity (α) was calculated by $α=k_2'/k_1'$, where k_1' and k_2' are the retention factors of the first and second eluted enantiomers, respectively. The resolution (Rs) was determined using Rs = $2×(t_{r2} -t_{r1})/(w_1 + w_2)$, where w is the base peak width.

2.4 Results and Discussion

2.4.1 Evaluation of binding chemistries

Normally, bonded chiral stationary phases are more stable and robust than coated ones, because the absorbed chiral selectors may be soluble in some solvents and can be removed by the mobile phases employed to affect the separation. The objective of this work is to synthesize the first LC CSP in which a chiral Ru complex was covalently bonded to a modern silica gel support.

The initial step was to compare the performances of different Ru complexes as chiral selectors. Two Ru *tris*(diimine) complexes with amino groups were selected: [Ru(phen)$_2$aminophen](PF$_6$)$_2$ and [Ru(phen)$_2$phendiamine](PF$_6$)$_2$.(structures shown in Figure 2.3)

30
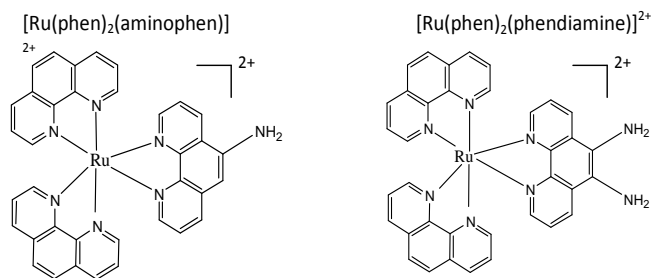
Figure 2.3 Structures of two Ru *tris*(diimine) complexes as chiral selectors

It was found that amino groups of these compounds were poorer nucleophiles than typical aliphatic amines due to the electron withdrawing nature of Ru^{2+}, and the fact that they are attached to an aromatic ring system. Therefore, nucleophilic coupling reactions that are commonly used to immobilize other chiral selectors to the surface of silica gel,[46,51] tend to be more difficult for these metal complexes. Λ-[Ru(phen)$_2$aminophen](PF$_6$)$_2$ and Λ-[Ru(phen)$_2$phendiamine](PF$_6$)$_2$ were chemically bonded to silica gel using the same binding method (binding method **1** in Figure 2.2). The carbon percentage of the final products is 4% for [Ru(phen)$_2$aminophen](PF$_6$)$_2$-bonded silica, and 7% for [Ru(phen)$_2$phendiamine](PF$_6$)$_2$-bonded silica, respectively. This indicates that replacing [Ru(phen)$_2$aminophen](PF$_6$)$_2$ with [Ru(phen)$_2$phendiamine](PF$_6$)$_2$ effectively improved the chiral selector loading. The enantiomeric performances of these two CSPs were evaluated by HPLC using the same experimental conditions. The chromatograms of cis-4,5-diphenyl-2-oxazolidinone separated on the [Ru(phen)$_2$aminophen](PF$_6$)$_2$-bonded CSP and the [Ru(phen)$_2$phendiamine](PF$_6$)$_2$-bonded CSP are shown in Figure 2.4.
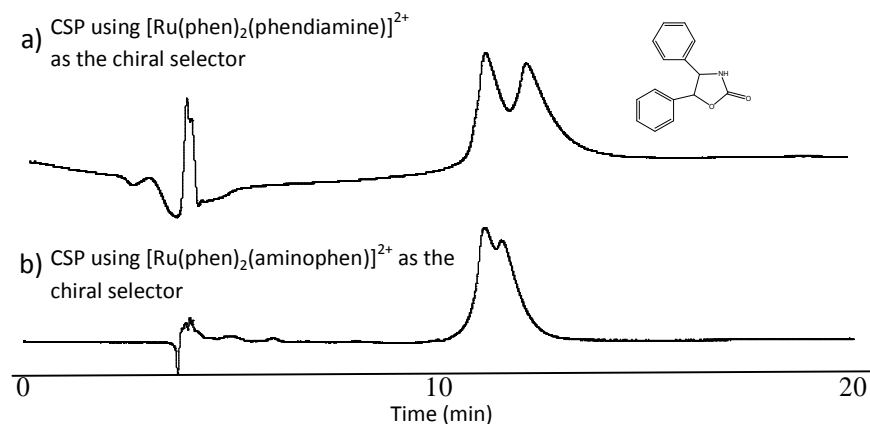
Figure 2.4 Comparison between two CSPs using a) Λ-[Ru(phen)$_2$(aminophen)]$^{2+}$ and b) Λ-[Ru(phen)$_2$(phendiamine)]$^{2+}$ as the chiral selectors. The analyte and mobile phase is cis-4,5-Diphenyl-2-oxazolidinone, and 95%water/5%acetonitrile, respectively.

It is evident that the CSP using Λ-[Ru(phen)$_2$(phendiamine)]$^{2+}$ provided higher selectivity and resolution, although similar retention was observed on these two columns. Both elemental analysis and chromatographic results show that [Ru(phen)$_2$(phendiamine)]$^{2+}$ is more suitable for preparing stationary phases, providing higher chiral selector loading and better enantioselectivity. Therefore, [Ru(phen)$_2$(phendiamine)]$^{2+}$ was selected to study further binding chemistries. In addition, the surface area of silica gel plays an important role in synthesis. Replacing 200Å silica (pore size, surface area is ~180m^2/g) with 100Å silica (pore size, surface area is ~450m^2/g) significantly improved the carbon loading from 3% to 7% using the same Ru complex. Therefore, 100Å silica was used for subsequent studies.

Special attention was paid to the chemical binding procedures in order to obtain stationary phases with good chiral selector loading. To determine the best immobilization process, reactions were carried out using three different methods (Figure 2.2), named isocyanate binding (Method **1**), diisocyanate binding (Method **2**) and aldehyde binding (Method **3**), which are commonly used to prepare macrocyclic glycopeptide and cyclodextrin CSPs.[46, 51] Small scale reactions were conducted due to limited availability of enantiopure Ru complex. The elemental analyses of three products are shown in Table 1.

Table 2.1 . Elemental analysis results of Ru complex-silica products synthesized by three different methods

	Description	C%	H%	N%
Method **1**	Isocyanate	7.2	1.2	1.5
Method **2**	Diisocyanate	13.5	2.2	4.5
Method **3**	Aldehyde	9.2	1.6	0.4

Also, comparison of the color of the final products allows a qualitative comparison of the binding methods, since these Ru complexes have a pronounced orange color. Diisocyanate binding chemistry (method **2)** gave a product with the highest carbon loading (13.5%), but the color of the final product was the lightest. This is explained by the fact that the high percentage of carbon originates mainly from the large quantity of the diisocyanate linkage present. Comparing isocyanate binding (method **1)** and aldehyde binding (method **3**), visual observation shows the darkness of products is similar and carbon percent of method **3** is higher than method **1** (9.2% versus 7.2%, shown in Table 2.1). These two methods were then utilized to provide sufficient media to pack into 25cm columns (i.e., 3.5 grams of each, respectively), which were evaluated using the same analytes and mobile phases. The chromatograms of 1,1'-bi-2-naphthol

separated on the CSPs prepared via isocyanate and aldehyde binding methods are shown in Figure 2.5. The enantioselectivity of the analyte separated on the CSP that utilized the aldehyde-binding is greater than that achieved on isocyanate-bound CSP.
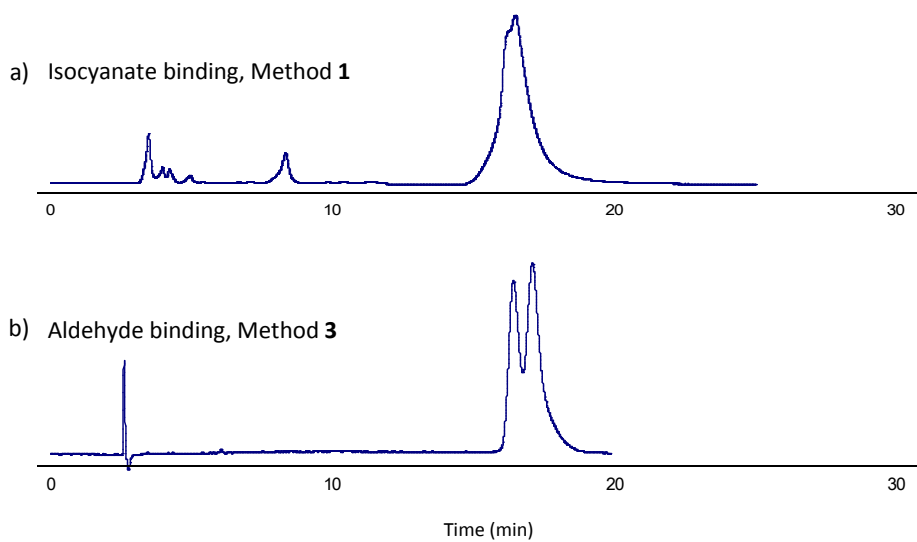
Figure 2.5 Comparison between two binding methods. The chromatograms were obtained on the CSPs prepared via a) isocyanate binding (method **1** in Figure 2) and b) aldehyde binding (method **3** in Figure 2), respectively. The chiral selectors ([Ru(phen)$_2$(phendiamine)]$^{2+}$) and silica (pore size: 100Å) used are the same for two CSPs. The analyte and mobile phase is 1,1'-bi-2-naphthol and 80%heptane/20%ethanol, respectively.

2.4.2 Evaluation of the CSP prepared via aldehyde binding method

In this study, the best CSP was obtained by binding [Ru(phen)$_2$(phendiamine)]$^{2+}$ to 100Å silica via aldehyde binding chemistry. A set of 155 chiral compounds with a wide variety of functionalities was used to test this Ru complex-bonded CSP. Three operation modes (normal phase, polar organic mode, and reversed phase) were studied. It should be noted that acidic compounds with –COOH group are not eluted with heptane/ethanol, or acetonitrile/water, due to strong charge-charge interaction with the Ru complex-bonded stationary phase. It was also observed that salts (such as ammonium nitrate) are

34

necessary to elute these acidic compounds in the polar organic mode. The other compounds without acidic groups did not give retention in the polar organic mode. Therefore, 35 acidic compounds were studied only in the polar organic mode and the other 120 compounds were injected in the normal phase and reversed phase modes. Table 2.2 lists the chromatographic data for all compounds separated in three chromatographic modes.

Table 2.2 Chromatographic data of enantiomers resolved by the Ru complex-based CSP
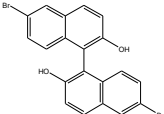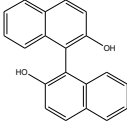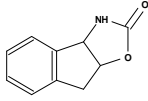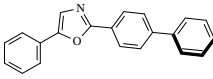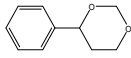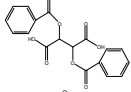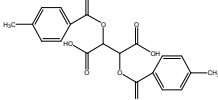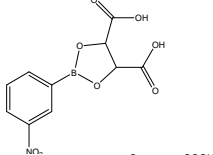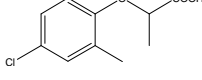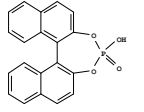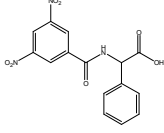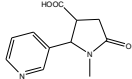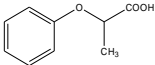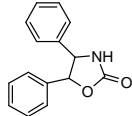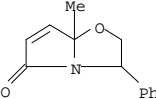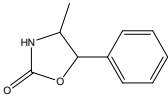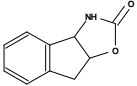
Mode	No.	Analyte name	Analyte structure	k1'	α	Rs	Mobile phase
Normal phase	1	6,6'-Dibromo-1,1'-bi-2-naphthol		11.69	1.17	1.5	A
	2	1,1'-Bi-2-naphthol		23.70	1.08	1.5	B
	3[c]	(3a(R,S)-cis)-(±)-3,3a,8,8a-Tetrahydro-2H-indeno[1,2-d]oxazol-2-one		2.72	1.08	0.6	C
	4	2-(4-Biphenylyl)-5-phenyloxazole		1.22	1.02	0.5	B
	5	4-Phenyl-1,3-dioxane		0.92	1.03	0.6	D
Polar organic	6	2,3-Dibenzoyl-DL-tartaric acid		17.34	1.07	1.5	E[a]
	7	O,O'-di-p-toluoyl-DL-tartaric acid		15.49	1.07	1.5	E[a]
	8	3-nitrophenylboronic acid tartaric acid ester		5.41	1.28	1.4	F
	9	2-(4-chloro-2-methyl-phenoxy)propionic acid		3.14	1.03	0.6	F
	10	(R/S)-(-/+)-1.1'-Binaphthyl-2,2'-diyl hydrogenphosphate		4.57	1.02	0.6	F
	11	N-(3,5-Dinitrobenzoyl)-DL-phenylglycine		2.14	1.02	0.5	F

36

Table 2.2 Continued

	12	trans-4-Cotininecarboxylic acid		1.28	1.05	0.6	F
	13	2-Phenoxypropionic acid		1.56	1.02	0.5	F
Reversed phase	14	cis-4,5-Diphenyl-2-oxazolidinone		3.70	1.05	0.9	G[b]
	15	2,3-Dihydro-7a-methyl-3-phenylpyrrolo[2,1-b]oxazol-5(7aH)-one		3.74	1.04	0.6	H[b]
	16	4-Methyl-5-phenyl-2-oxazolidinone		2.48	1.03	0.6	H[b]
	17[c]	(3a(R,S)-cis)-(±)-3,3a,8,8a-Tetrahydro-2H-indeno[1,2-d]oxazol-2-one		2.36	1.02	0.5	H[b]

Note: (a) The flow rate and the column temperature are 0.5 mL/min and 0 °C in order to improve the resolution; (b) The flow rate is 0.8 mL/min to avoid high pressure (>300bar), which could damage silica support. The mobile phase compositions are: (A) 90%heptane/10%isopropanol; (B) 95%heptane/5%isopropanol; (C) 80%heptane/20%ethanol; (D) 60%heptane/40%ethanol; (E) 100%methanol/15mM NH_4NO_3; (F) 100%methanol/12.5mM NH_4NO_3; (G) 90%water/10%acetonitrile; (H) 98%water/2%acetonitrile.

The chromatographic data include retention factor (k_1'), selectivity (α), and resolution (Rs). Examples of optimized separations in all three modes are shown in Figure 2.6.
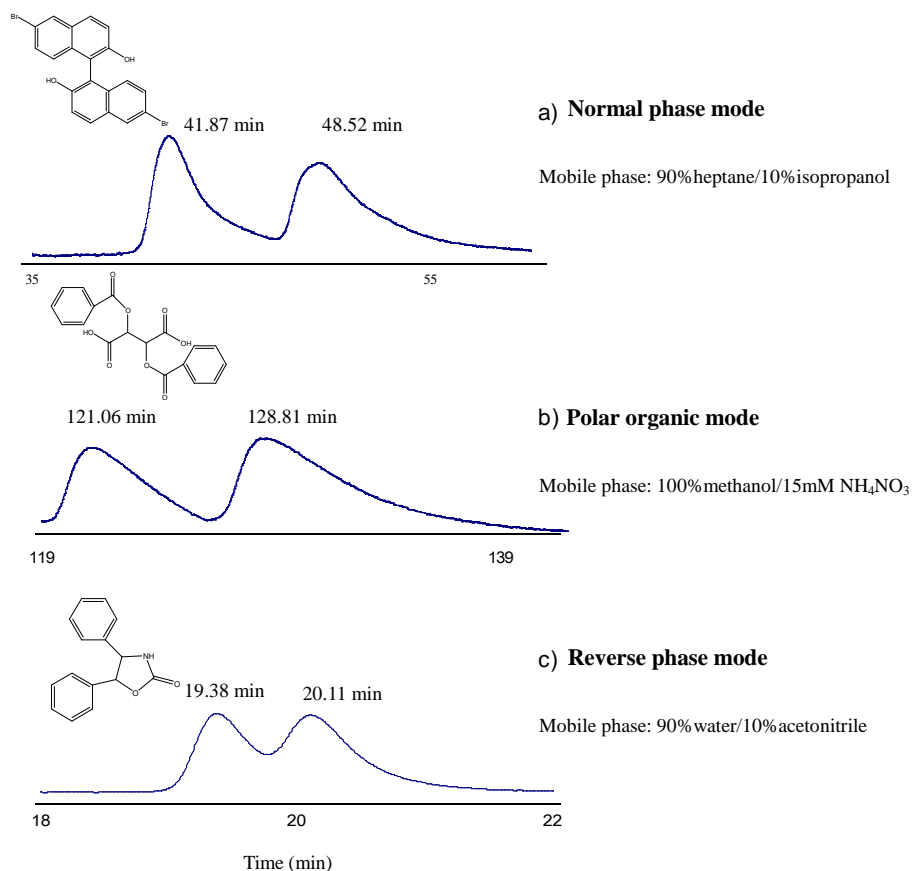
Figure 2.6 Optimized separations in three modes. Chromatographic data: (a) k_1'=14.26, α=1.11, R_s=1.5; (b) k_1'=17.34, α=1.07, R_s=1.5 (flow rate=0.5mL/min); (c) k_1'=3.70, α=1.05, R_s=0.9 (flow rate=0.8mL/min).

Overall, sixteen racemic compounds were separated on the best Ru complex-based CSP using three mobile phase modes mentioned above. The polar organic mode appeared to produce more successful separations than the other two modes. In the polar organic mode, eight compounds are separated, compared to five compounds separated

in the normal phase, and four in the reversed phase, respectively. Four compounds are baseline resolved ($R_s \geq 1.5$) and twelve were partially separated ($0.4 < R_s < 1.5$). One compound (No. 3 or No. 17 in Table 2) was partially enantioseparated in both the normal phase mode and the reversed phase mode. Although the enantioseparation capability of Ru complex-based CSP is relatively limited, Ru-CSP is selectively effective for acidic compounds, considering 8 racemic analytes were separated out of 35 tested.

A closer examination of the data reveals some interesting facts. Ru complex bonded stationary phase appears to be multimodal in that they can be used in normal phase, polar organic and reversed-phase modes. The CSP was not irreversibly altered when changing from one mobile phase mode to another. Previous papers[107,112-114] also indicate that the stereochemistry at these ruthenium centers is very robust and these compounds are not easily racemized or decomposed in ordinary protic or aprotic solvents.

The Ru complex-bonded CSP provides the best resolution for compounds of binaphthyl types in the normal phase mode. This indicates that different retention mechanisms may be involved in different mobile phase modes. In the normal phase mode where the non-polar solvents are used as the mobile phase, π-π interactions can play an important role in the chiral recognition process. The phenanthroline ring linked to Ru^{2+} is very electron deficient and π-π interactions are strong when it associates with π-basic compounds, such as 1,1'-bi-2-naphthol. Also, the carbamate linker provides additional sites for dipolar interactions. The helical chirality of Ru complex possibly provides a good fit with those analytes of helical chirality (such as binaphthyl compounds). Steric interaction may be important as well. These results are in agreement with previous reports on the $[Ru(phen)_3]^{2+}$-clay column, which was shown to separate 1,1'-bi-2-naphthol.[115]

39

In the polar organic mode, the dominant interactions between the analyte and CSP usually involve some combination of hydrogen bonding, electrostatic, and dipolar interactions. The fact that Ru complex column shows enantioselectivity toward acidic compounds demonstrates that electrostatic interaction between positively-charged Ru complex and negatively-charged acidic analyte plays an important role in chiral recognition. In addition, electrostatic interactions between a solute and the stationary phase may be associated with a slow adsorption-desorption process, giving rise to broad and more poorly-defined peaks.

In addition, the circular dichroism detector was applied to test the compounds with appropriate retentions ($1<k'<6$) in the normal phase and reversed phase. A positive-negative signal split in the circular dichroism chromatogram was observed in many cases (shown in Figure 2.7), where only one single peak was obtained in the UV chromatograms. This occurred when there was chiral recognition between the CSP and racemic analyte, but only moderate enantioselectivity and low efficiency.
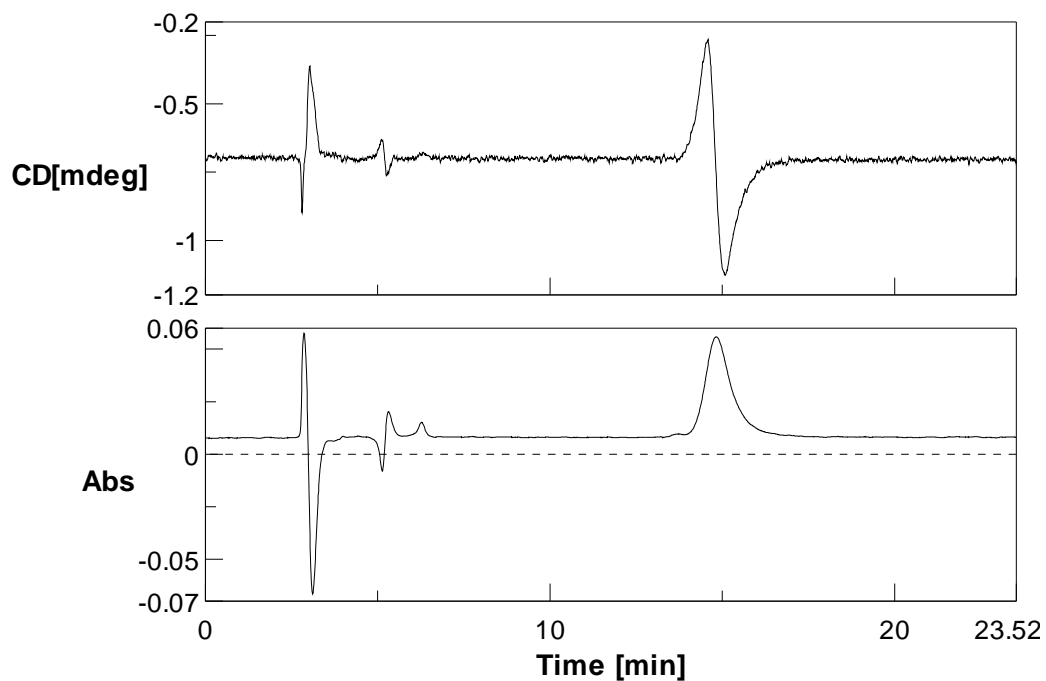
Figure 2.7 UV and CD chromatograms of the analyte retained on the Ru-complex column. The analyte is 4-(4-methoxy-phenyl)-6-methyl-2-thioxo-1,2,3,4-tetrahydro-pyrimidine-5-carboxylic acid allyl ester. The mobile phase and wavelength is 80%heptane/20%ethanol and 254 nm, respectively.

It is found that the Ru-complex CSP shows enantioselectivity to a wide variety of compounds when using CD detection. All the compounds showing selectivity in normal phase and reversed phase are listed in Table 2.3. In summary, 47 compounds were slightly separated in the reversed phase conditions, compared to 22 in the normal phase mode. Considering its broader selectivity, the reversed phase mode is more successful than the normal phase mode.

Table 2.3 Enantioselectivity of compounds observed by the circular dichroism (CD) detector

Normal phase		Reversed phase			
No.	Analyte structure	No.	Analyte structure	No.	Analyte structure
1		1		25	
2		2		26	
3		3		27	
4		4		28	
5		5		29	
6		6		30	
7		7		31	
8		8		32	
9		9		33	
10		10		34	
11		11		35	
12		12		36	
13		13		37	
14		14		38	
15		15		39	
16		16		40	

42

Table 2.3 Continued

17		17		41	
18		18		42	
19		19		43	
20		20		44	
21		21		45	
22		22		46	
		23		47	
		24			

2.4.3 Effect of mobile phase composition and temperature on enantioseparation.

In order to optimize enantioseparation on Ru complex-bonded stationary phase, effects of mobile phase compositions have been studied. In the normal phase mode, the concentration and nature of the alcohol modifier in the mobile phase affect the retention and selectivity of analyte.[116,117] Figure 2.8 shows effects of varying alcohol types. Five different alcohols were studied when the volume percentage of alcohols remained the same. Increasing alkyl chain length of primary and secondary alcohols enhances the retention, illustrated by comparison of ethanol, 1-propanol and 1-butanol, or comparison of isopropanol and 2-butanol. Using five alcohols, the enantioselectivities are different, ranging between 1.10 -1.21.
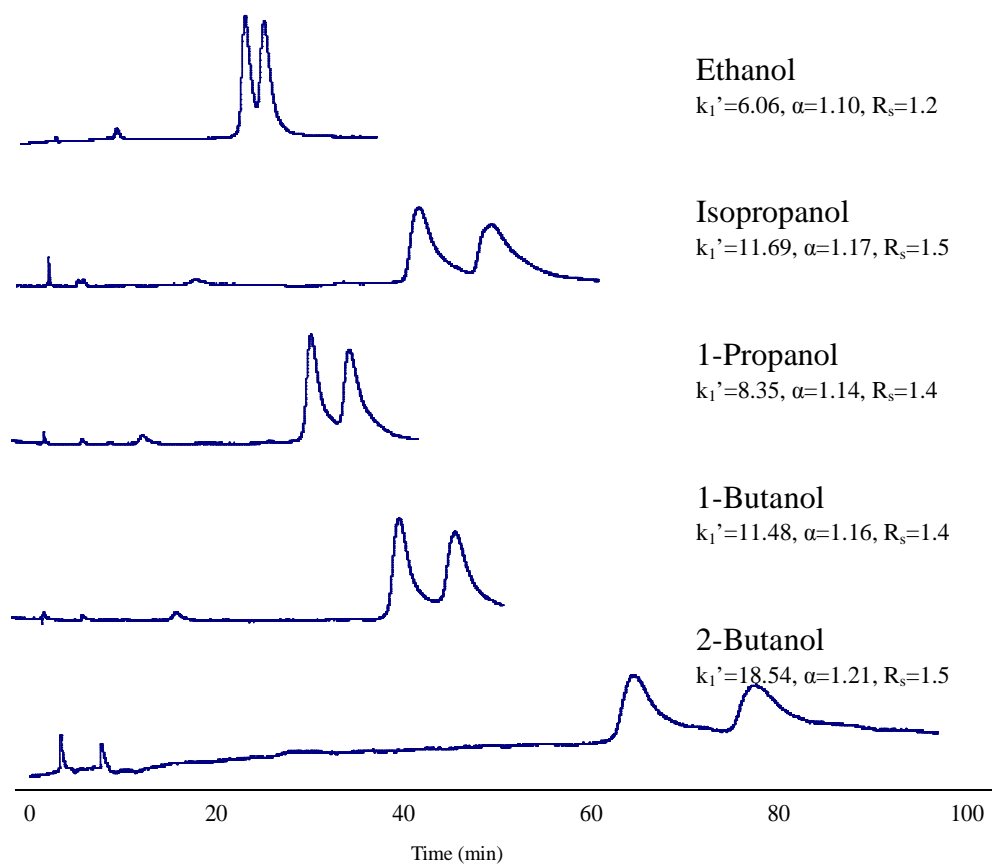
Figure 2.8 Effect of nature of alcohol on enantioseparations of 6,6'-dibromo-1,1'-bi-2-naphthol in the normal phase mode. The mobile phase is composed of 90%heptane/10%alcohol and all the other chromatographic conditions are kept the same.

The concentration of the alcohol modifier also affects enantioseparation greatly (results shown in Figure 2.9). The retention factor of the analyte increased from 1.60 to 16.59, when reducing ethanol percentage from 40% to 5%. The improvement in enantioresolution resulted from much longer retention, because selectivity remained unchanged.

44

40%Ethanol/60%Heptane

$k_1'=1.60$, $\alpha=1.06$, $R_s=0.7$

20%Ethanol/80%Heptane

$k_1'=3.98$, $\alpha=1.05$, $R_s=0.9$

5%Ethanol/95%Heptane
$k_1'=16.59$, $\alpha=1.06$, $R_s=1.3$

Time (min)
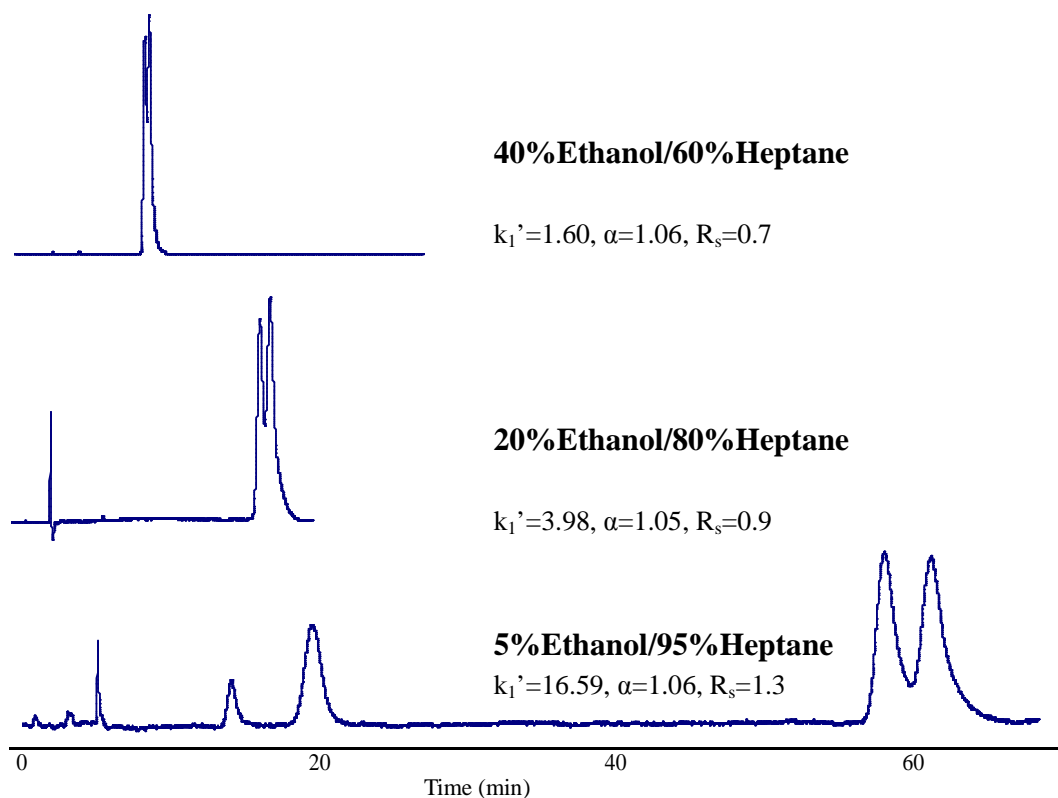
Figure 2.9 Effect of concentration of alcohol. The analyte and mobile phase are 6,6'-dibromo-1,1'-bi-2-naphthol.

In the polar organic mode, additives, such as acetic acid, triethylamine, and ammonium nitrate are often added. These additives in the mobile phase can usually shorten the retention time and improve chromatographic efficiency. In these studies, additives were necessary to elute acidic compounds by competing with analyte for strong binding sites. Different salts were tested as additives, while the salt concentration remained the same (12.5 mM). The chromatographic results are listed in Table 2.4 and it is evident that the type of salt addtive affects retention and resolution significantly. The highest selectivity and resolution were obtained with the mobile phase containing

45

ammonium nitrate. Furthermore, increasing the salt concentration was found to decrease retention (data not shown), which is a trend usually observed in the polar organic mode on other chiral stationary phases.

Table 2.4 Effect of salt type in the mobile phase on enantioseparation

Salt type	k_1'	$α$	Rs
NH_4NO_3	11.95	1.15	1.3
$N(CH_3)_4NO_3$	8.22	1.07	0.9
NH_4Cl	33.42	1.09	1.1
NH_4COOCF_3	12.76	1.09	1.2
NH_4COOCH_3	No elution		

In order to study the effect of temperature on enantioseparation of Ru complex-bonded CSP, a study of varying temperature between 0 ℃– 30 ℃ was carried out. Chromatograms at three specific temperatures are shown in Figure 2.10. When increasing temperature, enantioresolution decreases due to lower retention and selectivity. Resolution of chiral separation is often improved by lowering the column temperature.

a) **30 °C**
$k_1'=5.67, \alpha=1.09, R_s=0.9$

b) **15 °C**
$k_1'=7.19, \alpha=1.11, R_s=1.2$

c) **0 °C**
$k_1'=9.05, \alpha=1.14, R_s=1.4$

20   30   40

Time (min)
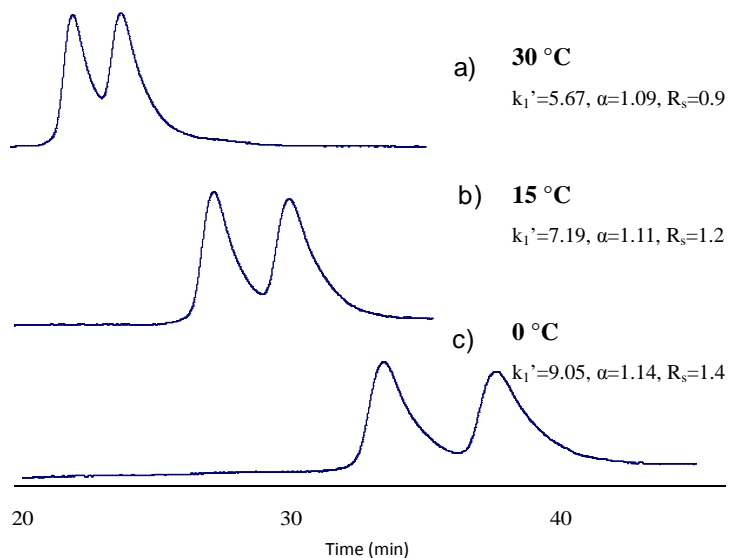
Figure 2.10 Effect of temperature on enantioresoluion of 6,6'-dibromo-1,1'-bi-2-naphthol at a) 30 ^{0}C, b)15 ^{0}C and c) 0 ^{0}C, The chromatographic conditions are the same as Figure 2.8.

2.5 Conclusions

Silica gel-based Ru complex-bonded chiral stationary phases have been developed for the first time. The best Ru-complex column was obtained using a reductive amination binding reaction and high surface area silica. Extensive liquid chromatographic studies with UV and CD detectors show Ru complex-bonded CSP provide enantioselectivity toward a wide variety of compounds, in particular, compounds with acidic groups. While the Ru complex-bonded CSP did not have high efficiency, the bonded phase is likely more robust than its coated predecessors. The development of the first transition metal complex-bonded chiral stationary phases and chromatographic studies provide insight concerning chiral stationary phase bonding strategies.

CHAPTER 3

EVALUATION OF AROMATIC-DERIVATIZED CYCLOFRUCTANS 6 AND 7 AS HPLC

CHIRAL SELECTORS

3.1 Abstract

The two best aromatic-functionalized cyclofrucan chiral stationary phases, R-naphthylethyl-carbamate cyclofructan 6 (RN-CF6) and dimethylphenyl-carbamate cyclofructan 7 (DMP-CF7), were synthesized and evaluated by injecting various classes of chiral analytes. They provided enantioselectivity toward a broad range of compounds, including chiral acids, amines, metal complexes, and neutral compounds. It is interesting that they exhibited complementary selectivities and the combination of two columns provided enantiomeric separations for 43% of the test analytes. These extensive chromatographic results provided useful information about method development of specific analytes, and also gave some insight as to the enantioseparation mechanism.

3.2 Introduction

In the past two and a half decades, enantiomeric separations have developed from a highly challenging method into a routine laboratory technique.[118] This is mainly because of the rapid development of a plethora of HPLC chiral stationary phases (CSPs). Given the large number and types of CSPs, method development for a specific enantiomeric compound can involve time-consuming screening of a large number of CSPs. Therefore, researchers continue to investigate new chiral stationary phases, in hopes of finding either a more universal column, which is widely effective for different classes of compounds, or columns with a well defined (and therefore predictable) selectivity.

48

Developing a new chiral selector with a broad range of enantioselectivies has been a challenge, and derivatization of a naturally-occurring molecule has proven to be a successful strategy, which can broaden the application range of the original chiral selector.[48,49,97,119-133] For example, aromatic derivatization (dimethylphenyl, R- and S-naphthylethyl, dinitrophenyl) of β-cyclodextrin greatly extended its utility in the normal phase mode.Native cellulose and amylose are known to be poor chiral selectors, while dimethylphenyl-substituted ones (Chiralpak AD and OD) are among the most widely useful CSPs.[123-126] Aided by additional π-π interactions and dipolar interactions, the aromatic-derivatized chiral selector may provide totally different mechanisms of chiral recognition, compared to the original one.

A new class of macrocyclic oligosaccharides, cyclofructans, has recently received considerable attention in the area of enantiomeric separations. Cyclofructans are composed of six or more β-(2→1) D-fructofuranose units, name as CF6, CF7, CF8, and etc.[134] They were first reported in 1989 and they have been used in a variety of industrial applications, such as moderators of food and drink bitterness and astringency, inhibitors for odor and taste of iron.[62-64] However, its application as a chiral selector for HPLC, CE and GC has been investigated only recently by our group.[66,135-137] Both LC and CE studies have demonstrated that native cyclofructan 6 (CF6) has limited capabilities for chiral recognition.[135,136] However, additional studies indicated that optimally derivatized-CF6 had considerable promise as a chiral selector.[66] By varying the nature and degree of substitution of the substituent(s), the functionalized cyclofructans could be "tuned" to separate different classes of molecules. While aliphatic-substituted CF6 has been thoroughly examined,[66] aromatic derivatives have not.

Therefore, the purpose of the present work is to examine the potential and overall chiral selectivities of aromatic-derivatized CF6 and CF7. In order to evaluate their

applicability, a large number of racemic compounds, including chiral acids, amines, metal complexes, and neutral compounds, were injected on the two best chiral stationary phases, R-naphthylethyl-carbamate CF6 (RN-CF6) and dimethylphenyl carbamate CF7 (DMP-CF7). Also, effects of the chiral selector structure on enantioseparations are discussed.

3.3 Experimental

3.3.1 Materials

Anhydrous toluene, anhydrous pyridine, trifluoroacetic acid (TFA), ammonium nitrate, 3-(triethoxysilyl)propyl isocyanate, 1,6-diisocyanatohexane, (3-aminopropyl)dimethylethoxysilane, R-1-(1-naphthyl)ethyl isocyanate, 3,5-dimethylphenyl isocyanate, and most of racemic analytes tested in this study were purchased from Sigma-Aldrich (Milwaukee, WI, USA). Ru(II) complexes were donated by Dr. Fred (Department of Chemistry and Biochemistry, the University of Texas at Arlington). CF6 was obtained by fermentation and crystallization as described previously.[138,139] CF7 was purified as reported previously.[140] Acetonitrile (ACN), isopropanol (IPA), heptane, ethanol (ETOH), and methanol (MEOH) of HPLC grade were obtained from EMD (Gibbstown, NJ). Water was obtained form Millipore (Billerica, MA). Kromasil and Daiso silica (5μm spherical diameter, 100 Å, 120 Å, 200 Å pore size) were obtained from Supelco (Bellefonte, PA). The aromatic-substituted CF6 and CF7 chiral stationary phases were synthesized, according to the previous paper.[136] Then it was slurry packed into a 25cm×0.46cm (i.d.) stainless steel column.

3.3.2 HPLC method

The chromatographic system used was an Agilent 1100 HPLC (Agilent Technologies, Palo Alto, CA, USA), consisting of a diode array detector, an autosampler, a binary pump and a temperature-controlled column chamber. For all HPLC experiments,

50

the injection volume and the flow rate were 5 μL, 1mL/min, respectively. The column temperature was 20 $^{\circ}$C, if not specified otherwise. The mobile phase was degassed by ultrasonication under vacuum for 5 min. The analytes were dissolved in ethanol, or the appropriate mobile phases. In the normal phase mode, heptane/ethanol (or isopropanol) with/without trifluoroactic acid was used as the mobile phase. The mobile phase of the polar organic mode was composed of acetonitrile/methanol with 0.2% ammonium nitrate (weight percentage).

For the calculation of retention factors (k_1, k_2), t_0 was determined by the peak of the refractive index change due to the sample solvent or by injecting 1,3,5-tri-*tert*-butylbenzene in the normal phase mode.

3.4 Results and Discussion

3.4.1 Screening chromatographic results of the RN-CF6 CSP and the DMP-CF7 CSP

Preliminary studies showed that aromatic functionalization of cyclofructans significantly broadened the application range of these CSPs.[136] Therefore, different aromatic-substitution groups on cyclofructan6 (CF6) and cyclofructan7 (CF7), including dimethylphenyl, methylphenyl, naphthylethyl, dichlorophenyl, and chlorophenyl, were tested. It was found that two of these CSPs provided the best performance and they showed the broadest selectivity for the tested racemic analytes. They are the R-naphthylethyl-carbamate CF6 (RN-CF6) and dimethylphenyl-carbamate CF7 (DMP-CF7). It was also found that better selectivity and resolution were often obtained in the normal phase mode on the aromatic functionalized cyclofructan stationary phases.[136] Therefore, the current study focuses on a systematic chromatographic evaluation of the RN-CF6 and DMP-CF7 stationary phases, mainly in the normal phase mode.

A set of 220 racemic compounds with various functionalities were used to evaluate these two columns. Racemic analytes were divided into five groups: acids,

amines (including primary, secondary and tertiary amines), alcohols, ruthenium complexes, and other neutral compounds. It was reported that enantiomers of ruthenium complexes were quickly separated with high selectivities by the R-naphthylethyl β-cyclodextrin column (Cyclobond RN),[107] which is closely related to the structure of the RN-CF6 stationary phase. Therefore, these Ru(II) complexes were tested in order to compare the performance of cyclofructan- and cyclodextrin-based stationary phases. Earlier studies indicated that the RN-CF6 CSP provided enantioselectivities for a few unique primary amines, which the isopropyl-CF6 column could not easily separate.[66] Therefore, in this study, several primary-amine containing compounds (grouped into "amines") were selected to investigate the capability of CF6- and CF7-based CSPs for separating primary amines.

Table 3.1 lists the chromatographic data for all compounds separated by the RN-CF6 and DMP-CF7 CSPs. The chromatographic data include retention factor (k_1), selectivity (α), and resolution (Rs). In the case of Ru complexes (group D in Table 3.1), it was necessary to use the polar organic mode plus salt addition (such as ammonium nitrate) to obtain elution in a reasonable time.Optimized separations of all other compounds were achieved in the normal phase mode. The chromatograms in Figure 3.1 (20 ˚C vs 0 ˚C) demonstrate effects of temperature on these enantioseparations. The selectivity of separating 4-chlorophenyl 2,3-epoxypropyl ether was improved from 1.07 to 1.12 when decreasing the column temperature. Usually, decreasing the column temperature increases enantioselectivity, retention, and resolution. Therefore, decreasing the column temperate to 0 ˚C can be an effective strategy during the optimization process.

Table 3.1 Summary of optimized chromatographic data achieved on RN-CF6 and DMP-CF7 CSPs
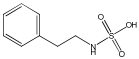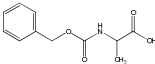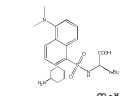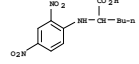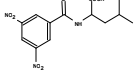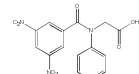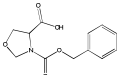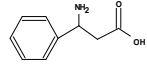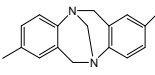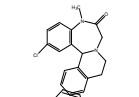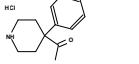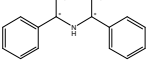
#	Compound name	Structure	CSP	k_1	α	Rs	Mobile phase[a]
A. Chiral acids							
1	Phenethylsulfamic acid		RN-CF6	1.52	1.20	1.6	60H40E0.1TFA
2	Carbobenzyloxy alanine		DMP-CF7	9.10	1.10	1.7	95H5E0.1TFA0C
3	Dansyl-norleucine cyclohexylammonium salt		DMP-CF7	2.42	2.03	8.6	80H20E0.1TFA
4	N-2,4-DNP-DL-norleucine		DMP-CF7	9.93	1.10	1.5	95H5E0.1TFA
5	N-(3,5-dinitrobenzoyl)-DL-leucine		RN-CF6	0.84	1.49	4.5	50H50E0.1TFA
			DMP-CF7	16.90	1.13	3.0	95H5E0.1TFA
6	N-(3,5-Dinitrobenzoyl)-DL-phenylglycine		RN-CF6	2.50	1.16	2.2	50H50E0.1TFA
			DMP-CF7	21.66	1.07	0.8	95H5E0.1TFA
7	3-(Benzyloxycarbonyl)-4-oxazolidinecarboxylic acid		DMP-CF7	4.11	1.05	0.9	95H5E0.1TFA
8	DL-3-Amino-3-phenylpropionic acid		DMP-CF7	8.25	1.04	0.7	80H20E0.1TFA
B. Amines							
1	Tröger's base		RN-CF6	0.79	1.50	5.2	70H30E
			DMP-CF7	3.19	1.29	3.7	80H20E0.1TFA
2	2-Chloro-5,9,10,14B-tetrahydro-5-Me-isoquino(2,1-d)(1,4)benzodiazepin-6(7H)-one		RN-CF6	2.58	1.02	0.4	60H40E0.1TFA
3	4-Acetyl-4-phenylpiperidine hydrochloride		DMP-CF7	5.14	1.05	0.7	80H20E0.1TFA
4	Bis-[(R/S)-1-phenylethyl] amine hydrochloride		RN-CF6	3.59	1.15	2.4	90H10E0.1TFA

Table 3.1 Continued
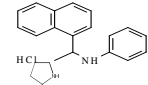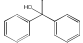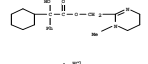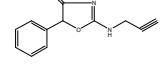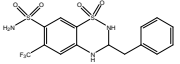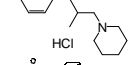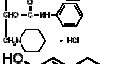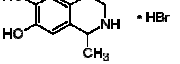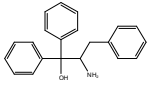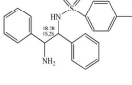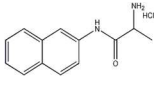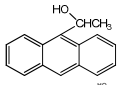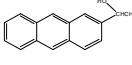
5	N-Benzyl-1-(1-naphthyl) ethylamine hydrochloride		RN-CF6	8.92	1.02	0.6	95H5E0.1TFA
6	α,α-Diphenylprolinol		RN-CF6	15.03	1.12	1.7	90H10E0.1TFA
7	Oxyphencyclimine hydrochloride		RN-CF6	13.68	1.12	1.5	60H40E0.1TFA
8	5-Phenyl-2-(2-propynyl-amino)-2-oxazolin-4-one		DMP-CF7	5.21	1.08	1.5	80H20E0.1TFA
9	Bendroflumethiazide		RN-CF6	1.81	1.16	2.0	60H40E0.1TFA
10	Tolperisone hydrochloride		RN-CF6	5.52	1.12	1.8	70H30E0.1TFA
11	Diperodon hydrochloride		RN-CF6	7.42	1.11	1.2	70H30E0.1TFA
12	1-Methyl-6,7-dihydroxy-1,2,3,4-tetrahydroisoquinoline hydrobromide		RN-CF6	4.33	1.17	2.0	60H40E0.1TFA
			DMP-CF7	12.12	1.05	0.6	80H20E0.1TFA
13	2-Amino-1,1,3-triphenyl-1-propanol		RN-CF6	3.40	1.10	1.5	80H20E0.1TFA
			DMP-CF7	3.12	1.02	0.5	80H20E0.1TFA
14	N-p-Tosyl-1,2-diphenylethylenediamine		RN-CF6	8.28	1.24	2.9	80H20E0.1TFA
			DMP-CF7	5.43	1.13	1.4	80H20E0.1TFA
15	DL-alanine-β-naphthylamide hydrochloride		RN-CF6	10.03	1.10	1.5	80H20E0.1TFA

C. Alcohols

1	α-Methyl-9-anthracenemethanol		RN-CF6	11.30	1.06	1.3	99H1I0.1TFA0C
2	1-Anthracen-2-yl-ethanol		DMP-CF7	14.59	1.05	1.0	99H1E

54

Table 3.1 Continued
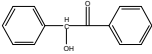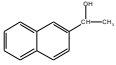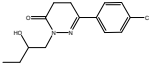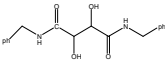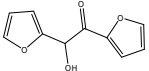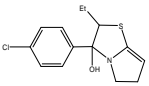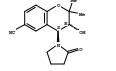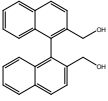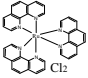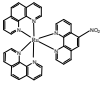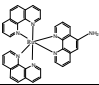
3	Benzoin		RN-CF6	9.30	1.06	1.5	99H1I0.1TFA0C
			DMP-CF7	7.79	1.09	1.5	99H1E
4	α-Methyl-2-naphthalenemethanol		DMP-CF7	9.90	1.02	0.5	99H1E
5	6-(4-chlorophenyl)-4,5-dihydro-2-(2-hydroxybutyl)-3(2H)-pyridazinone		DMP-CF7	13.63	1.03	0.6	95H5E0.1TFA
6	N,N'-Dibenzyl-tartramide		RN-CF6	8.21	1.04	0.9	90H10E0.1TFA
			DMP-CF7	22.76	1.03	0.8	95H5E0.1TFA
7	Furoin		RN-CF6	5.24	1.02	0.5	90H10E0.1TFA
			DMP-CF7	17.46	1.04	0.7	98H2E0.1TFA
8	3-(4-Chlorophenyl)-2-ethyl-2,3,5,6-tetrahydroimidazol[2,1-b]-thiazol-3-ol		DMP-CF7	5.05	1.10	0.7	80H20E0.1TFA
9	Cromakalim		DMP-CF7	17.24	1.08	1.5	95H5E0.1TFA
10	1,1'-Binaphthyl-2,2'-dimethanol		RN-CF6	6.37	1.02	0.6	95H5E0.1TFA
			DMP-CF7	7.44	1.05	0.7	80H20E0.1TFA

D. Ru(II) complexes

1	[Ru(phen)$_3$](Cl$_2$)		RN-CF6	0.62	1.49	3.8	60M/40A/0.2 NH$_4$NO$_3$[b]
			DMP-CF7	3.81	1.14	1.3	80M/20A/0.2 NH$_4$NO$_3$
2	[Ru(phen)$_2$nitrophen](Cl$_2$)		RN-CF6	0.46	1.65	4.1	60M/40A/0.2 NH$_4$NO$_3$
			DMP-CF7	3.52	1.25	1.8	80M/20A/0.2 NH$_4$NO$_3$
3	[Ru(phen)$_2$aminophen](Cl$_2$)		RN-CF6	0.54	1.53	3.9	60M/40A/0.2 NH$_4$NO$_3$

Table 3.1 Continued
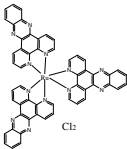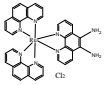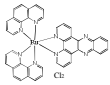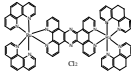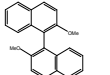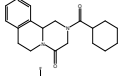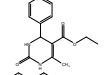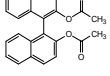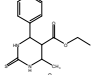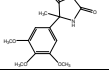
		DMP-CF7	2.81	1.15	1.3	80M/20A/0.2 NH_4NO_3
4	[Ru(dppz)$_3$](Cl$_2$)	RN-CF6	0.78	2.90	11.4	60M/40A/0.2 NH_4NO_3
		DMP-CF7	2.63	1.44	2.7	80M/20A/0.2 NH_4NO_3
5	[Ru(phen)$_2$phendiamine] (Cl$_2$)	RN-CF6	0.59	1.51	3.3	60M/40A/0.2 NH_4NO_3
		DMP-CF7	4.02	1.16	1.2	80M/20A/0.2 NH_4NO_3
6	[Ru(phen)$_2$dppz](Cl$_2$)	RN-CF6	0.67	1.80	5.8	60M/40A/0.2 NH_4NO_3
		DMP-CF7	6.25	1.32	2.2	80M/20A/0.2 NH_4NO_3
7	[Ru$_2$(phen)$_4$(tpphz)](Cl$_4$)	RN-CF6	2.24	2.67	6.9	60M/40A/0.2 NH_4NO_3
		DMP-CF7	16.24	1.30	0.9	80M/20A/0.2 NH_4NO_3

E. Others

1	2,2'-Dimethoxyl-1,1'-binaphthyl	RN-CF6	6.20	1.02	0.5	95H5E0.1TFA
2	Praziquantel	RN-CF6	9.69	1.05	1.0	95H5E0.1TFA
3	4-(4-Fluoro-phenyl)-6-methyl-2-oxo-1,2,3,4-tetrahydro pyrimidine-5-carboxylic acid ethyl ester	DMP-CF7	14.85	1.12	2.6	95H5E0.1TFA
4	1,1'-Bi(2-naphthyl diacetate)	RN-CF6	0.83	1.12	1.5	70H30E0.1TFA
		DMP-CF7	4.18	1.13	2.2	99H1E
5	N-2'-Acetylamino-[1,1']binaphthalenyl-2-yl)-acetamide	DMP-CF7	23.45	1.04	0.9	95H5E0.1TFA
6	6-Methyl-4-phenyl-2-thioxo-1,2,3,4-tetrahydro-pyrimidine-5-carboxylic acid ethyl ester	DMP-CF7	12.92	1.11	1.5	98H2E0.1TFA
7	5-Methyl-5-(3,4,5-trimethoxyphenyl)hydantoin	RN-CF6	13.08	1.04	1.1	90H10E0.1TFA

Table 3.1 Continued
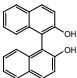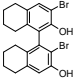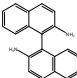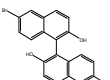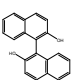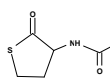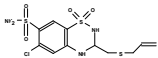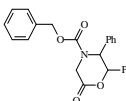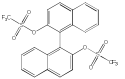
#	Name	Structure	Column				
			DMP-CF7	13.36	1.05	1.5	90H10E0.1TFA
8	5,5',6,6',7,7',8,8'-Octahydro(1,1'-binaphthalene)-2,2'-diol		RN-CF6	6.80	1.20	4.9	99H1I0.1TFA
			DMP-CF7	5.13	1.05	0.7	80H20E0.1TFA
9	3,3'-Dibromo-5,5',6,6',7,7',8,8'-octahydro(1,1'-binaphthalene)-2,2'-diol		RN-CF6	4.89	1.28	5.2	99H1I0.1TFA
			DMP-CF7	5.13	1.04	0.7	80H20E0.1TFA
10	2,2'-Diamino-1,1'-binaphthalene		RN-CF6	2.03	1.18	2.7	70H30E
			DMP-CF7	4.36	1.48	5.0	80H20E0.1TFA
11	6,6'-Dibromo-1,1'-bi-2-naphthol		RN-CF6	3.67	1.11	2.3	90H10E0.1TFA
			DMP-CF7	3.70	1.17	2.6	90H10E0.1TFA
12	1,1'-Bi-2-naphthol		RN-CF6	3.33	1.07	1.7	90H10E0.1TFA
			DMP-CF7	3.91	1.23	5.0	90H10E0.1TFA
13	DL-N-Acetylhomocysteine thiolactone		RN-CF6	12.08	1.03	0.8	90H10E0.1TFA
14	Althiazide		RN-CF6	3.04	1.20	2.7	60H40E0.1TFA
			DMP-CF7	12.42	1.09	1.5	80H20E0.1TFA
15	Benzyl-6-oxo-2,3-diphenyl-4-morpholine carboxylate		RN-CF6	7.08	1.05	1.6	95H5E0.1TFA
			DMP-CF7	6.26	1.06	1.5	95H5E0.1TFA
16	1.1'-Bi-2-naphthol bis(trifluoromethanesulfonate)		RN-CF6	7.80	1.07	1.2	100HEP0C

Table 3.1 Continued
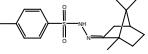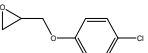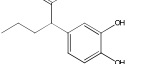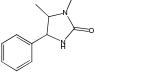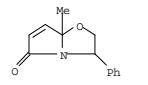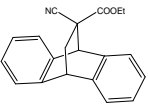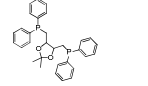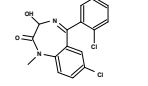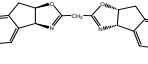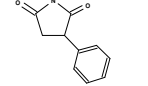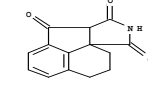
17	Camphor p-tosyl hydrazon		DMP-CF7	7.53	1.18	3.4	95H5E0.1TFA
18	4-Chlorophenyl 2,3-epoxypropyl ether		DMP-CF7	2.52	1.12	1.9	95H5E0.1TFA0C
19	3,4-dihydroxyphenyl-alfa-propylacetamide		DMP-CF7	6.15	1.06	1.0	80H20E0.1TFA
20	1,5-Dimethyl-4-phenyl-2-imidazolidinone		RN-CF6	11.17	1.06	1.5	95H5I0.1TFA
			DMP-CF7	11.10	1.07	1.5	95H5E0.1TFA
21	2,3-Dihydro-7a-methyl-3-phenylpyrrolo[2,1-b]oxazol-5(7aH)-one		RN-CF6	2.19	1.15	2.1	90H10E0.1TFA
			DMP-CF7	8.26	1.07	1.6	99H1E
22	Ethyl 11-cyano-9,10-dihydro-endo-9,10 - ethanoanthracene-11-carboxylate		RN-CF6	3.07	1.08	1.7	99H1E0.1TFA
			DMP-CF7	1.94	1.57	5.2	95H5E0.1TFA
23	2,3-O-Isopropylidene 2,3-dihydroxy-1,4-bis(disphenylphosphino)butane		RN-CF6	10.89	1.05	0.8	90H10E0.1TFA
			DMP-CF7	5.80	1.02	0.5	80H20E0.1TFA
24	Lormetazepam		RN-CF6	9.57	1.04	0.8	90H10E0.1TFA
25	[3aS/R-[2(3'aR*,8'aS*),3'aα/β, 8'aα/β]] -(-)-2,2'-Methylenebis [3a,8a-dihydro-8H-indeno[1,2-d]oxazole]		RN-CF6	9.84	1.21	1.2	70H30E0.1TFA
26	Phensuximide		RN-CF6	6.12	1.05	1.5	95H5E0.1TFA
			DMP-CF7	15.98	1.09	1.2	98H2E0.1TFA
27	3a,4,5,6-Tetrahydro-succininido[3,4-b]acenaphthen-10-one		RN-CF6	4.31	1.08	1.5	80H20E0.1TFA
			DMP-CF7	12.60	1.10	2.1	90H10E0.1TFA

58

Table 3.1 Continued
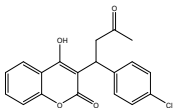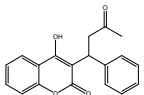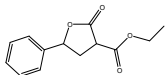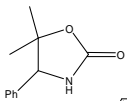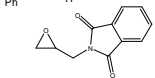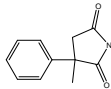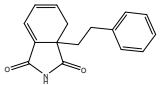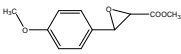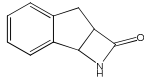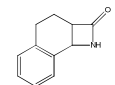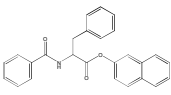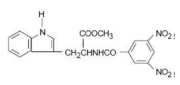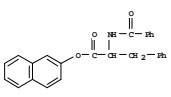
28	3-(α-Acetonyl-4-chlorobenzyl)-4-hydroxycoumarin		RN-CF6	11.54	1.10	1.8	95H5E0.1TFA
			DMP-CF7	12.16	1.30	4.5	95H5E0.1TFA
29	Warfarin		RN-CF6	12.20	1.10	1.9	95H5I0.1TFA
			DMP-CF7	11.54	1.17	2.6	95H5E0.1TFA
30	2-Carbethoxy-gamma-phenyl-gamma-butyrolactone		RN-CF6	12.79	1.09	1.0	99H1I0.1TFA0C
			DMP-CF7	11.79	1.12	2.4	98H2E0.1TFA0C
31	5,5-dimethyl-4-phenyl-2-oxazolidinone		DMP-CF7	8.26	1.08	1.8	95H5E0.1TFA
32	N-(2,3-Epoxypropyl)-phthalimide		DMP-CF7	14.59	1.08	1.7	98H2E0.1TFA
33	α-Methyl-alpha-phenyl-succinimide		RN-CF6	10.28	1.05	1.5	95H5E0.1TFA0C
			DMP-CF7	9.77	1.09	2.0	95H5E0.1TFA
34	Phenethylphthalimide		RN-CF6	4.07	1.08	1.3	99H1I0.1TFA0C
			DMP-CF7	3.82	1.25	3.2	99H1E
35	Methyl trans-3-(4-methoxyphenyl)glycidate		RN-CF6	7.22	1.02	0.6	90H10E0.1TFA
			DMP-CF7	14.07	1.09	1.9	95H5E0.1TFA
36	cis-3,4-benzo-6-azabicyclo[3.2.0]heptan-7-one		RN-CF6	5.31	1.07	1.5	90H10E0.1TFA0C
			DMP-CF7	22.03	1.04	0.8	98H2E0.1TFA
37	cis-4,5-benzo-7-azabicyclo[4.2.0]octan-8-one		RN-CF6	8.27	1.05	1.3	95H5E0.1TFA0C

Table 3.1 Continued

			DMP-CF7	17.70	1.03	0.6	98H2E0.1TFA
38	Fipronil		RN-CF6	17.42	1.07	1.7	98H2E0.1TFA0C
39	5-Methyl-5-phenyl hydantoin		DMP-CF7	14.73	1.16	5.0	95H5E0.1TFA
40	trans-Stilbene oxide		RN-CF6	1.70	1.05	1.1	100HEP0C
41	Thalidomide		RN-CF6	12.65	1.05	1.1	80H20E0.1TFA
42	3,5-DNB-2-aminoheptane		RN-CF6	0.86	1.13	1.5	70H30E0.1TFA
43	3,5-Dinitro-N-(1-phenylethyl)benzamide		RN-CF6	0.96	2.05	9.8	50H50E0.1TFA
44	4-Phenyl-2-oxazolidinone		DMP-CF7	7.12	1.05	1.0	90H10E0.1TFA
45	4-Phenylthiazolidine-2-thione		RN-CF6	13.27	1.04	1.3	95H5E0.1TFA0C
46	4-Benzyloxazolidine-2-thione		RN-CF6	6.98	1.02	0.5	90H10E0.1TFA
			DMP-CF7	6.90	1.15	2.9	90H10E0.1TFA
47	4-Benzylthiazolidine-2-thione		DMP-CF7	4.25	1.09	1.9	90H10E0.1TFA
48	4-Benzyl-5,5-dimethyl-2-oxazolidinone		RN-CF6	7.06	1.02	0.6	90H10E0.1TFA
49	4-Benzyl-3-chloroacetyl-2-oxazolidinone		RN-CF6	3.73	1.02	0.5	90H10E0.1TFA
50	4-Isopropylthiazolidine-2-thione		DMP-CF7	5.65	1.08	1.8	95H5E0.1TFA
51	cis-4,5-Diphenyl-2-oxazolidinone		RN-CF6	14.80	1.05	1.5	95H5E0.1TFA0C
			DMP-CF7	13.63	1.09	1.9	95H5E0.1TFA

Table 3.1 Continued

52	N-Benzoyl-DL-phenylalanine beta-naphthyl ester		RN-CF6	5.92	1.06	0.5	90H10E0.1TFA0C
			DMP-CF7	14.80	1.08	1.5	95H5E0.1TFA0C
53	3,5-DNB-Tryptophan methyl ester		RN-CF6	5.52	1.12	1.8	70H30E0.1TFA
			DMP-CF7	5.75	1.14	5.0	80H20E0.1TFA
54	N-Benzoyl-DL-phenylalanine beta-naphthyl ester		DMP-CF7	8.52	1.06	1.1	95H5E0.1TFA

a) Abbreviation:Mobile phases: H: heptane; I: isopropanol; E: ethanol; A: acetonitrile; M: methanol; TFA: trifluoroacetic acid.OC: the column temperature is 0 ˚C.
(b) 0.2% NH_4NO_3 is the weight percentage.

a) **20 ºC**
kı'=1.78, α =1.07
Rs =1.3

b) **0 ºC**
k_1'=2.52, α =1.12
R_s=1.9
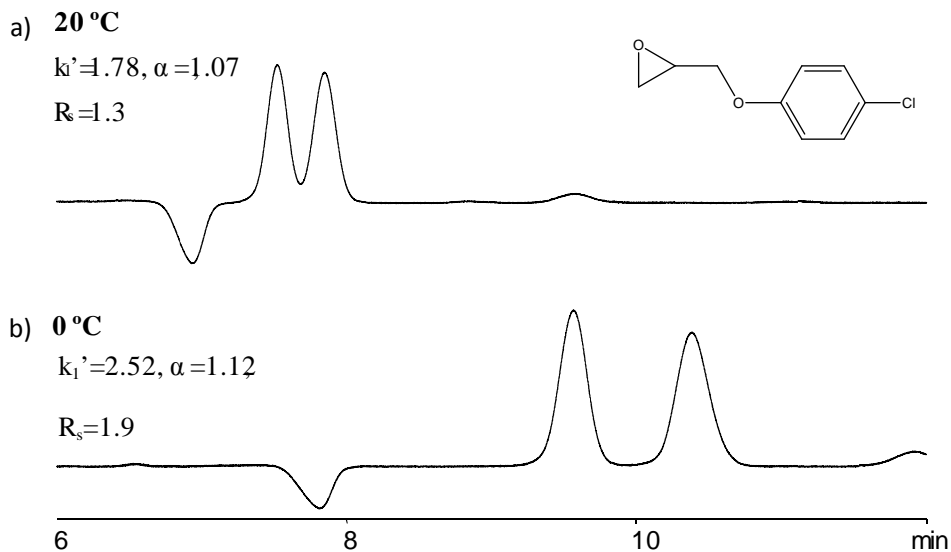
Figure 3.1 Effects of the column temperature a) 20 ^{0}C and b) 0 ^{0}C on enantioseparations by the DMP-CF7 CSP. The analyte and mobile phase are 4-chlorophenyl 2,3-epoxypropyl ether and 95Hep5EtOH0.1TFA, respectively.

The data in Table 3.1 indicates that the number of separations for each class of analyte obtained on two columns is 8, 15, 10, 7, 54, respectively. The total number of separations achieved on the combination of RN-CF6 and DMP-CF7 are 94. Enantiomers of 63 compounds out of 94 were baseline separated. 43% of the tested compounds, which were randomly chosen, were separated on these two CSPs. The representative chromatograms of a chiral acid, secondary amine, tertiary amine, alcohol, Ru(II) complex, and a neutral compound, are shown in Figure 3.2.

a) Acid b) Secondary amine

c) Tertiary amine d) Alcohol

e) Ru(II) complex f) Other type
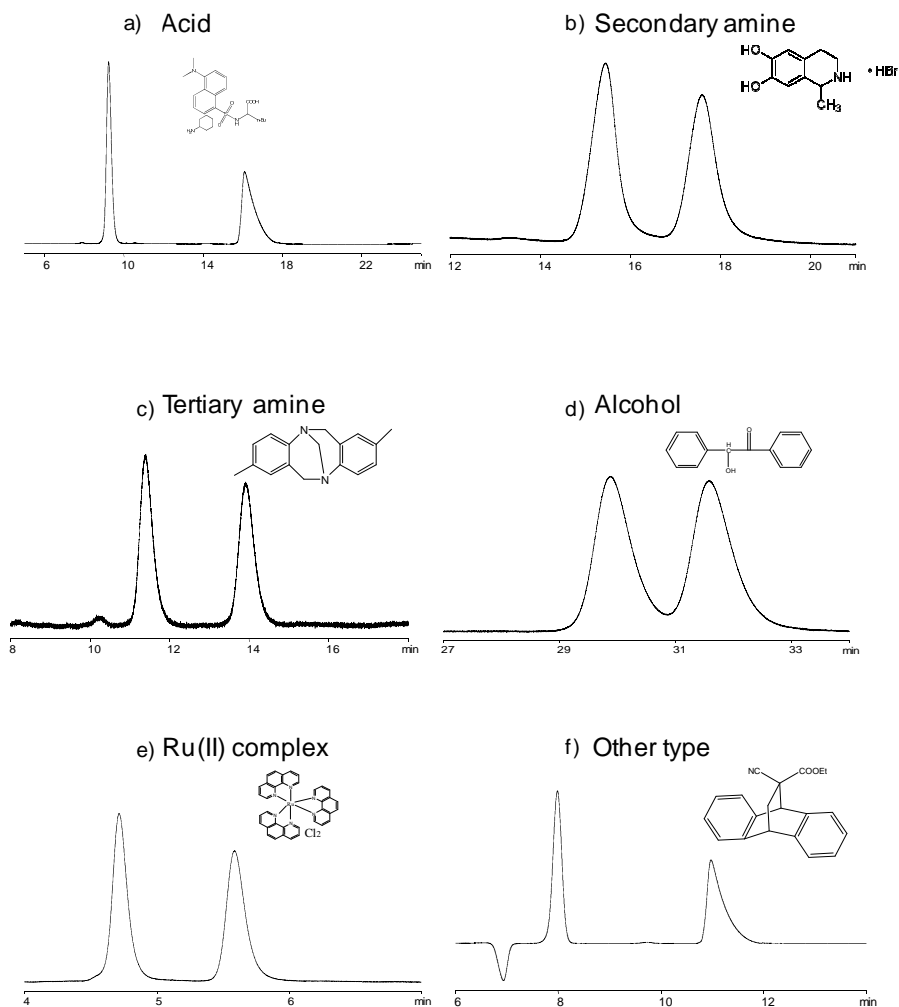
Figure 3.2 Representative chromatograms showing enantioseparations of various types of compounds. The analytes, stationary phases, and d mobile phases are: (a) Dansyl-norleucine cyclohexylammonium salt, DMP-CF7, 80H20E0.1TFA; (b) 1-Methyl-6,7-dihydroxy-1,2,3,4-tetrahydroisoquinoline hydrobromide, RN-CF6, 60H40E0.1TFA; (c) Tröger's base, DMP-CF7, 80H20E0.1TFA; (d) Benzoin, RN-CF6, 99H1I0.1TFA (0˚C); (e) [Ru(phen)$_3$]Cl$_2$, RN-CF6, 60M/40A/0.2 NH$_4$NO$_3$; (f) Ethyl 11-cyano-9,10-dihydro-endo-9,10 - ethanoanthracene-11-carboxylate, DMP-CF7, 95H5E0.1TFA.

The data in Table 3.1 and Figure 3.2 indicates that the RN-CF6 and DMP-CF7

CSPs provide excellent enantioselectivity toward a wide range of analytes. Compared to

native CF6 and CF7, their capabilities for chiral recognition were significantly improved.

63

This can be explained by the fact that derivatization of native cyclofructans effectively disrupts internal hydrogen bonding, relaxing (denaturing) the molecule and exposing its entire surface.[66,136] In addition, the presence of the aromatic and carbonyl groups provide ample opportunities for π-π interactions and dipolar interactions, as well as additional steric interaction sites. These are the type of interactions that play a pronounced role in chiral recognition in nonpolar solvents (the normal phase mode) rather than in polar solvents. It should be also noted that the CF-based chiral stationary phases were very robust and not irreversibly altered when changing from one mobile phase mode to another. The cyclofructan-bonded CSPs did not show a detectable deterioration in the separation performance after extensive use (~ 1000 injections in six months).

These results also indicate that the performance of cyclofructan stationary phases was significantly different from other known crown-ether based CSPs, although cyclofructans also contain crown-ether cores. CF-based CSPs provided chiral recognition toward a variety of compounds in the normal phase mode, while other known crown-ether CSPs show limited selectivity except for primary amines and they are preferably used with acidic aqueous mobile phases.[45,141-144]

3.4.2 Complementary selectivity provided by RN-CF6 and DMP-CF7

Figure 3.3 summarizes the separations obtained on the RN-CF6 CSP, the DMP-CF7 CSP and a combination of the two columns. The total number of separations achieved on the RN-CF6 CSP and the DMP-CF7 CSP are 69, and 69, respectively. Of these, there were 43 baseline separations on the RN-CF6 column and 41 on the DMP-CF7 column. Enantiomers of 25 compounds were separated only by the RN-CF6 CSP, while another 25 were separated only with the DMP-CF7 CSP. It was often observed that some analytes were baseline separated on the RN-CF6 column, while only a partial separation or no separation was observed on the DMP-CF7 CSP, and vice versa.

Therefore, the RN-CF6 and DMP-CF7 CSPs demonstrated complementary enantioselectivities.
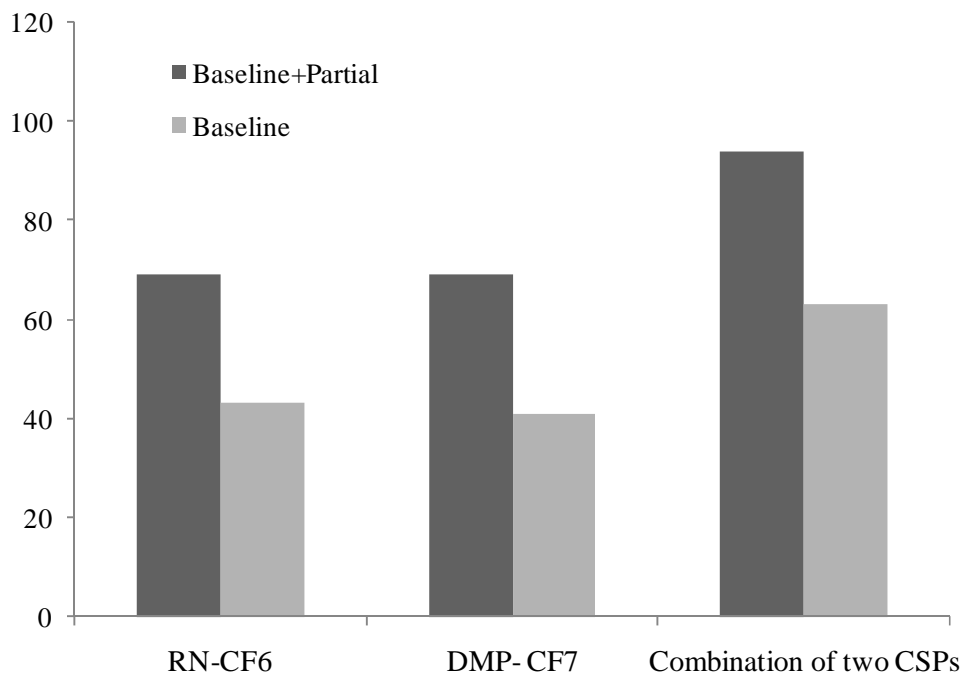
Figure 3.3 Summary of enantioseparations obtained on RN-CF6 and DMP-CF7 based chiral stationary phases.

Figure 3.4 gives two examples of the complementary selectivity provided by these columns. Enantiomers of bendroflumethiazide were baseline separated with the RN-CF6 CSP with a high selectivity (α=1.16) while no separation was observed on the DMP-CF7 CSP (Fig.4a). The RN-CF6 column gave a partial separation of 4-benzyloxazolidine-2-thione with a tiny shoulder (α=1.02) while the DMP-CF7 column provided high selectivity (α=1.15) and a baseline separation (Fig.4a).
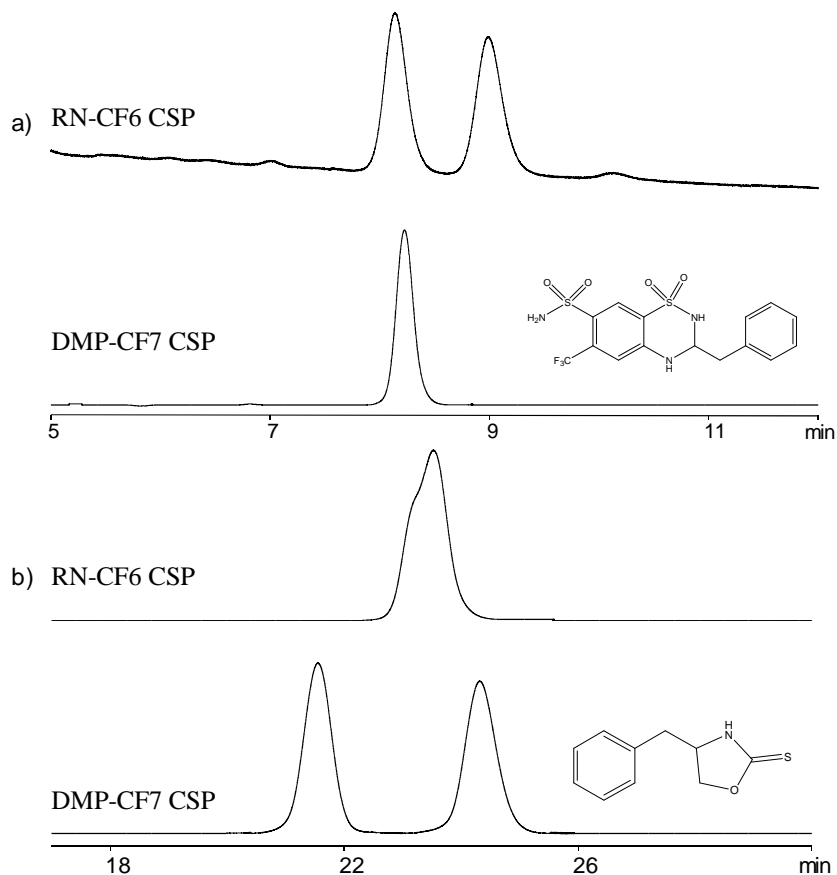
Figure 3.4 Comparison between RN-CF6 and DMP-CF7 stationary phases. The analyte and mobile phase are a) bendroflumethiazide, 60heptane/40ethanol/0.1TFA; b) 4-benzyloxazolidine-2-thione, 90heptane/10ethanol/0.1TFA.

Although the overall success rates of the RN-CF6 and DMP-CF7 CSPs are the same (31%), their capabilities for chiral recognition for various classes of compounds are different. For example, only 2 out of 8 in group A (chiral acids), 4 out of 15 in group B (amines), and 4 out of 10 in group C (alcohols) were separated by both columns. The others compounds (over 60%) in these three groups were only separated by one column (either the RN-CF6 or the DMP-CF7 CSP). However, for group E (others), these two stationary phases shared a bigger overlap and about 50% analytes in group E (Table 3.1)

were separated by both columns. For Ru complexes (group D), both columns provided enantiomeric separation, although the RN-CF6 CSP gave a much higher selectivity than the DMP-CF7 CSP.

Considering the success rate of two columns for different groups of compounds, the DMP-CF7 CSP obtained greater success than the RN-CF6 CSP when separating chiral acids, based on the fact that 8 analytes were separated by the DMP-CF7 CSP compared to 3 by the RN-CF6 CSP. It was also found that the RN-CF6 CSP provided a higher enantioselectivity toward chiral amines (group B) than the DMP-CF7 CSP in most of cases. The characteristic that the RN-CF6 and DMP-CF7 columns offered complementary selectivities for different groups of compounds is advantageous when selecting columns for separating a large number of different compounds.

3.4.3 Effects of the size of the cyclofructan ring, i. e., CF6 vs CF7 on enantioseparations

The effects of the size of the central crown ether core (i. e., 18-crown-6 vs 21-crown-7) in CF6 and CF7 can be examined by comparing DMP-CF6 (data shown in ref.[136]) and DMP-CF7 as LC chiral selectors. The capabilities of chiral recognition provided by DMP-CF6 and DMP-CF7 CSPs are quite different. The DMP-CF7 column provided significantly different resolution for over 60 % of analytes separated by the DMP-CF6 CSP. Generally, the DMP-CF7 CSP gave better performance than the DMP-CF6 CSP for separating acidic and neutral analytes. For example, enantiomers of dansyl-norleucine cyclohexylammonium salt were well separated with an extremely high selectivity (α=2.03) by the DMP-CF7 CSP while only a partial separation was obtained on the DMP-CF6 CSP (shown in Figure 3.5). For amine containing compounds, the DMP-CF6 column gave higher selectivity than the larger DMP-CF7 based CSP. Also, this was true for all derivatized-CF6 stationary phases and respective CF7 columns. Therefore,

the size of the cyclofructan ring plays a significant role in interactions between amine containing analytes and the chiral selector.
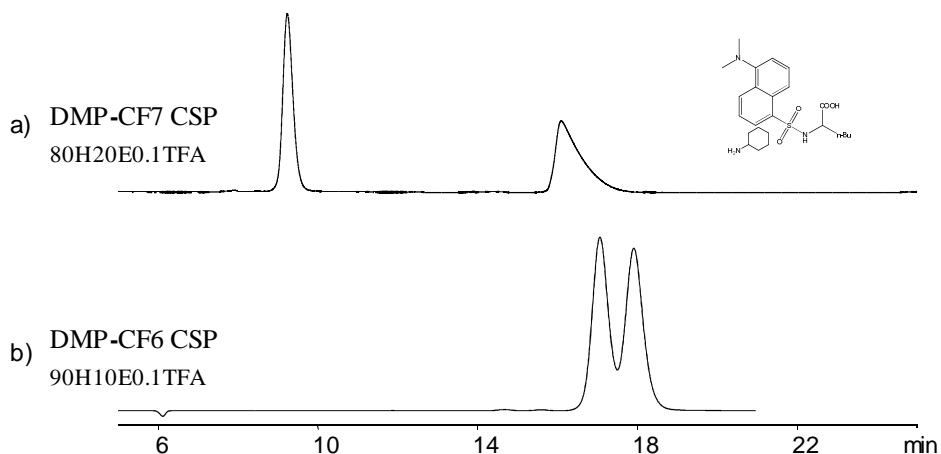
Figure 3.5 Comparison between a) DMP-CF6 and b) DMP-CF7 CSPs. The analyte is dansyl-norleucine cyclohexylammonium salt.

The selectivity of the RN-CF6 and RN-CF7 stationary phases also were compared. The relative performance of the RN-CF6 and RN-CF7 CSPs was opposite to that found for the DMP functionalized cyclofructans. Indeed, it was the smaller RN-CF6 CSP that usually provided better resolution than the larger RN-CF7 CSP. Also, it is noted that the chromatographic differences between the RN-CF6 and RN-CF7 CSPs are much smaller compared to the more substantial difference between the DMP-CF6 and DMP-CF7 columns.

The difference between CF6 and CF7 is the central crown ether size and the number of available hydroxyl groups. Although CF6 and CF7 differ only by one fructose unit, their spatial structures are quite different according to computational modeling studies.[145] Also, the separation of CF6 and CF7 on a HILIC stationary phase showed that their number of available hydroxyl groups was quite different.[140] There is a much bigger difference in the separation of CF6 and CF7, than is found for the comparable separation

of α-, β-, and γ-cyclodextrin. This may be due to the extensive internal hydrogen bonding of cyclofructans.[140]

Currently, there is no reported crystal structure of CF7 and it is difficult to give more detailed explanations about the chromatographic differences between CF6 and CF7-based stationary phases without further study. However, the chromatographic results clearly indicated that the size and geometry of cyclofructan is an important factor in interactions between cyclofructans and chiral analytes.

3.4.4 Effects of the nature of the derivatization group on enantioseparations

The nature of the derivatization group also contributes to chiral recognition. Our earlier studies of various aliphatic- and aromatic-derivatized CF6 stationary phases support this contention.[136] The nature of the aromatic group plays an important role since the derivatizing groups change the interactions between analyte and stationary phase (i.e., steric repulsion, π-π interaction, dipolar interactions, etc). Also, the R-naphthylethyl moiety itself is chiral, and its defined stereogenic configuration may contribute additional interaction sites.

Special attention was paid to the separations of racemic ruthenium (II) complexes. The RN-CF6 stationary phase provided significantly better selectivity toward Ru complexes than other derivatized-CF6 stationary phases, such as DMP-CF6, R/S-methylphenyl-CF6.[136] This fact indicated that the nature of the derivative plays a major role in the chiral recognition process between the Ru complex and the chiral selector. Comparisons between RN-CF6 and SN-CF6 provide further insights about the chiral recognition mechanism. The configuration of the naphthylethyl carbamate moieties is opposite for the "RN" (R-naphthylethyl) and "SN"-CF6 (S-naphthylethyl) stationary phases. RN-CF6 easily separates enantiomers of Ru (II) complexes, with enantioselectivities ranging from 1.49-2.90. The SN-CF6 column can also baseline

separate all of the tested complexes, with enantioselectivities ranging from 1.17-1.97 (data not shown). The most important fact is that enantiomers of these metal complexes were separated on RN- and SN-CF6 columns with opposite elution orders. This indicates that the substituent significantly contributed to the chiral recognition. The stereogenic configuration of the naphthylethyl carbamate group is a major factor for chiral recognition, and the cyclofructan6 plays a secondary role. If CF6 played no role in the enantiomeric selectivity for these complexes, then the SN-CF6 CSP would produce exactly opposite enantiomeric separations. However, this is not the case.

Although the exact orientation of the aromatic groups of derivatized-CFs is not known, it is likely that chiral recognition is the sum of many different interactions arising from different parts of the bonded chiral selector. Both the derivative group and the core cyclofructan play an important role in enantiomeric separations.

3.4.5 Effects of the analyte structure

To try to understand the separation mechanism, it helps to look at closely related compounds, where slight structural changes greatly alter enantioselectivity. In Group E, compounds 44-51 are a series of structurally related compounds, which all contain a five-member ring, having -O-CO-NH-, or -S-CO-NH-, or -S-CS-NH- units.

For example, 4-phenyl-2-oxazolidinone (E44) and 4-phenylthiazolidine-2-thione (E45) have similar chemical structures, in which the only difference is that the -O-CO-NH-moiety in compound E44 is replaced by -S-CS-NH- in E45. Chromatographic results indicate that the RN-CF6 stationary phase provided enantioselectivity toward E45, but not E44, while the DMP-CF7 column separated racemic E44, but not E45. Another analogous example is the comparison of 4-benzyloxazolidine-2-thione (E46) and 4-benzylthiazolidine-2-thione (E47). E46 contains a -O-CS-NH- unit, while E47 has a -S-CS-NH unit. The other functionalities are the same. The RN-CF6 CSP provided

enantioseparation only for E46. The DMP-CF6 column showed significantly different selectivity toward E46 and E47 (1.15 vs 1.09). The structural difference between E44/E45, and E46/47 mainly affected dipolar interactions or hydrogen bonding interactions. The facts that the CSPs provided hugely different selectivities indicated that dipolar interactions or hydrogen bonding interactions play an import role in chiral recognition of cyclofructan chiral selctors.

π-π interactions and steric interactions may significantly contribute to enantiomeric separations on cyclofructan-based stationary phases as well. For example, compared with E44, compound E51 has an additional phenyl group, which can provide additional π-π interactions and increase the steric bulkiness of the analyte. The fact that the DMP-CF7 stationary phase only separated racemic E44 while the RN-CF6 CSP exhibited chiral recognition only for E51, demonstrated that π-π and/or steric interactions can significantly affect chiral recognition interactions between the chiral selector and analyte.

3.5 Conclusions

The RN-CF6 and DMP-CF7 stationary phases provided chiral recognition toward a variety of compounds, including acidic, basic, neutral organic compounds, and metal complexes. It is interesting that they exhibited complementary selectivity and the combination of two columns provided enantioseparations for 43% of test analytes. Generally, better separation of amine containing compounds was obtained on the RN-CF6 stationary phases, while the DMP-CF7 column worked more effectively for acidic compounds in most cases. It was found that both the crown ether ring and the nature of the derivative group on the cyclofructans affected selectivity and enantiomeric separations.

These extensive chromatographic results offered useful information for method development of specific chiral analytes and a better knowledge of enantioseparation mechanism. Also, they provide insight concerning design of new chiral stationary phases. Currently, the studies in which both ionic groups (anionic or cationic) and aromatic groups are inserted in one CF molecule, are underway, in hopes of finding more widely-applicable chiral selectors.

CHAPTER 4

THE ENANTIOMERIC SEPARATION OF TETRAHYDROBENZIMIDAZOLE

INTERMEDIATES BY HPLC AND CE USING CYCLODEXTRIN AND CYCLOFRUCTAN

BASED CHIRAL SELECTORS

4.1 Abstract

High performance liquid chromatography (HPLC) and capillary electrophoresis (CE) were used to examine the enantiomeric separation of a series of seventeen racemic tetrahydrobenzimidazole analytes. These compounds were prepared as part of a synthetic program directed towards a select group of pyrrole-imidazole alkaloids. This group of natural products have unique frame works of pyrrole and guanidine-containing fused rings which can be constructed through the intermediacy of tetrahydrobenzimidazole scaffold. Several bonded cyclodextrin (both native and derivatized) and derivatized cyclofructan - based chiral stationary phases were evaluated for their ability to separate these racemates via HPLC. Similarly, several cyclodextrin derivatives and derivatized cyclofructan were evaluated for their ability to separate this set of chiral compounds via CE. Enantiomeric selectivity was observed for the entire set of racemic compounds using HPLC with resolution values up to 3.0. Among the twelve different CSPs, enantiomeric recognition was most frequently observed with the Cyclobond RN and LARIHC CF6-P while Cyclobond DMP yielded the greatest number of baseline separations. Fifteen of the analytes showed enantiomeric recognition in CE with resolution values as high as 5.0 and hydroxypropyl-γ-cyclodextrin was the most effective chiral additive.

4.2 Introduction

Enantiomeric separations play a major role in the pharmaceutical and agrochemical industries involving the production of safer and more effective drugs, pesticides and herbicides. High performance liquid chromatography (HPLC) in combination with effective chiral stationary phases is one of the most widely tools used to separate enantiomers given its good reproducibility, wide selectivity and its potential for preparative and semipreparative separations.[46,48,51,96,97,146,147] Although a large number of HPLC chiral stationary phases (CSPs) are available[25,51,52,59,148-156] the macrocyclic oligosaccharide family of chiral selectors has remained an influential and popular class of chiral selector for decades. Cyclodextrin based chiral stationary phases are likely the most widely recognized member of this CSP family and they have proven to have broad enantioselectivity towards a large number of racemic analytes.[46-48,119,120,157,158] Recently three new cyclofructan (CF) based CSP have been developed. Two of them show broad enantiomeric selectivity towards a plethora of analytes and one of them is particularly well suited for the separation of primary amine containing racemates.[66,67] These cyclofructan CSPs broaden the applicability of the cyclic oligosaccharides chiral selector family. Both CDs and CFs are evaluated as HPLC chiral selectors herein.

Capillary electrophoresis (CE) is a good alternative to chromatography for enantiomeric separations due to its high efficiency, short analysis time and low sample consumption.[159-161] Unlike HPLC using chiral stationary phases, enantiomeric separations in CE are accomplished by adding the chiral selector into the run buffer. Although there are a wide number of chiral selectors applicable to CE, cyclodextrins and their derivatives dominate in CE for enantiomeric separations.[162]

To test the effectiveness of cyclodextrin and cyclofructan chiral selectors towards the enantiomeric separation of chiral synthetic intermediates of natural products, a set of

probe analytes based on a 4,5,6,7-tetrahydrobenzimidazole (THB) scaffold with benzyl protection at the N1 position and varying substituents at the 5-, 6-, and 7- positions on the tetrahydrobenzimidazole were evaluated (Figure 1). These compounds were prepared as part of synthetic study toward the construction of several pyrrole-imidazole alkaloids (PIAs). This class of natural products is notable for their high content of nitrogen atoms within a structural framework of complex heterocyclic moieties and strained rings. Also this class of compound has shown diverse biological activities.[163-166] These compounds include well known members like ageliferin and palau'amine.[163,167,168] Due to the pharmacological importance of these natural products and to facilitate asymmetric syntheses, it would be advantageous to be able to separate and analyze these functionalized intermediates.

Enantioselective separation of these precursors is important since it will allow access to intermediates with the same absolute configuration as the natural product. The purpose of this work is to examine the enantiomeric separation of seventeen newly synthesized polysubstituted THB's (Figure 1). Furthermore, the ability to determine enantiomeric ratios during asymmetric syntheses will be greatly facilitated by this work. In order to evaluate the enantiomeric separation of these potential precursors both HPLC and CE were tested. To our knowledge, there have been no previous reports of these compounds being subjected to any chiral chromatographic or electrophoretic technique.

4.3 Materials and Methods

4.3.1 Materials and Chemicals

Figure 4.1 shows the chemical structures of the seventeen synthetic racemic analytes. This group of natural products has unique frame of pyrrole and guanidine containing fused rings which having 4,5,6,7-tetrahydrobenzimidazole scaffold with benzyl

protection at the N1 position and varying substituents at the 5,6,7-portions on the tetrahydrobenzimidazole.
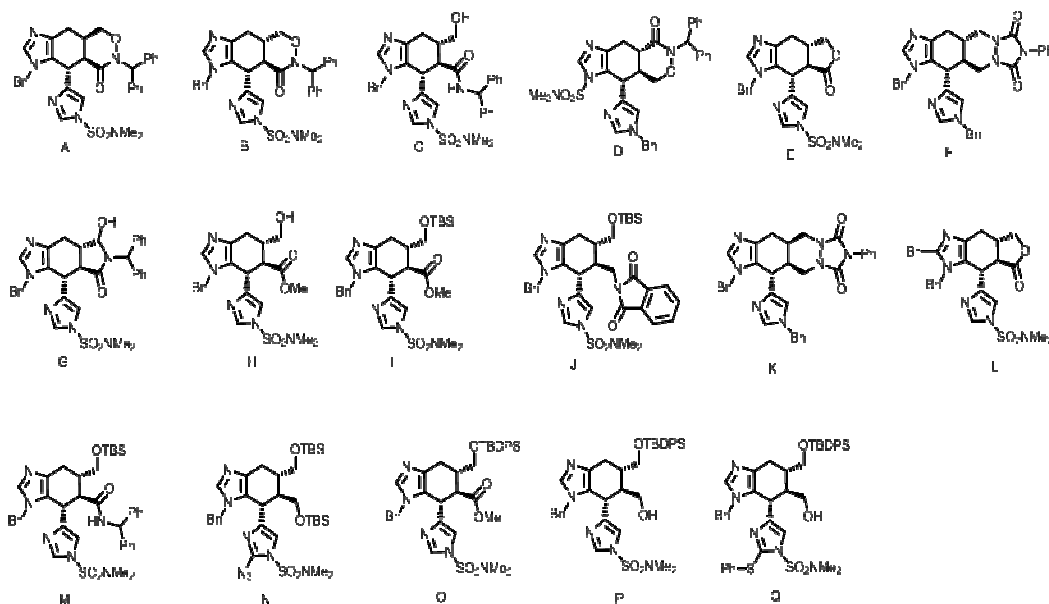
Figure 4.1 The chemical structures of the seventeen synthetic racemic tetrahydrobenzimidazole analytes that were subjected to enantioselective HPLC and CE analysis. Note : Bn: Benzyl, Ph: Phenyl, TBS: *tert*-butyldimethylsilyl, TBDS: *tert*-butyldiphenylsilyl

Heptane, ethanol (EtOH), acetonitrile (ACN) and methanol (MeOH) of HPLC grade were purchased from EMD Chemicals Inc. (Gibbstown, NJ, USA). Deionised water was obtained from a Milli-Q system (Billerica, MA, USA). Sodium phosphate monobasic and dibasic, phosphoric acid, sodium hydroxide (NaOH), ammonium acetate (H_4NOAc), glacial acetic acid (HOAc), and triethylamine (TEA), were obtained from Sigma-Aldrich (Milwaukee, WI, USA). All the racemic analytes listed in Figure 1 were synthesized as previously reported.[169-171] All of the columns [250 × 4.6 mm (i.d.)] were obtained from Supelco (Whippany, NJ, USA) and AZYP (Arlington, TX, USA). The columns used were: native β-CD (β-cyclodextrin), HP-RSP (high performance hydroxypropyl ether

β-cyclodextrin), RSP (hydroxypropyl ether - β cyclodextrin), AC (acetylated β-cyclodextrin), RN and SN (R- and S-naphthylethyl carbamate β-cyclodextrin), DMP (dimethylphenyl carbamate β-cyclodextrin), DNP (2,6-dinitro-4-trifluoromethylphenyl ether β-cyclodextrin), DM (dimethylated β-cyclodextrin), LARIHC-P (LARIHC CF6-P), LARIHC-RN (LARIHC CF6-RN) and CF7-DMP (LARIHC CF7-DMP). Chiral selectors for CE were obtained from Sigma-Aldrich (Milwaukee, WI, USA) and are as follows: γ-CD (γ-cyclodextrin), HP-β-CD (hydroxypropyl-β-cyclodextrin), and HP-γ-CD (hydroxypropyl-γ-cyclodextrin). The untreated fused silica capillaries (50 μm i.d.) for CE were purchased from Polymicro Technologies (Phoenix, AZ, USA).

4.3.2 Instruments and Measurements

HP (Agilent Technologies, Palo Alto, CA, USA) 1050 system was used, which consists of a UV VWD detector, an autosampler, a quaternary pump and Chemstation software as a first chromatographic system. The second HPLC system was composed of a pump (Shimadzu, LC-6A) and a circular dichroism detector (Jasco, CD-2095 plus). All CE experiments were performed on Beckman Coulter P/ACE MDQ (Fullerton, CA, USA) CE system equipped with an on-column UV–visible detector.

4.3.3 HPLC analyses

All samples were dissolved in ethanol, or the appropriate mobile phases for analyses done in reversed phase, normal phase and polar organic mode. H_4NOAc buffers were used and HOAc used to adjust the desired pH in the reversed phase mode. The mobile phase compositions are in volume to volume ratios. All the mobile phases were degassed by ultrasonication under vacuum for 5 min. The injection volume, the flow rate, and the detection wavelength are 5 μL, 1 ml/min and 254 nm, respectively. Separations were carried out at room temperature (~22 °C) if not otherwise

77

specified.

4.3.4 CE analyses

All CE experiments were carried out using a Beckman Coulter P/ACE MDQ (Fullerton, CA, USA) CE system equipped with an on-column UV-visible detector. Bare fused silica capillary (50 μm ID $\times$ 358 μm OD, 30 cm in length, 20 cm to the detector) purchased from Polymicro Technologies (Phoenix, AZ, USA) was maintained at 20 ^{o}C during analysis. UV detection was accomplished at 214 nm. The capillary was conditioned before its first use by rinsing with 1M sodium hydroxide for 5 min, water for 5 min. Between each run, the capillary was flushed with 1 M sodium hydroxide for 2 min, water for 2 min and buffer solution for 2 min. Buffers of the desired pH were prepared by mixing equimolar solution of phosphoric acid and $NaH_2PO_4.$ Buffer additives as chiral selectors were added directly into the buffer. Voltages were applied across the capillary in between 7 to 12 kV at normal polarity mode to optimize enantioselective separation. Samples were dissolved in 20% ethanol in water and injected hydrodynamically at 0.5 psi for 5 sec.

4.4 Results and Discussion

4.4.1 HPLC analyses

The enantiomeric separation of the seventeen racemic analytes listed in Figure 4.1 was evaluated by HPLC using cyclodextrin and cyclofructan - based CSPs. An understanding of the means by which these types of compounds can be separated is of great imporazance to synthetic chemists. Reversed phase, polar organic and normal phase modes were tested in this study. During optimization of reverse phase separations, both ACN and methanol were tested as organic modifiers. Considering that all the tested compounds are ionizable, (see Figure 4.1) an ammonium acetate buffer was

78

used in all reversed phased mode separations. During the optimization process both the pH and buffer concentrations were examined. Figure 4.2(a)　and Figure 4.2(b) show chromatograms for the enantiomeric separation of compound A (Figure 4.1) at varying pHs and buffer concentrations. For screening purposes, pH and buffer concentration were 4.1 and 20 mM, respectively, which resulted in the greatest selectivity within a reasonable analysis time.
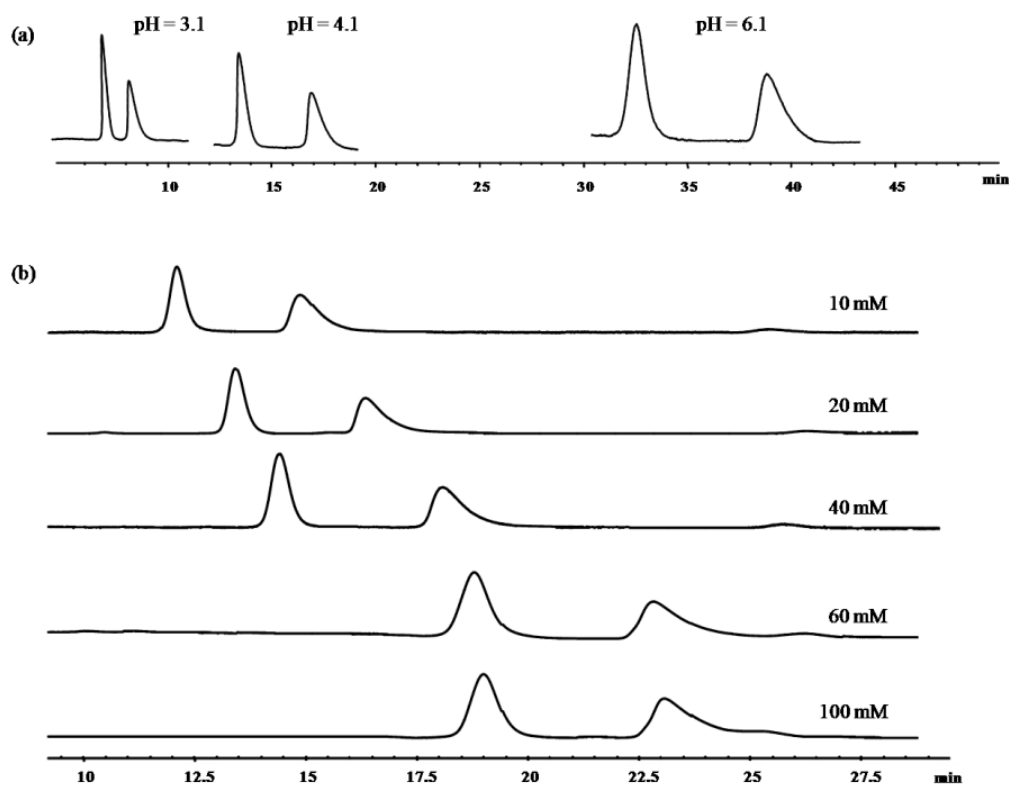
Figure 4.2 The effect of the buffer pHs (a) effect of the buffer concentrations (b) on enantiomeric separation of compound A resolved by CYCLOBOND I 2000 DMP, Eluent: 20mM NH$_4$OAc / ACN (60/40,v/v) ; flow rate: 1.0 ml/min, UV detection : 254 nm.

Table 4.1 summarizes the optimized chromatographic conditions for the each analyte. Optimized conditions were those which resulted in maximum resolution (R_S)

values with reasonable retention factors (k_1') values. All chiral compounds showed enantioselectivity (α) with the macrocyclic stationary phases. The enantioselectivity values ranged from 1.03 (compound J) to 1.81 (compound O). While the R_s values ranged from 0.6 (compound J) to 3.0 (compound A). Among all the racemates, twelve of the compounds showed R_s values greater than or equal to 1.5 meaning they were baseline separated.

Table 4.1 Summary of the optimized HPLC enantiomeric separations.

Compounds	CSP[a]	k_1	α	R_s	Mobile phase
A	DMP	3.65	1.28	3.0	60/40 20mM NH4OAc/ACN
B	DM	4.80	1.42	2.3	85/15 20mM NH4OAc/ACN
C	RN	4.11	1.04	0.7	99ACN/1MeOH/0.3AA/0.2TEA
D	DM	3.14	1.18	1.8	80/20 20mM NH4OAc/ACN
E	DMP	2.64	1.30	2.0	60/40 20mM NH4OAc/MeOH
F	RN	5.13	1.27	1.8	50/50 20mM NH4OAc/MeOH
G	SN	9.14	1.17	1.6	80/20 20mM NH4OAc/ACN
H	LARIHC	2.02	1.11	1.0	80/20 20mM NH4OAc/MeOH
I	DMP	2.86	1.25	1.3	80/20 20mM NH4OAc/MeOH
J	RN	14.10	1.03	0.6	70/30 20mM NH4OAc/ACN
K	AC	1.90	1.50	1.7	70/30 20mM NH4OAc/MeOH
L	SN	3.76	1.17	1.7	60/40 20mM NH4OAc/MeOH
M	HP-RSP	3.06	1.21	1.5	50/50 20mM NH4OAc/MeOH
N	RSP	13.53	1.26	0.9	75/25 20mM NH4OAc/ACN
O	β-CD	1.76	1.81	1.6	60/40 20mM NH4OAc/MeOH
P	β-CD	3.00	1.54	2.1	60/40 20mM NH4OAc/MeOH
Q	β-CD	5.33	1.39	1.7	60/40 20mM NH4OAc/MeOH

[a] For a list of the defined CSP abbreviations, see the Materials and Chemicals section. For the structures of the analytes, refer to Figure 1.
Flow rate, 1.0 ml min^{-1}; detection, 254 nm; temperature, ambient

The 3,5-dimethylphenyl derivatized β-cyclodextrin (DMP) and native β-cyclodextrin (β-CD) chiral stationary phases (CSPs) combined to give five of the baseline separations and proved to be two of the more effective chiral selectors for these types of racemates. The dimethylated β-cyclodextrin (DM) and S-naphthylethyl carbamate β-

cyclodextrin (SN) chiral stationary phases, each accounted for two baseline separations. The high performance hydroxypropyl ether β-cyclodextrin (HP-RSP), acetylated β-cyclodextrin (AC), R-naphthylethyl carbamate β-cyclodextrin (RN) accounted for one baseline separation each. To obtain the twelve baseline separations, five different CSP's were used, owing to the complementary nature of the chiral selectors. The Cyclobond DMP column yielded the largest enantiomeric resolution value (compound A, $R_S = 3.0$). The supporting information (Figure 4.3) shows the optimized separation of compound A on the Cyclobond DMP column using both UV and CD detection. Enantiomeric separations were confirmed using a CD detector in all cases.
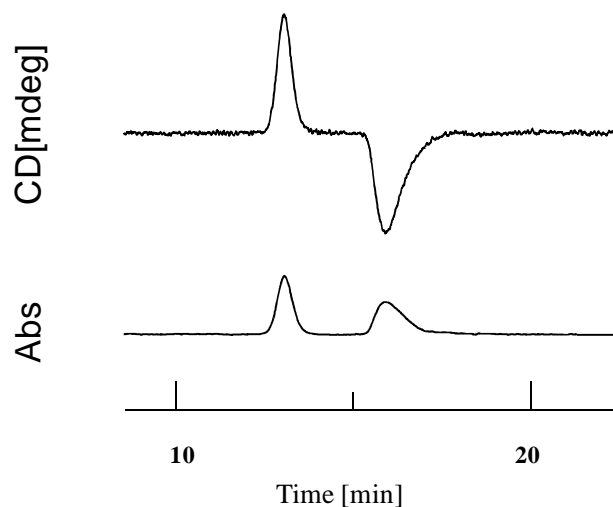
Figure 4.3 Chromatograms of compound A resolved by CYCLOBOND DMP CSP. The top and bottom chromatograms are circular dichroism and UV signal at 254nm. Eluent: 20mM NH_4OAc / ACN (60/40, v/v); flow rate: 1.0 ml/min.

Figure 4.4 summarizes the total number of partial ($0.4 < R_S < 1.5$) and baseline ($R_S > 1.5$) enantiomeric separations obtained using each chiral selector in all the three modes of operations. The Cyclobond RN and LARIHC CF6-P chiral

stationary phases showed enantiomeric selectivity for the greatest number of compounds. Each of these two the stationary phases displayed enantiomeric recognition for thirteen out of seventeen of the compounds tested. However, the Cyclobond RN and LARIHC CF6-P CSPs produced only three total baseline separations. Cyclobond DMP, native β-CD and RSP had the second greatest success rate, shown enantiomeric recognition for 71% of the tested compounds.
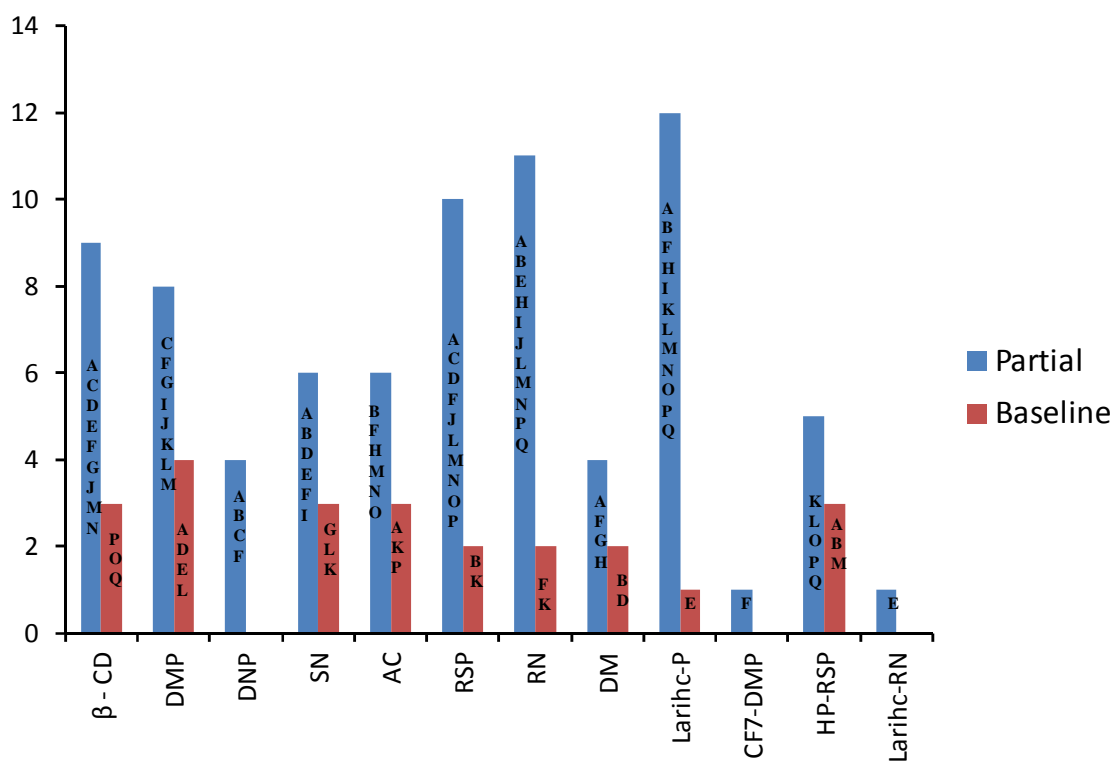
Figure 4.4 A representation of the total number of partial and baseline separations obtained using HPLC with different chiral stationary phases with all mobile phases including reversed phase (RP), polar organic (PO) and normal phase (NP) modes. For a list of the defined CSP abbreviations, see the Experimental section. The letters in the Bars represent the compound code as listed in Figure 4.1.

Typically, cyclodextrin based CSPs in the reversed phase mode form strong inclusion complex between the hydrophobic portions of the analytes and the cyclodextrin

cavity.[47,158,172,173] During this work, optimal aqueous/organic ratios were varied from 50/50 to 85/15. Compound C was the only analyte that had an optimized separation using the polar organic mode (Table 4.1). Overall, the polar organic mode performed poorly when using all CSP's and only resulted in five total separations.

The supporting information (Figure 4.5) is compared the separation of compound A in both polar organic and reversed phase modes on Cyclobond DMP CSP. Figure 4.5(a) shows the separation in polar organic mode and Figure 4.5(b) shows the separation in the reversed phase.
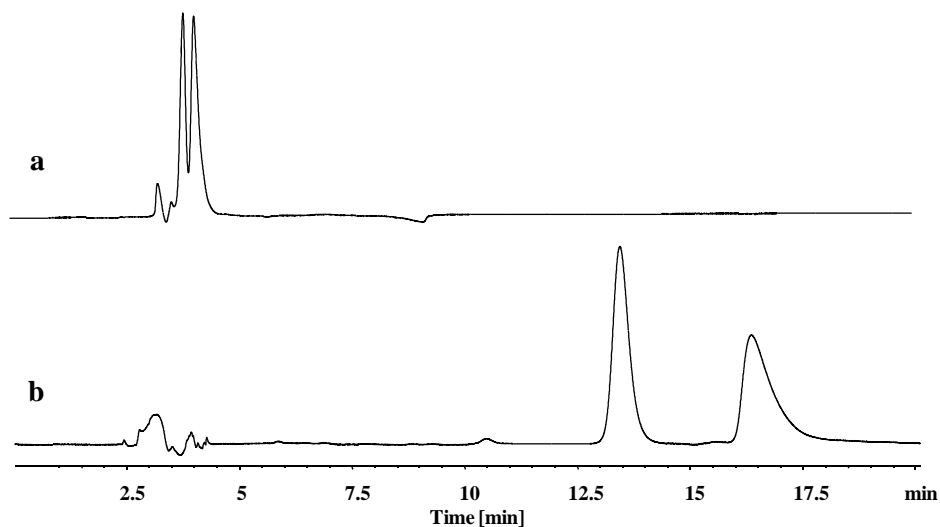
Figure 4.5 HPLC enantiomeric separation of compound A in the polar organic mode (a) and in reversed phase (b) resolved by CYCLOBOND DMP. Eluent: ACN/MeOH/AA/TEA (99/1/0.3/0.2, v/v) (a) and 20mM NH$_4$OAc / ACN (60/40, v/v) (b); flow rate: 1.0 ml/min, UV signal at 254nm. See Figure 1 for analyte structures.

Figure 4.6 compares retention curves for two different analytes, compounds A and F. The retention factors in the reversed phase mode are shown in the left side of the plot and the retention factors in the polar organic mode are shown to the right. This shows that compound A forms a stronger inclusion complex than compound F, likely due to the greater number of phenyl rings in the structure. Compound F has longer retention

83

compare to compound A in the polar organic mode where inclusion complexation is not available due to the high concentration of organic solvent occupying the CD cavity. Comparing the structure of these two analytes reveals an additional urazole ring in compound F, resulting in more hydrogen bonding sites than compound A. Hydrogen bonding is the main interaction mechanism in the polar organic mode. So it is reasonable that compound F retained longer than compound A under polar organic conditions.
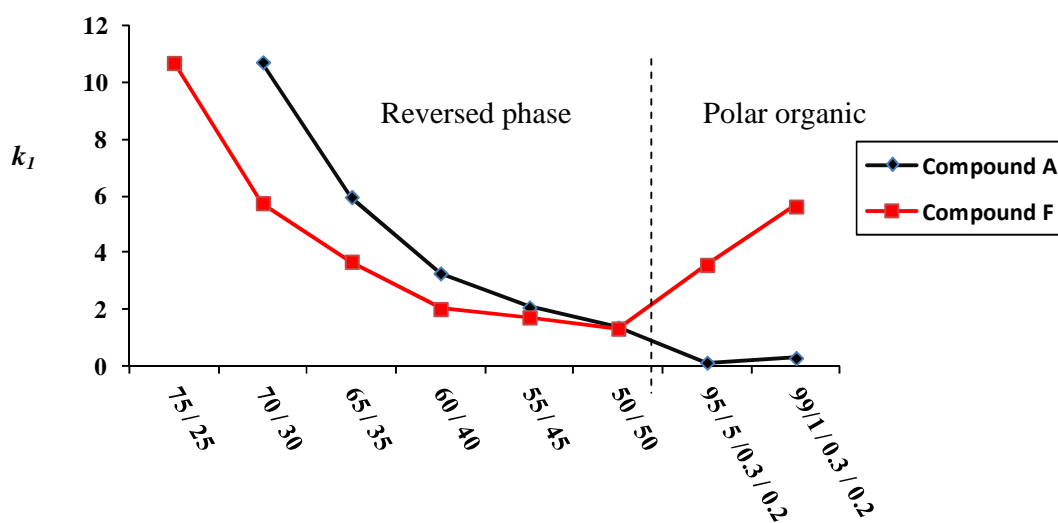
Figure 4.6 Retention curves for two of the compound A and F resolved by CYCLOBOND DMP. The Eluent: The reverse phase 20mM H_4NOAc (pH=4.1)/ACN, polar orgnic ACN/MeOH/AA/TEA. See Figure 1 for analyte structures.

Among the seventeen compounds, sixteen compounds were separated using reversed phase conditions with twelve being baseline separations.(Table 4.1) The analytes which had *tert*-butyldiphenylsilyl (TBDPS) groups, such as compounds O, P and Q were more easily separated. TBDPS moieties groups can form strong hydrophobic inclusion complexes with the cavity of the cyclodextrin and may be part of the reason they separated relatively easily. Among the screened chiral intermediates compound N was the only analyte contained two *tert*-butyldimethylsilyl (TBS) groups. Compound J

84

possesed one TBS and one imide group on the 5 and 6 positions of tetrahydrobenzimidazole ring. These two analytes had the longest retention among the seventeen compounds due to the strong hydrophobic interaction with the cyclodextrin cavity. In most cases, it was difficult to elute these analytes from the stationary phase. Both Cyclobond AC and RN CSPs were able to recognize the stereoselectivity at the 5 and 6 positions of compound K and F in reversed phase conditions. (see Table 4.1) Comparing compounds P and Q there is an additional thiophenyl group on compound Q which resulted in longer retention on the native β-CD CSP due to stronger hydrophobic interactions. (Table 1) Comparing compound I and O there is an additional hydrophobic functional group (diphenyl in TBDPS) on compound O which leads a better separation compared to compound I.

4.4.2 CE analysis

All the compounds studied by HPLC were also investigated by CE using derivatized cyclodextrins as chiral selectors. In a related study, sulfated-β-CD was reported as an optimum chiral selector for similar compounds.[172] However, when using sulfated-β-CD in this study, no enantiomeric separations was observed in either normal or reverse polarity modes. Clearly, this set of alkaloid compounds behave much differently than those studied previously.[172]

Alternatively, neutral chiral selectors were considered for separating the tetrahydrobenzimidazoles. As is typical to capillary zone electrophoresis (CZE) separations, alterations in pH were extremely important in achieving enantiomeric separations. Using neutral chiral selectors requires that the analytes are be charged. Thus, acidic conditions were required for all CE separations. Figure 4.7 shows electropherograms for compound C at various pH buffers using HP-β-CD. No

enantiomeric separations were observed at pHs $\geq$ 6.0. Lower pHs provided increased

resolution (R_S) up to 1.5 at pH 2.5.
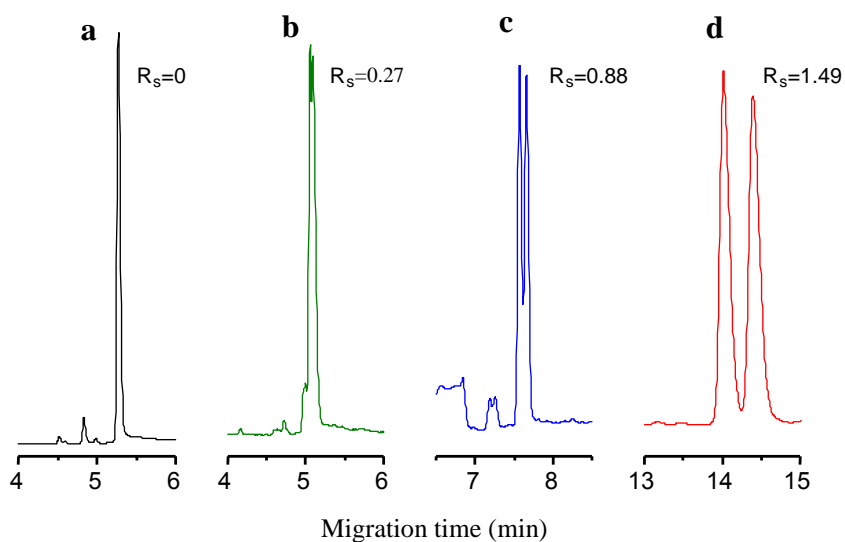
Figure 4.7 Electropherograms of compound C using 30 mM of of HP-β-CD in (a) 50 mM tris-phosphate buffer pH 6.0, (b) 25 mM ammonium acetate buffer pH 5.0, (c) 25 mM ammonium acetate buffer pH 4.0 and (d) 50 mM sodium phosphate buffer pH 2.5. at 7 kV at normal polarity.

Increasing the applied voltages from 7 to 12 kV resulted in improved resolution

as well as an increase in apparent mobility, allowing for shorter analysis times. In

addition, when the concentration of the chiral selector was increased from 30 to 70 mM in

the BGE for compound C (Figure 4.8), enantiomeric selectivity values were remained

constant whereas the number of theoretical plates (N) improved slightly.
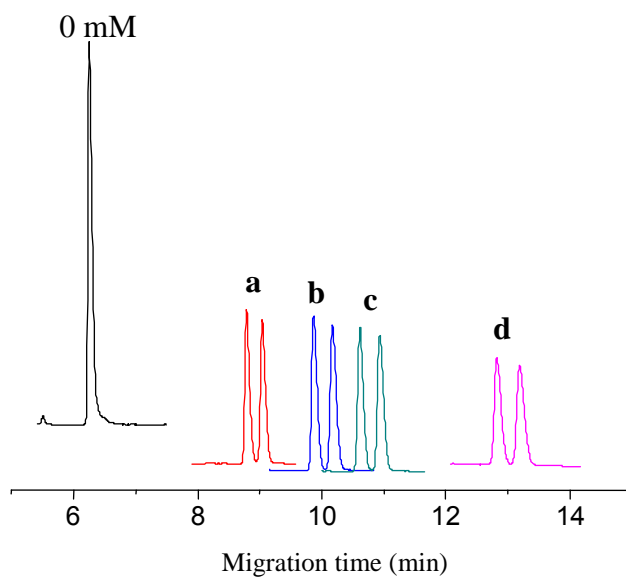
Figure 4.8 Electropherograms of compound C using (a) 30, (b) 40, (c) 50 and (d) 70 mM of HP-β-CD in 50 mM phosphate buffer pH 2.5 at 12 kV of normal polarity. The enantioselective resolution values were 1.68 for (a), 1.73 for (b), and 1.75 for (c) and 1.68 for (d).

The most important factor in the enantiomeric separation of the tetrahydrobenzimidazoles was the nature of the chiral selector used. Figure 4.9 shows the enantiomeric separations obtained using each chiral selector. Of the seventeen compounds studied, fifteen were enantiomerically separated using γ-CD, HP-β-CD, HP-γ-CD and IP-CF6 chiral selectors. HP-γ-CD provided to be the most effective chiral selector, showed enantiomeric recognition for eleven racemates. It is especially important to note that this is the first report of using IP-CF6 as a chiral selector in CE. Compound C was only separated when cyclodextrin chiral selectors were used. In contrast, compound A was only separated when using the cyclofructan selector. This shows the potential for complementary separations to be obtained using this novel cyclofructan based chiral

87

selector. However, compound H could be separated using all chiral selectors studied. It was observed that the larger cavity of HP-γ-CD relative to HP-β-CD provided better separation of the compounds which contained a t-butyl silanol substituent. Clearly, this bulky hydrophobic moiety forms enantioselective inclusion complexes more easily with the γ-CD.
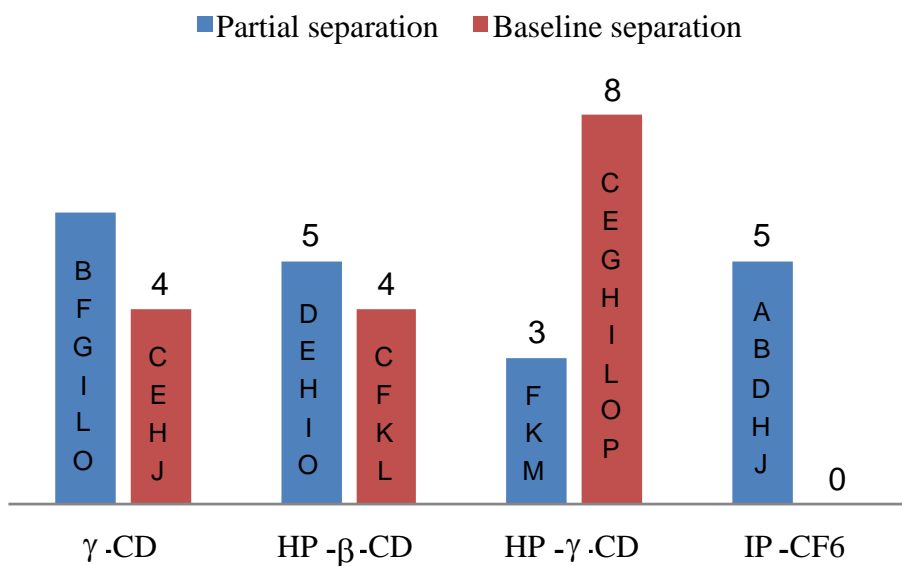
Figure 4.9 Bar graph representing the ability of chiral recognition depending on different chiral selectors. The letters in the Bars represent the compound code.

A summary of the optimized enantiomeric recognitions obtained by CE is given in Table 4.2. It was determined that a buffer solution of 50 mM of phosphate at pH 2.5 provided the most successful enantiomeric separations as described above. Enantiomeric selectivity values (α) ranged from 1.01(compound D) to 1.13 (compound L). Separation efficiency (N) values were observed from 8000 (compound M) to 70000 (compound F). Lastly, resolution values (R_S) ranged from 0.3 (compound M) to 5.0 (compound L). Among the fifteen compounds separated using CE, eight of them were

baseline separations, which were obtained using only two chiral selectors. (HP-β-CD and

HP-γ-CD)

<div align="center">Table 4.2 Summary of the optimized CE enantiomeric separations[a]</div>

Compounds	t_{m1}[b]	α	R_s	N[c]	Chiral selectors[d]
A	10.76	1.02	0.7	32000	70 mM IP-CF6
B	12.21	1.02	1.2	48000	70 mM γ-CD
C	10.61	1.03	1.8	55000	50 mM HP-β-CD
D	17.71	1.01	0.5	32000	100 mM HP-β-CD
E	7.31	1.04	1.2	16000	50 mM HP-γ-CD
F	10.44	1.03	1.7	70000	100 mM HP-β-CD
G	17.41	1.04	2.6	64000	100 mM HP-γ-CD
H	7.39	1.04	1.6	30000	50 mM HP-γ-CD
I	7.50	1.04	2.1	58000	50 mM HP-γ-CD
J	11.60	1.03	1.4	27000	70 mM γ-CD
K	8.33	1.03	1.6	53000	70 mM HP-β-CD
L	13.25	1.13	5.0	23000	30 mM HP-γ-CD
M	19.09	1.02	0.3	8000	150 mM HP-γ-CD
N	-	-	-	-	-
O	19.05	1.04	2.2	57000	150 mM HP-γ-CD
P	32.25	1.02	1.1	41000	200 mM HP-γ-CD
Q	-	-	-	-	-

[a] All separation were performed with 50 mM of Phosphate buffer at pH 2.5, 12 kV, 30 capillary (20 cm to detector) with 50 μm I.D.
[b] t_{m1} is migration times in minutes of the first enantiomeric peak.
[c] N is the average number of theoretical plates (N = 16(t_m/w)).
[d] The chiral selectors were added into the buffer solution.

4.4.3 Comparison between HPLC and CE enantiomeric separations

HPLC was able to show enantiomeric recognition for all the seventeen compounds, whereas using CE; only fifteen showed enantiomeric selectivity. However, compared to HPLC, CE produced more rapid separations and greater resolution with higher efficiencies; characteristics which are typical for CE analyses.
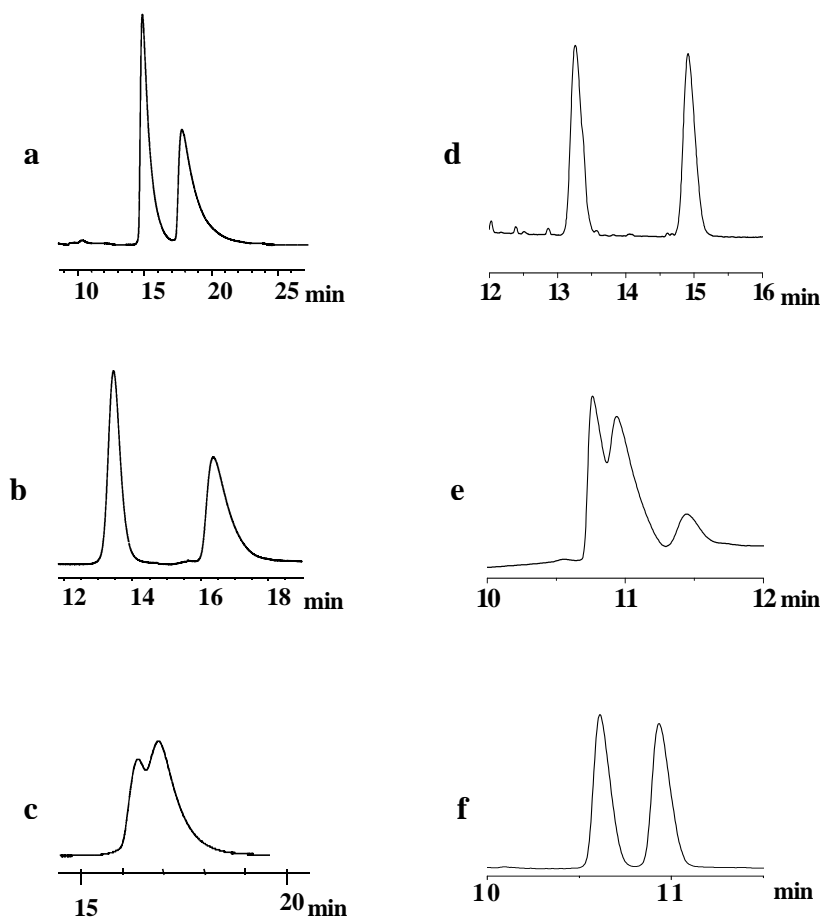
Figure 4.10 Enantioselective HPLC (a, b and c) and CE (d, e and f) analyses of compounds L (a and d), A (b and e) and C (c and f). The optimized conditions used on HPLC and CE were described in Table 1 and 2.

The greatest R_S found using HPLC was 3.0, while the best CE separation had a R_S of 5.0. Figure 10 compares some separations obtained using HPLC [Figure 4.10(a), (b) and (c)] and CE [Figure 4.10(d), (e) and (f)]. The comparison made in the separation of compound L by HPLC [Figure 4.10(a) and by CE (Figure 4.10(d)] shows the characteristic advantage of using CE. HPLC separation was greater in some cases as shown in Figure 4.10(b) (separation of compound A by HPLC) and Figure 4.10(e) (separation of

90

compound A by CE). Hence, it is clear that both techniques have different advantages for this set of analytes. It is important to note that compound C, which was separated only in the PO mode by HPLC, was well separated by CE. [Figure 4.10(c) and Figure 4.10(f)] Compound N and Q did not give any enantioselecitvity in CE. However, compound N was separated by HPLC with resolution of 0.9 with the Cyclobond RSP and compound Q with resolution of 1.7 on the native β-CD column. (Table 4.1 and Table 4.2) Therefore both techniques gave complementary selectivities towards these alkaloid compounds.

4.5 Conclusions

In this study, seventeen chiral tetrahydrobenzimidazole compounds were subjected to enantioselective HPLC and CE analyses using cyclodextrin, cyclofructan and its derivatives.   In HPLC, the Cyclobond RN and LARIHC CF6-P yielded enantiomeric selectivities for the greatest number of racemates while the Cyclobond DMP phase showed the greatest number of baseline separations towards the analytes. In CE, HP-γ-CD was the most successful chiral additive for the enantiomeric recognition for racemic tetrahydrobenzimidazole analytes. Although IP-CF6 could not provide baseline separation on most of the compounds, it showed enantiomeric selectivity on a specific compound that was not separated with native or derivatized cyclodextrins.

CHAPTER 5

BONDED IONIC LIQUID POLYMERIC MATERIAL FOR SOLID PHASE MICRO EXTRACTION GC ANALYSIS.

5.1 Abstract

Four new ionic liquids (IL) were prepared to be bonded onto 5 μm silica particles for use as adsorbent in solid phase micro extraction (SPME). Two ILs contained styrene units that allowed for polymerization and higher carbon content of the bonded silica particles. Two polymeric ILs differing by the anion were used to prepare two SPME fibers that were used in both headspace and immersion extractions and compared to commercial fibers. In both sets of experiments, ethyl acetate was used as an internal standard to take into account adsorbent volume differences between the fibers. The polymeric IL fibers are very efficient in headspace SPME for short chain alcohols. Immersion SPME can also be used with the IL fibers for short chain alcohols but also for polar and basic amines that can be extracted at pH 11 without damage to the fiber contained silica particles. The sensitivities of the two IL fibers differing by the anion were similar. Their efficacy compares favorably to that of commercial fibers for polar analytes. The mechanical strength and durability of the polymeric IL fibers were excellent.

5.2 Introduction

Solid phase microextraction (SPME) was developed by Pawliszyn in the early 1990s as a simple and "green" technique for sample preparation without the use of any solvent.[174-176] SPME is simply performed by exposing a silica fiber covered by an absorbing agent to the headspace (HS) volume of a vial or directly immersing into the matrix of the liquid sample. A rapid preconcentration of analytes into the fiber surface is

observed if the coating absorbing agent is appropriate. The extracted agents are analyzed by simply placing the fiber into the injection port of a gas chromatograph (GC). The injector is heated at an elevated temperature that will cause the vaporisation of the absorbed analytes into the GC insert and a classical GC chromatogram can be developed for full identification and quantitation of all extracted compounds.

The chemistry of the sorptive SPME coating layer plays a significant role in enhancing the extraction of specific classes of compounds and discriminating against others.[177,178] The SPME extractant must primarily be thermally stable so as not to decompose during the GC injection process. It must also be mechanically strong to support agitation and manipulation. Finally, it must be able to withstand harsh chemical media when immersed in the sample solution including extreme pHs, high ionic strengths, and organic solvent concentrations. Bare silica gel, polydimethylsiloxane (PDMS), divinylbenzene (PDMS-DVB), polyacrylate (PA), high density polyoxyethylene (Carbowax) are used in commercially available SPME fibers.[179,180] Since higher selectivity as well as higher sensitivity are needed as the technique gains wide-spread popularity, the quest for new coating adsorbents is the goal of numerous research teams.[69,71,181]

Ionic liquids are a new class of non molecular solvents with unique properties such as a very low volatility, often good thermal stability, electrical conductivity, good solvating properties associated to adjustable polarity, and water or solvent solubility.[78,182-186] Ionic liquids are actually salts with a melting point close to or below room temperature. Their low volatility and peculiar solvating properties were soon considered as attractive properties that would make them very useful for use in separation techniques[187] and especially, possible candidates for new adsorbents for SPME fibers.

93

Considerable insights into solute-IL interactions and affinities were obtained during the development and evaluation of GC stationary phases made with ILs.[79,188-190] This experience was first used to develop microextractions on a single ionic liquid drop, i.e. without fiber support.[174,191] Next ionic liquid coated fibers were prepared for a single determination of trace amount of polyaromatic hydrocarbons in water samples.[192] The contamination of the GC injection liner precluded the widespread use of this method. Polymerized ionic liquids were used to coat on the silica fiber and obtain thermally stable and reusable SPME fibers for esters[73] and amphetamine metabolite[193] determination.

So far, the works reported with ionic liquid SPME fibers were successful with mixtures containing mainly hydrophobic and semi-polar compounds. It was found in GC analyses on ionic liquid stationary phase[79,189,190] and in ionic liquid-water liquid-liquid extractions[184] that alcohols had an unusually high affinity for ILs. In this work, attention will be given to hydrophilic and polar compounds such as short chain alcohols and amines. For this purpose, completely new and different ionic liquids were prepared and tested as new adsorbents for SPME. To reduce contamination and/or loss of adsorbent, the different ionic liquid derivatives were bonded to silica microparticles that were used to prepare a porous and mechanically strong fiber coating. Both headspace and immersion techniques were tested to evaluate the capabilities of the newly developed bonded ionic liquid sorbents with a large variety of polar solutes.

5.3 <u>Experimental</u>

5.3.1 Materials and Reagents

The reagents imidazole, 1-methylimidazole, 1-hydroxyethyl imidazole, triethylene glycol, phosphorous tribromide, ethyl acetate, toluene, 4-vinyl chlorotoluene, tetrahydrofurane (THF), *n*-butanol, methylene chloride, chloroform, dioxane, butyric acid, phenol, dimethylamine, trimethylamine, pyridine and aniline were purchased from Sigma-

Aldrich, Milwaukee, WI, USA. The common HPLC solvents: acetonitrile (ACN), isopropyl alcohol (IPA), ethanol and methanol were OmniSolv™ solvents obtained from EMD Merck, Darmstadt, Germany. Kromasil spherical silica gel with 5 µm particle diameter, 10 nm pore size and 310 m^2 surface area was obtained from Supelco, Sigma-Aldrich.

The beverages tested were obtained from different local grocery stores. The standard reference material used for calibration was SRM 1828b from the National Institute of Standards and Technology (Gaithersburg, MD, USA).

5.3.2 Synthesis of the ionic liquid derivatives

5.3.2.1 Bis-hydroxyethyl imidazolium trioxyethylene derivatives

Bis-hydroxyethyl imidazolium trioxyethylene bis-(trifluoromethylsulfonyl) imide, noted $(HeIM)_2PEG_3$, $2NTf_2^-$ was synthesized following a method previously reported.[194] Trioxyethylene dibromide was reacted with hydroxyethyl imidazole, in a one to two mole ratio, in isopropyl alcohol (IPA) at 83^oC under reflux overnight. The bromide ionic liquid obtained was dissolved in methanol with Li NTf_2 and mixed for two hours. The NTf_2 ionic liquid was extracted with methylene chloride, washed with water and ether and dried in a vacuum oven with P_2O_5. It was reacted with triethoxysilane ethylisocyanate in dry ACN in a one to one mole ratio for four hours. The ethoxysilane derivative was bonded to half its weight of silica particles to give IL 1 (Figure 5.1, top). The elemental analyses and coverage are listed in Table 5.1.

5.3.2.2 1,1´-(1,6-hexanediyl)bisimidazole derivative

A 250 ml round bottom flask was filled with 100 mL anhydrous dimethylformamide (DMF) and 2.0 g sodium imidazole (22.2 mmoles). Next 3.8 mL of 1,6-dichlorohexane (3.8 mmoles) were slowly added into the DMF solution and stirred overnight at room temperature. Then the solvent was removed under reduced pressure and the resulting crude mixture was purified by column chromatography (stationary

95

phase: SiO$_2$ 20 µm, 60 Å; mobile phase: CH$_2$Cl$_2$/Methanol 9:1) to yield the desired product 1,1´-(1,6-hexanediyl) bisimidazole (88 %) (Figure 5.1, bottom).
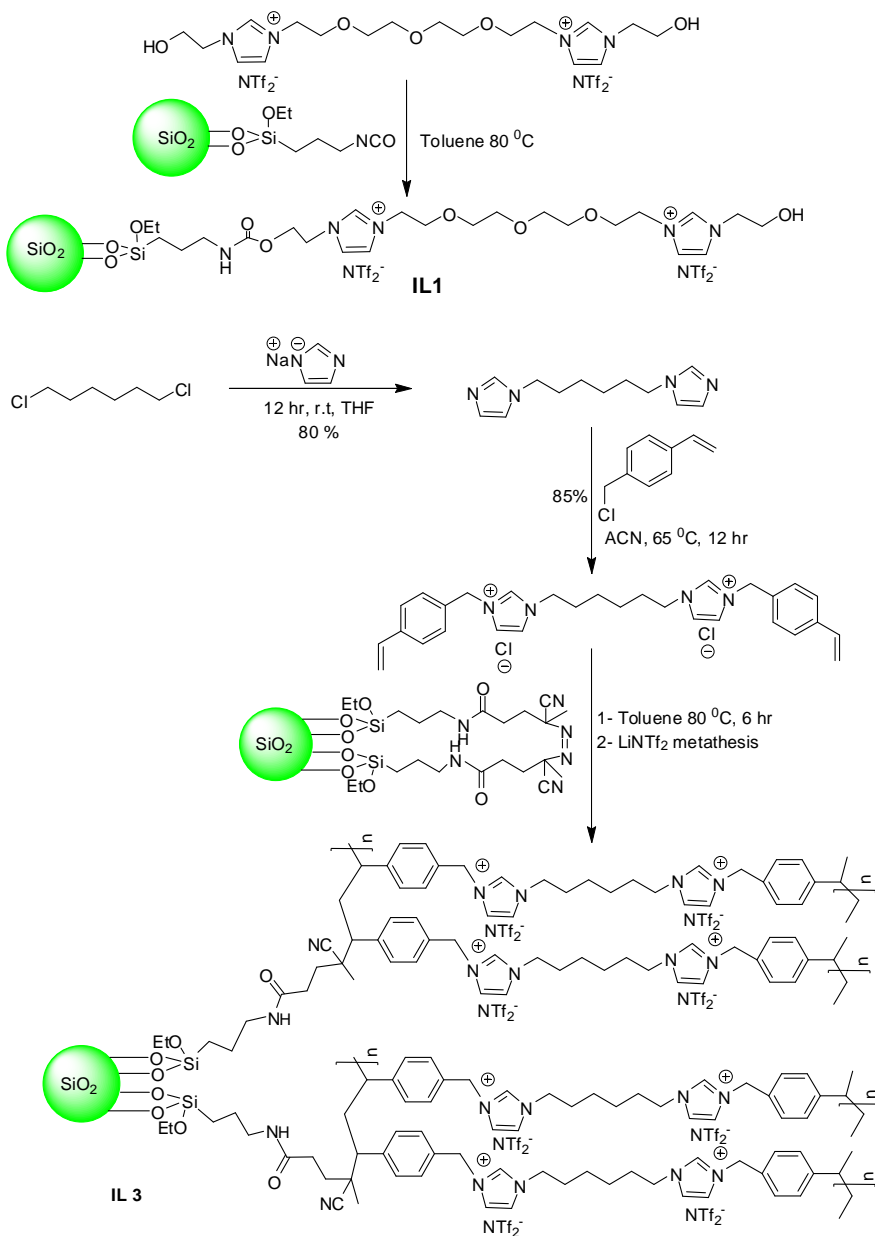
Figure 5.1 Top: Final chemical step for the attachment of the polar bonded ionic liquid derivative **1** to silica particles.Bottom: Synthesis of the polymeric bonded ionic liquid derivative **3.**

Table 5.1 Characteristics of the silica bonded ionic liquid derivative adsorbent for SPME

fiber #	bonded moiety	C%	coverage $\mu mol/m^2$
1	$(HeIM)_2PEG_3$, 2 NTf_2^-	9.2	1.5
2	$(HeIM)_2PEG_3$, 2 TfO^-	8.5	1.2
3	$[(StyrIM)_2C_6$, 2 $NTf_2^-]_n$	21	Polymeric
4	$[(StyrIM)_2C_6$, 2 $TfO^-]_n$	23	Polymeric

5.3.2.3 Styrene dicationic imidazolium monomer

One gram of 1,1´-(1,6-hexanediyl) bisimidazole (4.6 mmoles) was dissolved in 20 mL CH_3CN in a 100 mL round bottom flask. 1.5 g of 4-chloromethylstyrene (10.1 mmoles) was added with a syringe and the reaction was heated at 65^oC overnight. The reaction was then allowed to cool to room temperature and was poured into 100 mL diethyl ether. A precipitate formed immediately, and the crude product was cooled to -10^oC in the freezer. Et_2O was decanted and the product dissolved in 20 mL deionized water. The aqueous phase was washed with ethyl acetate (3×50 mL) and water was removed by reduced pressure to obtain the dicationic imidazolium monomer in the chloride form (Figure 5.1, bottom).

5.3.2.4 Synthesis of the silica bonded polymer

To a suspension of 4 g of azobis-isobutyronitrile (AIBN) derivatized silica (Supelco) in toluene was added the 1 g of dicationic monomer and the mixture was heated to 80°C for 6 h. Then it was allowed to cool to room temperature with continued stirring overnight. Next the content was filtered through fine pore sintered glass filter. The collected silica bonded polymeric product was successively washed with 100 mL of toluene, ethanol, acetone, methanol, and chloroform. The final product was dried under vacuum at 50 °C.

5.3.2.5 Metathesis reaction

The bonded silica is in the chloride form. 1 g of silica bonded ionic liquid polymer in chloride form was mixed with 3 g of sodium triflate (NaTfO) and stirred overnight. After filtration it was washed with deionized water until no white precipitate was seen testing the filtrate with dilute silver nitrate. The resulting silica bonded polymer was vacuum dried overnight to obtained the bonded silica in the triflate form. Similar metathesis was carried out to obtain the silica bonded ionic liquid polymer in its bis-trifluoromethane-sulfonimide (NTf_2^-) form. The $(StyrIM)_2C_6$, 2 TfO^- ionic liquid was prepared on a similar manner exchanging the bromide ions for triflate ions before polymerization and bonding on silica particles. Table 5.1 lists the elemental carbon analyses of the bonded silica particles.

5.3.3 Methods

5.3.3.1 Solid phase microextraction

For all headspace extraction, a Supelco SPME fiber assembly and holder Model 57330 was used with a 57357-U sampling stand, a 57358-U heater block holding 8 18-mm vials of 15 mL and a Corning PC420-D heat/stir plate, all provided by Supelco (Sigma-Aldrich). Immersion extractions were done using the Supelco fiber assembly and a Varian CX 8200 autosampler (Varian Inc. Palo Alto, CA, USA) using 2 mL mini-vials. The ionic liquid derivative bonded silica particles were sent to Supelco Bellefonte to be glued as a 50 µm layer onto SPME flexible core Nitinol wire fitting the holder (Stableflex® proprietary protocol). Figue 5.2 shows scanning electron microphotographs of Fiber 3. A very porous 50 µm layer is coated on the solid core. At high magnification (Figure 5.2, bottom) it is possible to see the polymeric IL bonded onto each silica particle. For comparison, commercial fibers were used in the same conditions as the newly developed fibers. They were a 65 µm polydimethylsiloxane / divinylbenzene fiber (PDMS/DVB)

98

Stableflex 57326-U, a 60 µm polyoxyethylene glycol (PEG) 57354-U, a 100 µm PDMS 57300-U and an 85 µm polyacrylate fiber (PA) fused silica 57304 (Supelco). Before use, all the fibers were conditioned at 220oC in the GC injection port under a flow of helium for 15 min.
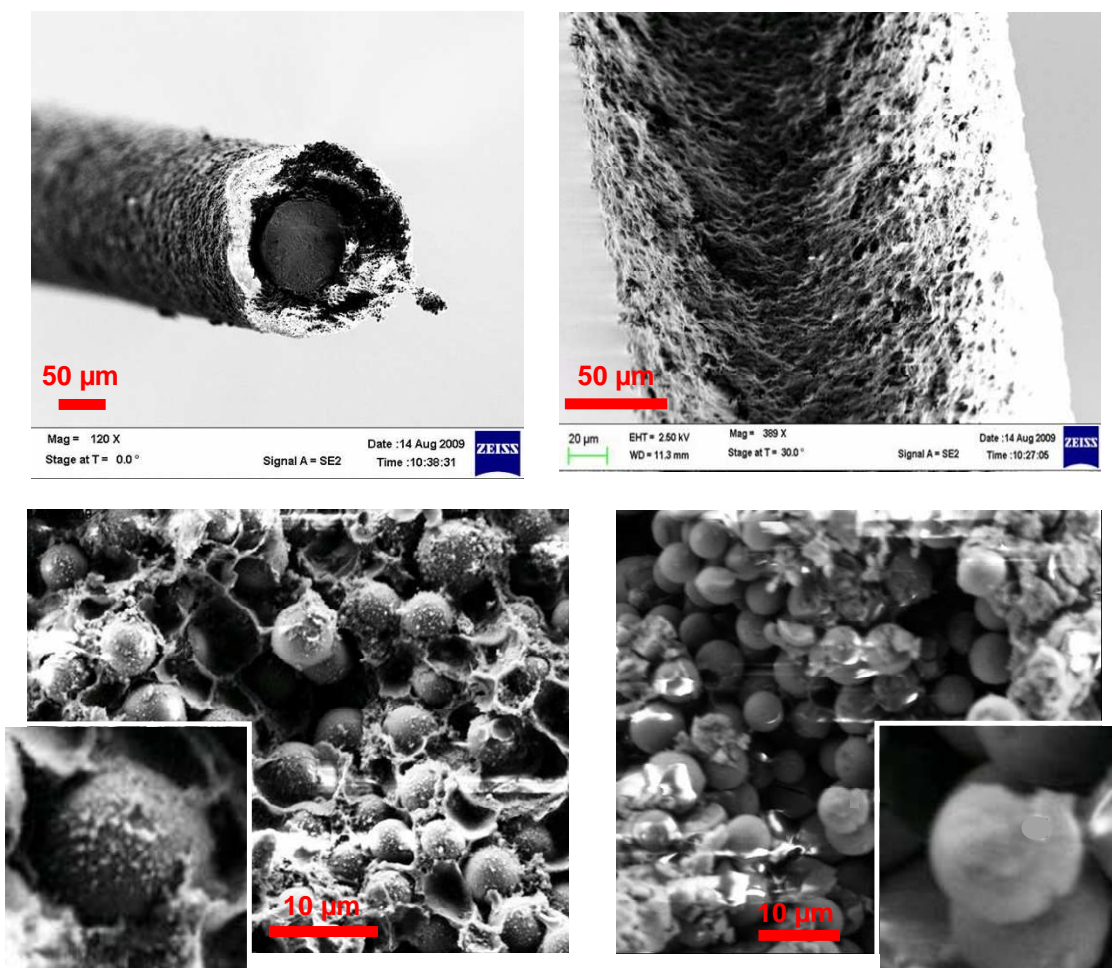
Figure 5.2 Scanning electron microphotographs of Fiber 3. Top left: side view of the fiber. Top right: granular structure of the coating due to the silica particles. Bottom right: enlargement of the coated layer showing the porous structure of the Stableflex® layer holding the bonded silica particles. The left inset is an enlargement of a single silica particle showing the IL polymeric coating as white spots covering the particles. Bottom

right: for comparison, the same procedure was followed with bare silica particles. The IL coating is not seen.

5.3.3.2 Gas chromatography

An Agilent GC 6850 was used with a split injector and FID detector both set at 300°C. A Chemstation software (Agilent, Palo Alto, CA, USA) was used to drive the chromatograph and process the chromatograms. The column for polar compounds and headspace analysis was a 30 m, 250 μm i.d., 0.25 μm film thickness Supelcowax^{TM} 10 capillary column (Supelco). The column for polar and amine compounds analyzed by immersion was a 30 m, 320 μm i.d., 4 μm film thickness SPB-1 Sulfur PDMS capillary column (Supelco). Both columns were operated with helium as the carrier gas.

5.3.3.3 SPME protocol - Headspace analysis

A known amount of the polar test compounds: ACN, methanol, ethanol, n-propanol, IPA, n-butanol, acetone, and ethyl acetate, were added to 2.5 mL distilled water in a Teflon® capped 4 mL vial. 750 mg of sodium chloride and a magnetic stir bar were added to the solution. The fiber holder needle was then inserted in the vial headspace. The fiber covered by the desired adsorbent was exposed for 15 min to the headspace vapors obtained at 50°C under fast 1000 rpm stirring. After 15 min, the fiber was retracted inside the needle and the fiber holder was withdrawn from the vial. The needle containing the fiber was next inserted into the GC split injector set with a low split ratio of 5 to 1. The fiber was immediately exposed for thermal desorption of the adsorbed compounds at 200°C for two minutes. After two minutes, the fiber was retracted inside the needle, the later being simultaneously withdrawn from the injector. The chromatogram was developed with the capillary column maintained at 50°C for 4 min followed by a temperature gradient of 15°C per min for 6 min and 40 s up to 150°C, with one minute at 150°C. The helium carrier gas linear velocity was 12 cm/s (hold up time

100

4.16 min) with an average flow rate of 0.35 mL/min. The FID solute peak areas were used for quantitation rather than the peak heights.

5.3.3.4 SPME protocol - Immersion analysis

Stock solutions of the volatile analytes were prepared at concentration in the g/L range in water. 1.2 mL of buffer at different pH and containing 30% w/v NaCl was introduced in a 2 mL vial. Spiking additions using the stock solutions were made to prepare the mixture with known concentrations of the desired analytes at the selected pH. A total of 5 to 6 extractions by fully immersing the fiber in the liquid mixture for 10 min with agitation at room temperature were made with each sample. In all cases the first extraction was excluded because results from the first extraction were usually not consistent with the remaining extractions. After 10 min the agitation is stopped, the fiber is retracted inside the needle and withdrawn for the vial for immediate GC analysis. The needle is inserted into the GC injector at 220°C or 250°C and the fiber is exposed in splitless condition for 45 s then the split is opened at a ratio of 20 to 1 (total helium flow is ~30 mL/min) for 1 min 15 s before being retracted into the needle and withdrawn from the injector. The chromatogram was developed with the capillary column maintained at 45°C for 1.5 min followed by a temperature gradient of 8°C per min for 4 min and 22 s up to 80°C, followed by a faster gradient of 20°C per min for 8 min and 30 s up to 250°C with a five minute hold at 250°C. The helium carrier gas linear velocity was 30 cm/s (hold up time 1.67 min) with an average flow rate of 1.5 mL/min. The FID detector was set at 290°C. The solute peak areas were used for quantitation rather than the peak heights.

5.4 Results and Discussion

5.4.1 Ethoxylated and polymeric alkylated ionic liquid derivatives

Polar analytes are hydrophilic. As such, they are more difficult to extract by the SPME protocol even maximizing the salting-out effect adding sodium chloride close to

the saturation concentration (359 g/L or 28% w/w).[175] SPME was used to identify the fuel used in arson cases and was very effective with gas or petroleum derivatives but was much less so when alcohols were used as fuel source igniters.[175,195] Thus enhancing the capabilities of SPME with new adsorbents that have a high affinity for polar compounds is of considerable interest. The specific affinity of ionic liquids for alcohols and polar compounds may be used for this purpose. Considering the problems due to ionic liquid coated fibers (liner contamination in the GC injector and irreproducibility)[192], a silica coated material was tailored for the task. Oxyethylene adducts were also selected to enhance to polarity of the ionic liquid derivative.

The **1** and **2** derivatives were bonded as oxyethylene adduct monomers onto the silica particle surface (Figure 5.1, top and Table 5.1). The carbon loading and moiety molecular weight (Table 5.1) allows for an estimate of the bonding density as 1.2-1.5 $\mu mol/m^2$. Such bonding density would be somewhat low for bonded silica particles dedicated to be sorbent in stationary phase HPLC. The 8.5 to 9.2 % carbon loading makes it acceptable for SPME extraction. Derivatives **3** and **4** were designed to increase even more the carbon load by polymerizing a hexyl ionic liquid monomer. The significantly higher carbon loads between 21 and 23% cannot be related to a coverage density since the additional carbon is strictly the results of the chain lengthening polymerization reaction up to the point that spots can be seen onto the silica particle surface (Figure 5.2, bottom).

The specific role of the anion in selectivity was pointed out previously.[194,196-198] Specifically, linear solvation energy relationship (LSER) studies found that the triflate anion had less proton acceptor ability than the bis-(trifluoromethylsulfonyl)imide anion (lower *b* coefficient in the Abraham LSER regression equation).[194,196,198] This is not surprising since triflyl acid is one of the strongest acids known. TfO⁻ also had a

significantly higher *a* parameter (acidity) than NTf_2^-.[194,196,198] It is then interesting to compare the effect of the anion in our ionic liquid sorbent derivatives.

5.4.2 Headspace analyses

5.4.2.1 Effect of the fiber exposure time

The same trend was observed for all studied new SPME fiber coated sorbents used in headspace extractions. The adsorbed amount of all analytes increases up to a plateau value reached after about 15 min of headspace exposure at 50^oC. A small decrease may be observed for some compounds exposed for times greater than 20 min. Figur 5.3 shows the results obtained with the polymeric IL sorbent **3** using the relative response value: {peak area (p.a.) at time t} over {p.a. at time 15 min}. The trend is the same for all compounds in this study. The absolute response in concentration depended on the nature of the solute as shown by the inset of Figure 5.3. Similar sorption-time profiles were obtained for polymeric IL coated fibers (30 min plateau time at 25^oC)[73] or IL coated fibers for amphetamine detection (20 min plateau time at 50^oC).[193]
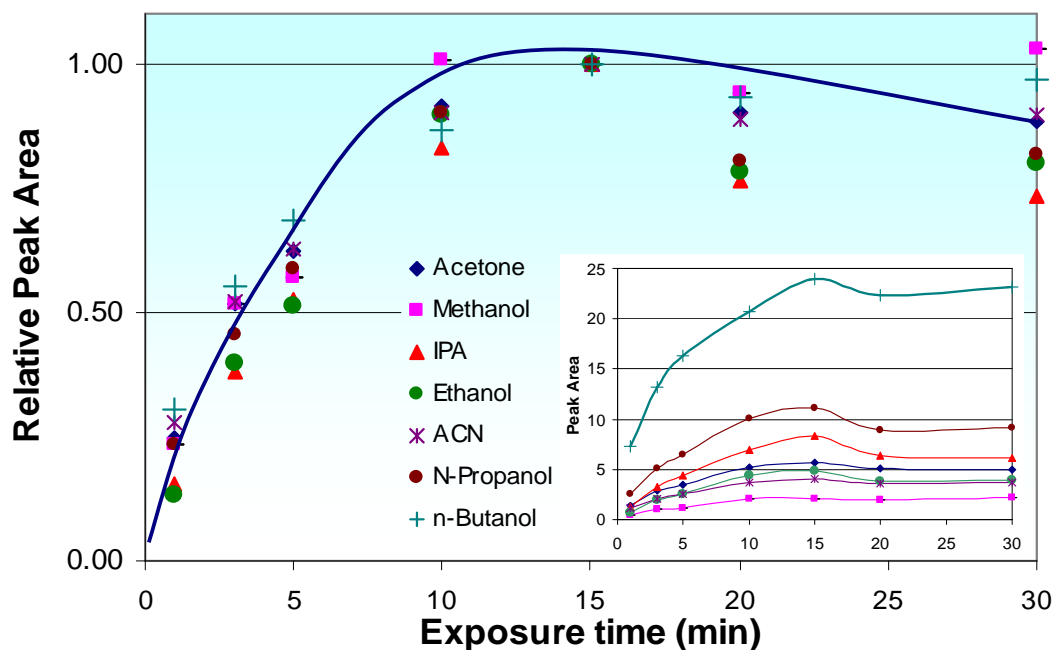
Figure 5.3 Profiles of the relative sorption expressed as [p.a. (t) over p.a. (15 min)] versus headspace exposure time for the polymeric ionic liquid 3 SPME fiber. The insert shows the corresponding raw data with peak areas (p.a.) expressed as FID picoampere time second. All solute concentrations were 5 μg/ml (ppm). Exposure temperature 50°C, 3 g NaCl added to 10 mL as salting out agent.

5.4.2.2 Extraction parameter optimization

NaCl salting out agent. Sodium chloride is added to the solution as a salting out agent. Previous work showed that the maximum amount of added NaCl produces the highest partial pressure of volatile analytes in the headspace volume and, consequently, the highest amount of analytes extracted by the fiber.[174-176,191-193] This result was confirmed with our fibers. A saturated NaCl solution at 20 °C contains 316 g/L and has a density of 1.20 g/mL. To avoid any precipitation and/or solubility problems, the amount of NaCl added to all solutions was 30% w/w (750 mg NaCl in 2.5 mL water) just below the saturation concentration.

104

5.4.2.3 Extraction temperature.

Temperature is another parameter increasing the partial vapor pressure of the analytes in the headspace volume. However, it also increases the vapor pressure of water making the pressure of the headspace volume higher than atmospheric pressure. If leaks occur, the concentration of the extracted analytes may be biased. The working extraction temperature for all headspace experiments was set at 50 $^{\circ}$C.

5.4.2.4 Analytical figures of merit

Table 5.2 lists the analytical figures of merit of the four fibers made with silica coated ionic liquid particles (as listed in Table 5.1), along with those of two commercial fibers: a polyacrylate (PA) fiber and a polydimethylsiloxane / divinylbenzene (PDMS/DVB) fiber. The listed sensitivity value is the slope of the calibration line for the given analyte extracted by the given fiber. It is expressed in {units of GC peak area} per {analyte ppm (= µg/mL) concentration}. The limits of detection (LOD) listed are given in µg/L or ppb. They were computed as the ratio of three times the baseline noise over analyte sensitivity. The curves regression coefficient and calibration ranges are also listed.

Table 5.2 Analytical figures of merit for polar solutes extracted for 15 min at 50 ^{o}C by headspace SPME with different fibers

Solute	fiber	Sensitivity p.a. per (µg/mL)	LOD µg/L or ppb	Correlation coefficient	Calibration range µg/mL or ppm
acetonitrile					
	IL 1	0.47	40	0.992	0.5-50
	IL 2	0.40	40	0.991	0.5-50
	IL 3	1.05	10	0.991	0.5-50
	IL 4	1.54	10	0.994	0.5-50
	PA	0.99	20	0.993	1-50
PDMS/DVB		1.56	10	0.998	1-50
methanol					
	IL 1	0.64	35	0.995	0.5-50
	IL 2	0.70	30	0.997	0.5-50
	IL 3	0.62	30	0.994	0.5-50
	IL 4	1.31	10	0.993	0.5-50
	PA	0.71	30	0.998	1-50
PDMS/DVB		0.70	30	0.996	1-50
ethanol					
	IL 1	0.92	20	0.993	0.5-50
	IL 2	0.91	20	0.991	0.5-50
	IL 3	0.95	20	0.993	0.5-50
	IL 4	1.76	10	0.995	0.5-50
	PA	1.33	15	0.996	1-50
PDMS/DVB		1.17	20	0.993	1-50
***n*-propanol**					
	IL 1	1.77	10	0.997	1-100
	IL 2	1.62	10	0.992	1-100
	IL 3	2.12	10	0.996	1-100
	IL 4	3.23	5	0.998	1-100
	PA	2.98	5	0.996	1-100
PDMS/DVB		3.05	7	0.997	1-100
***i*-propanol**					
	IL 1	1.29	15	0.993	1-100
	IL 2	1.31	15	0.991	1-100
	IL 3	1.56	15	0.998	1-100
	IL 4	2.66	8	0.991	1-100
	PA	2.02	10	0.995	1-100
PDMS/DVB		2.34	9	0.999	1-100
***n*-butanol**					
	IL 1	4.50	4	0.993	1-100
	IL 2	4.21	5	0.992	1-100
	IL 3	5.40	3	0.992	1-100
	IL 4	6.52	2	0.994	1-100
	PA	8.16	1	0.991	1-100
PDMS/DVB		11.5	0.5	0.992	1-100

Table 5.2 Continued

acetone					
	IL 1	0.99	20	0.996	1-100
	IL 2	0.82	25	0.993	1-100
	IL 3	1.36	15	0.997	1-100
	IL 4	1.95	10		1-100
	PA	1.25	15	0.995	1-100
	PDMS/DVB	2.60	5	0.999	1-100
ethyl acetate					
	IL 1	3.12	10	0.992	1-100
	IL 2	3.04	10	0.992	1-100
	IL 3	3.20	10	0.994	1-100
	4	4.88	5	0.995	1-100
	PA	6.59	4	0.995	1-100
	PDMS/DVB	8.70	3	0.996	1-100

Fibers 1 to 4: see full structures in Table 1; PA: polyacrylate fiber 85 μm coating thickness; PDMS/DVB: polydimethylsiloxane/divinylbenzene fiber 65 μm coating thickness; p.a.: peak area; LOD: limit of detection; ppm: part per million or mg/L; ppb: part per billion or μg/L.

The sensitivities obtained with the two monomeric IL fibers (#1 and #2, Tables 5.1 and 5.2) are clearly lower than the corresponding sensitivities obtained with the polymeric IL fibers #3 and #4. The two polymeric bonded IL fibers have a better absolute sensitivity than the commercial PA and PDMS-DVB fibers for the three lightest polar analytes: acetonitrile, methanol and ethanol. The commercial fibers PA and especially PDMS-DVB have better sensitivities than the new IL based fibers for all other tested polar compounds. Fiber #4 (bonded polymeric [(StyrIM)$_2$C$_6$, 2 TfO$^-$]$_n$, Table 5.1) showed higher absolute sensitivities than its triflate Fiber #3 counterpart for all analytes (Table 5.2). It should be noted that, with the IL coated fibers, both the binder and silica used to prepare the adsorbing layer take a significant percentage of the coating volume having limited extraction capabilities. Furthermore, the coating volume of the IL based fibers with a coating thickness of around 50 μm (Figure 2) is itself lower than the coating volume of the commercial PA fiber (85 μm) and the PDMS-DVB fiber (65 μm). To take in account these

composition and volume differences, we thought to use ethyl acetate as an internal standard to normalize the results.

Figure 4 presents the Table 5.2 absolute results as relative results i.e. plotting for each analyte the ratios of the analyte absolute response over the same fiber ethyl acetate response. This representation shows that the IL fibers have a better relative response for all selected analytes. For the polymeric bonded IL fibers #3 and #4, the short chain alcohols' relative response can be twice higher than that of the commercial fibers. For n-butanol that shows the highest absolute response for all fibers, the polymeric IL #3 (NTf_2 anion) relative response is 20% higher than the other fiber response (Figure 5.4).
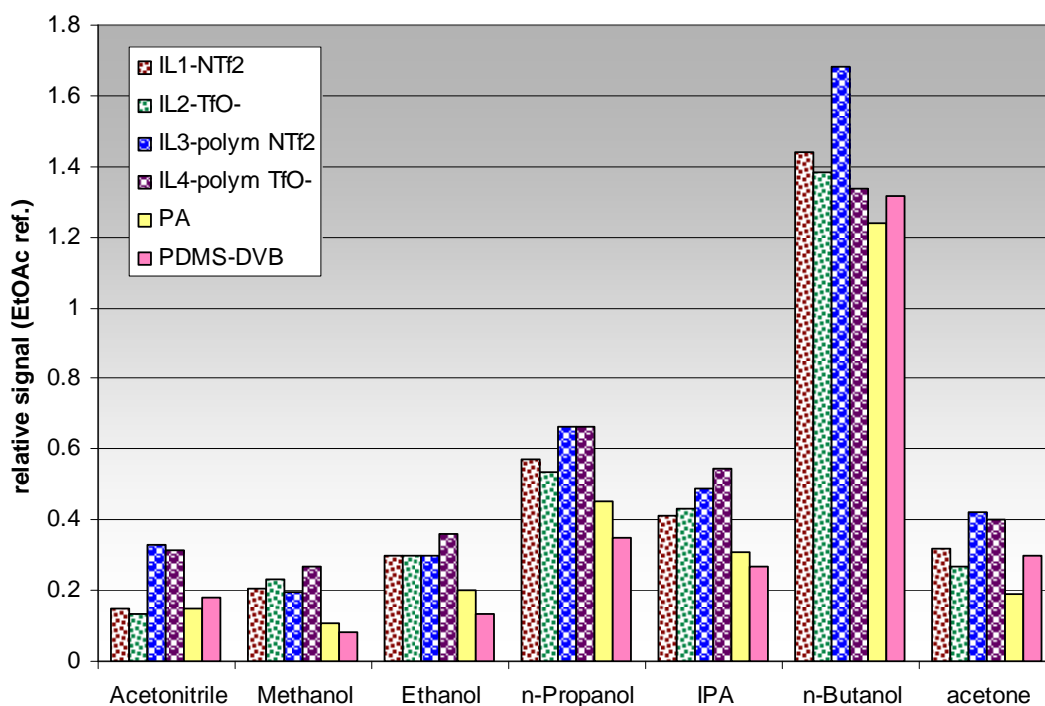
Figure 5.4 Relative response ratios of analytes in headspace analyses with four ILs and two commercial fibers. The Table 2 sensitivity factors for each analyte and each fiber are expressed as their ratio over the ethyl acetate corresponding factor to take in account the differences between adsorbent masses.

However, the relative representation of the results in Figure 5.4 shows that, except for n-butanol, there is no significant difference between the NTf_2 and TfO- IL fiber response. The higher absolute values obtained for Fiber #4 (Table 5.2) compared to Fiber #3 may be due to a higher silica particle density formed during the coating procedure. The relative response in headspace analysis for the two polymeric IL fibers is very similar being somewhat better than the two monomeric IL fibers. The enhanced affinity of ILs for short chain alcohols observed with IL gas chromatography stationary phases[79,189,190] is confirmed in headspace analysis with IL based adsorbents.

5.4.2.5 Use of the polymeric IL fiber for ethanol determination in beverages

The headspace analysis process was validated using the reference material NIST SRM 1828b and it was used with Fiber #4 to assess the ethanol content of several alcoholic beverages. A calibration curve was prepared between 5 and 100 ppm in volume (µL of ethanol per L of water). The NIST reference material is calibrated in mass. The beverage items were all labeled in ethanol %v/v. Considering the low concentrations involved, the water density was taken as 1 g mL^{-1} and the ethanol density (0.789 g mL^{-1}) was used to establish the correspondence: 1000 ppm in mass = 0.1%w/w = 0.1267%v/v. Table 5.3 lists the results obtained comparing them with the beverage labels. The relative standard deviation (RSD) on 4 experiments were between 6 and 12%. These RSDs may appear high for an analytical technique; they are the usual SRD values obtained in quantitative SPME experiments.[175-177,179, 180] The average values obtained for the SPME ethanol extraction of the two reference materials with certified 0.02% and 0.1%w/w values, were respectively 0.0193±0.0013%w/w and 0.097±0.0079%w/w validating the method with a 8% SRD.

Five different beers and two liquors were analyzed for their ethanol content. The samples were diluted using the label indication in %v/v so that the ethanol content for

SPME analysis was around 50 ppm in volume, a value in the middle of the calibration curve. Ethanol being rapidly eluted in gas chromatography, no interferences were encountered in the sample analyses. Except for the beer sample containing the highest ethanol percentage, all SPME results, including the two certified samples, were found slightly below the label values (Table 5.3). SPME headspace extraction could be used to estimate the ethanol content of blood samples in a non-destructive way.

Table 5.3 SPME results obtained with Fiber #4 in the ethanol analysis of real samples.

Sample[a]	Label indication	SPME value[b] % v/v	RSD[c]	Deviation[d]
NIST SRM 1828b	0.02%w/w or 0.0253%v/v	0.0245	7.1%	-3.2%
NIST SRM 1828b	0.1%w/w or 0.1267%v/v	0.123	8.2%	-3.1%
Miller Lite beer	3%v/v	2.9	11.7%	-3.3%
Coors original	5%v/v	4.8	9.4%	-4.0%
Shiner beer	4.4%v/v	4.3	8.6%	-2.3%
Dos Equis XX	4.2%v/v	4	7.6%	-5.0%
Steel Reserve 211	8.1%v/v	8.6	6.4%	+6.2%
Crown Royal	40%v/v	38	8.1%	-5.0%
Antique Whiskey	30%v/v	29.5	11.9%	-1.7%

a) SRM = standard reference material, the other samples were obtained from local groceries stores (Arlington, Texas).
b) Average values of 4 measurements, headspace protocol.
c) Relative standard deviation on 4 measurements.
d) Relative difference with the label indication and SPME result.

5.4.3 Immersion extractions

This study is carried out by Supelco R&D laboratories Bellefonte, PA. The protocol for immersion extractions is necessarily different from the headspace protocol (see Experimental section). Only the two polymeric fibers #3 and #4 were evaluated. Six

extractions were done successively for each sample at room temperature. The very first extraction of a new sample always gave results that differed significantly from the five following extractions, it was discarded. Ion-exchange could be responsible for this phenomenon. Since the cationic part of the IL is chemically attached to the fiber and the anion is bound by electrical interaction only, the fiber can behave as an anion-exchanger. Ion-exchange can occur between the high ionic strength solution and the fiber anions. The fiber can exchange its triflate or bis-triflylimide anions for chlorine and/or phosphate anions in the sample.

5.4.3.1 Extractions at pH 2

Since bonded silica is known to be sensitive to pH, extraction at pH 2 and pH 11 were done with different analytes. Table 5.4 lists the results obtained with the two polymeric IL fibers #3 and #4, two commercial fibers: a 60 µm thickness PEG fiber and a 100 µm thickness PDMS fiber, and same compounds that were used in headspace analyses plus a variety of other less volatile compounds. The listed values are the average value of five successive experiments. The low percent RSD for most of the extracted analytes indicate that the fibers are quite stable. The relatively higher RSD for methanol, phenol and butyric acid were associated to a response slowly declining with repeated extractions.

The IL fibers were compared to a polar 60 µm PEG coated fiber and to a non polar 100 µm PDMS coated fiber. Table 5.4 lists the sensitivity obtained for each fiber expressed as GC peak area per ppm (µg/mL) of analyte concentration. As observed in the headspace extraction study, the amount of extracting material has a great influence on the experimentally observed fiber sensitivity. Therefore, in the immersion extraction study also, ethyl acetate was used as an internal standard. Figure 5.5 presents the relative response ratios for each analyte and each fiber expressed as the absolute value

111

for analyte on a given fiber (from Table 5.4) divided by the corresponding ethyl acetate value.

Table 5.4 SPME results obtained with different fibers by immersion in two different pH solutions.

Solute	Fiber[a]	Sensitivity pH 2 p.a. per (µg/mL)	RSD[b] %	Sensitivity pH 11 p.a. per (µg/mL)	RSD[b] %
acetonitrile	IL 3	47.2	0.5%	43.5	0.8%
	IL 4	27.4	0.5%	24.3	1.2%
	PEG	67.9	2.1%		
	PDMS	15.8	1.6%		
methanol	IL 3	11.1	13.0%	25.1	1.5%
	IL 4	12.6	13.6%	25.4	2.8%
	PEG	54.0	49%		
	PDMS	6.8	17%		
ethanol	IL 3	23.2	0.9%	34.8	1.7%
	IL 4	18.5	1.2%	27.8	3.7%
	PEG	62.4	2.4%		
	PDMS	12.2	1.5%		
n-propanol	IL 3	176	0.6%	91.8	1.0%
	IL 4	97.0	2.1%	49.3	1.2%
	PEG	381	2.2%	185	-
	PDMS	123	0.8%	55	-
isopropanol	IL 3	49.4	1.3%	49.1	1.5%
	IL 4	27.2	2.8%	26.6	1.3%
	PEG	104	2.2%	96	-
	PDMS	41.4	0.6%	60	-
n-butanol	IL 3	331	1.0%	69.9	0.9%
	IL 4	131	2.6%	27.0	2.8%
	PEG	611	1.7%		
	PDMS	327	1.2%		
acetone	IL 3	78.0	0.5%	75.7	1.2%
	IL 4	32.9	1.0%	30.9	1.4%
	PEG	65.7	2.3%		
	PDMS	58.6	0.8%		
ethyl acetate	IL 3	90.3	1.1%	93.1[c]	-
	IL 4	44.8	0.9%	75.1[c]	-
	PEG	129	2.1%	290[c]	-
	PDMS	178	1.5%	1036[c]	-
	PDMS/DVB			2704[c]	-
methyl-ter-butyl ether	IL 3	235	1.2%		
	IL 4	89.8	2.8%		
	PEG	245	2.5%		
	PDMS	4580	1.2%		
dioxane	IL 3	33.7	0.9%	28.6	1.2%
	IL 4	12.1	2.6%	10.9	2.4%
	PEG	41.3	2.7%		
	PDMS	67.2	1.1%		

Table 5.4 Continued

butyric acid	IL 3	323	6.7%	ion.	-
	IL 4	143	24%	ion.	-
	PEG	585	7.8%	ion.	-
	PDMS	48.7	6.0%	ion.	-
phenol	IL 3	2200	12%		-
	IL 4	1220	12%		-
	PEG	11600	2.6%		-
	PDMS	477	7.4%		-
methylamine	IL 3	ion.	-	105	0.8%
	IL 4	ion.	-	34.7	5.6%
	PEG	ion.	-	191	-
	PDMS	ion.	-	137	-
	PDMS/DVB	ion.	-	288	-
dimethylamine	IL 3	ion.	-	135	1.7%
	IL 4	ion.	-	81	1.4%
	PEG	ion.	-	229	-
	PDMS	ion.	-	319	-
	PDMS/DVB	ion.	-	684	-
trimethylamine	IL 3	ion.	-	115	1.1%
	IL 4	ion.	-	200	1.1%
	PEG	ion.	-	213	-
	PDMS	ion.	-	2082	-
	PDMS/DVB	ion.	-	699	-
isopropylamine	IL 3	ion.	-	134	1.7%
	IL 4	ion.	-	161	0.7%
	PEG	ion.	-	470	-
	PDMS	ion.	-	492	-
	PDMS/DVB	ion.	-	1594	-
diethylamine	IL 3	ion.	-	216	1.8%
	IL 4	ion.	-	161	0.7%
	PEG	ion.	-	602	-
	PDMS	ion.	-	1220	-
	PDMS/DVB	ion.	-	3390	-
butylamine	IL 3	ion.	-	556	1.2%
	IL 4	ion.	-	353	1.8%
	PEG	ion.	-	1560	-
	PDMS	ion.	-	2334	-
	PDMS/DVB	ion.	-	9228	-
triethylamine	IL 3	ion.	-	365	1.4%
	IL 4	ion.	-	815	1.9%
	PEG	ion.	-	960	-
	PDMS	ion.	-	11570	-
	PDMS/DVB	ion.	-	12600	-

a) Fiber #3 is polymeric $[(StirIM)_2C_6, 2\ NTf_2^-]_n$; Fiber #4 is the triflate version of #3 (Table 1); PEG: polyethylene glycol, fiber 60 µm coating thickness; PDMS: polydimethylsiloxane, fiber 100 µm coating thickness; PDMS/DVB: polydimethylsiloxane divinylbenzene, fiber 65 µm coating thickness.
b) RSD: relative standard deviation on six successive extractions of the same sample.
c) Ethyl acetate decomposes in ethanol and sodium acetate at pH 11. The measurements were especially done at pH 7.
p.a.: peak area; ion.: the compound ionizes at the measurement pH.

In absolute results, Fiber #3 (polymeric IL with NTf$_2$ anion) gives higher sensitivity factor for all studied analytes compared to its counterpart Fiber #4 with the triflate anion (Table 5.4). The absolute factors for the PEG fiber are also higher than these obtained with the two IL fibers for all analytes. The picture is completely different when looking the relative fiber responses. Figure 5.5 shows that the two ILs fibers gave similar results in this relative representation. The IL fibers' results compare well with the polar PEG fiber and are clearly superior to the PDMS results except for MTBE (Figure 5.5). The relative results obtained in headspace extraction (Figure 5.4) and immersion extraction (Figure 5.5) are quite coherent. Compared to the two IL fibers, the PEG fiber seems to be slightly more efficient in immersion extractions than in headspace extractions in acidic media.

Figure 5.5 Relative response ratios of analytes in immersion analyses at pH 2 with two ILs and two commercial fibers. The Table 4 sensitivity factors for each analyte and each fiber are expressed as their ratio over the ethyl acetate corresponding factor to take in account the differences between adsorbent masses.

114

5.4.3.2 Extractions at pH 11

Phosphate buffer was used to obtain a stable pH 11 allowing an evaluation of fiber stability. Since the polymeric ionic liquids are bonded to silica particles, alkaline solutions could damage the particle and/or deteriorate the bonding. Many of the pH 2 neutral analytes and seven basic analytes were used as test solutes. Table 4 lists all the results in the two rightmost columns.

The first observation is ample stability and good reproducibility of the results at pH 11. The relative standard deviations on the experiments were similar to the pH 2 values. Experiments at different pHs were repeated with the same fibers over several months to study different mixtures. The reproducibility of the silica based fibers was comparable to that of the polymer based commercial fibers. Table 5.4 lists also the sensitivity factors obtained for seven small amines at pH 11. The two polymeric IL fibers were able to extract all tested amines with sensitivity factors equal or higher to those obtained for short chain alcohols at both pHs (Table 5.4). The amine sensitivity factors are however significantly lower than the corresponding factors obtained with the three commercial fibers. It must be pointed out that the 65 μm PDMS/DVB commercial fiber was specially designed to extract basic compounds. It did produce sensitivity factors for amines higher than those of all other fibers except for trimethylamine.

When considering these extractions in relative terms, the picture is different. Figure 5.6 (top chart) shows the relative response ratios (ethyl acetate reference compound) of the amines extracted by immersion at pH 11. The IL fiber sensitivities for the amine compounds seem significantly better than the commercial fibers sensitivities. This figure will not be commented on any further because it was not obtained with a true internal standard. The internal standard, ethyl acetate, used to prepare Figure 5.4 and Figure 5.5 is not stable at pH 11 decomposing to ethanol and sodium acetate. So its

sensitivity factor was specially measured at pH 7 meaning that the standard was not present with the amine compounds as a true internal standard should be. This could induce a bias in Figure 5.6 (top chart). Figure 5.6 (bottom chart) shows the same Table 5.4 data using n-propanol as an internal standard. n-Propanol is not the same standard as the one used in Figure 5.4 and 5.5 but is was present with the amine compounds since it is stable at pH 11. Figure 5.6 top and bottom show very similar results for the two IL fibers compared to one another and also compared to the commercial PEG fiber. The PDMS and PDMS/DVB commercial fiber relative responses look very different and much higher than those of the two IL fibers when the true internal standard n-propanol is the reference compound. Polar n-propanol is not as good as less polar ethyl acetate as an internal standard. Since n-propanol adsorbs more on the polymeric IL fibers and PEG fiber than on the less polar PDMS/DVB fiber (Figure 5.5), used as the internal standard, it tends to produce underestimated relative sensitivity factors for the IL fibers and/or overestimated factors for the PDMS based fibers. There is no definitive conclusion comparing the new polymeric IL fibers to the commercial PDMS and PDMS/DVB fibers; however, there is no doubt that the IL fibers are able to extract short amines effectively.
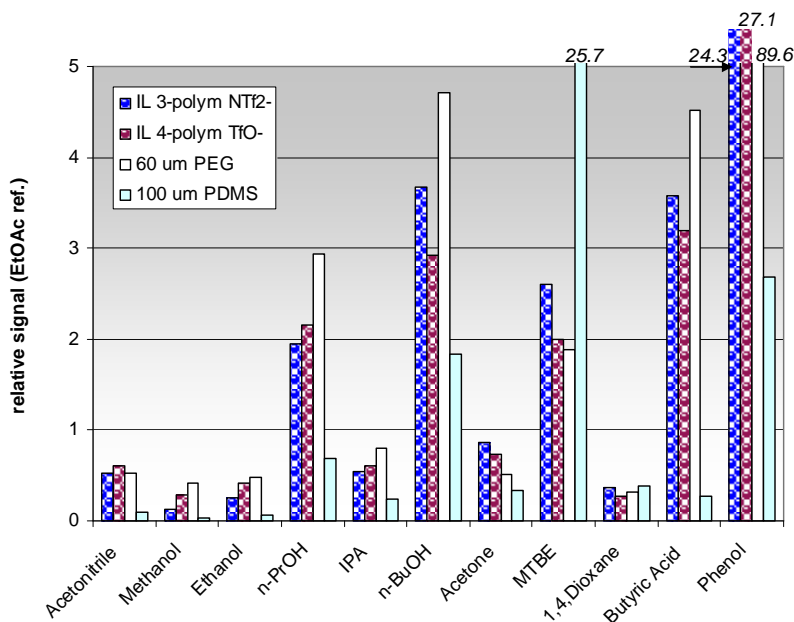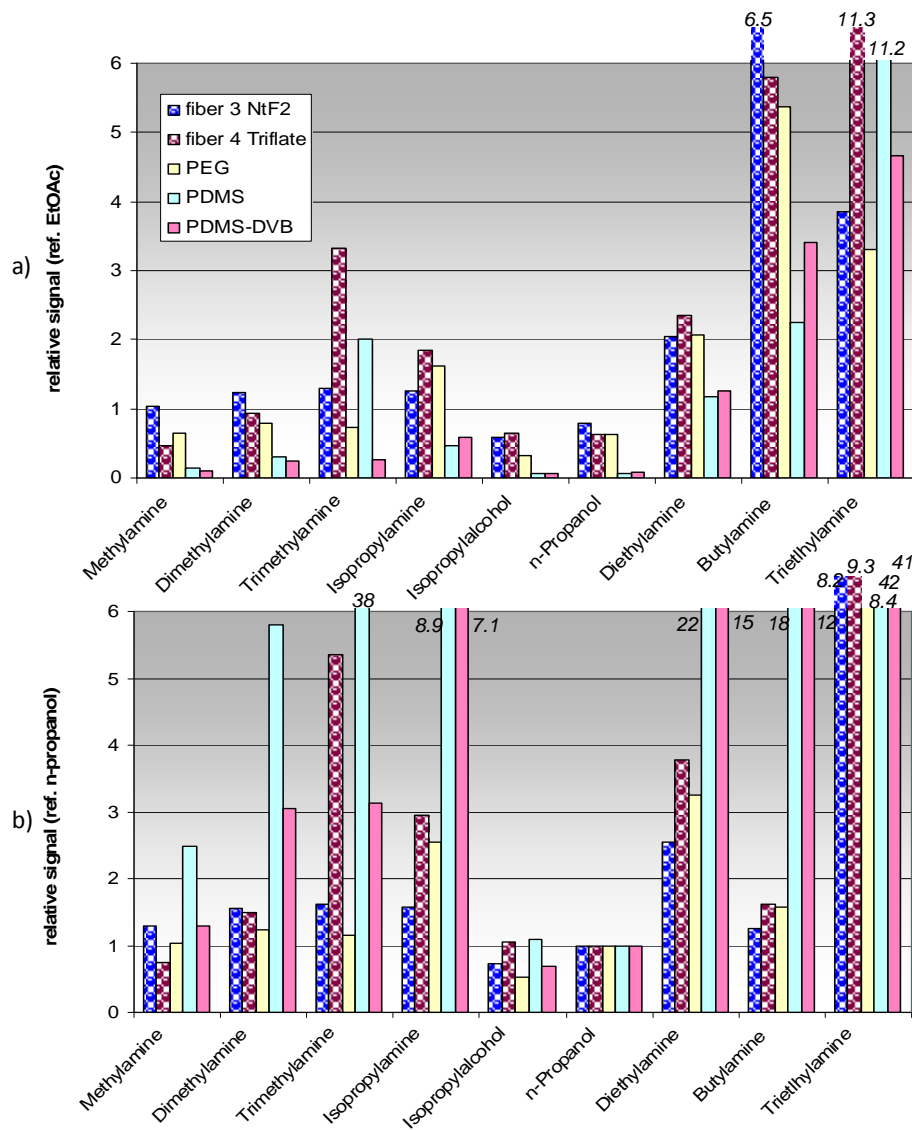
Figure 5.6 Relative response ratios of analytes in immersion analyses at pH 11 with two ILs and three commercial fibers. The Table 5.4 sensitivity factors for each analyte and each fiber are expressed as their ratio over, a) the ethyl acetate corresponding factor (obtained at pH 7) and, b) n-propanol factor to take in account the differences between adsorbent masses.

5.4.3.3 Durability of the IL fibers

The headspace procedure is very gentle process for the fibers and did not pose any durability problems. The immersion procedure put much more mechanical strain on the fiber itself since the Varian 8200 auto sampler uses a strong vibrator similar to that used in an electrical razor. It is extremely harsh on the fiber coating vibrating it at about 50 Hz. However a single triflate Fiber #4 was used to do all the more than 50 immersion experiments done in this study. If two fibers #3 were needed, it is because one broke due to improper installation into the auto sampler. The fibers were very durable. The thickness of the fiber coating remained the same. The fiber coloration did change after the initial $220^{o}C$ conditioning but remained stable and consistent after all immersions and GC analyses done for the study. No indications of visual fiber coating deterioration were noted throughout the study.

Peak tailings were observed on the GC peaks of amines. A $30^{o}C$ desorption temperature increase was tried to improve the peak shape increasing the amine desorption rate. The GC injector temperature was raised to 250 ^{o}C. No significant changes were observed in either the analyte sensitivities or the GC peak shapes. However, the IL fibers withstood this temperature increase without damage further showing their durability.

5.5 Conclusions

Ionic liquids were found to have an intermediate polarity comparing to that of ethanol.[184] Upon polymerization and bonding to silica particles, the liquid state of ILs is lost but the other unique properties, such as low volatility and polarity associating apolar and charge-charge interactions, are maintained. It was demonstrated that the polymerized IL bonded silica particles could be coated on SPME fibers to be used for the extraction of small and polar molecules. The headspace as well as the immersion SPME

protocols were used to quantitate short chain alcohols down to the 10 ppb level. The efficacy of the method was tested checking the ethanol content of a variety of beverages and a NIST standard material. Small amines were extracted using the immersion procedure at pH 11 demonstrating the stability of the polymerized IL coated silica particles. The nature of the anion, triflate or bis-triflyl amide, could influence the overall polarity of the IL. However, no clear differences were found between the two fibers made respectively with these two anions.

CHAPTER 6

COUPLING SOLID PHASE MICRO-EXTRACTION AND LASER DESORPTION

IONIZATION FOR RAPID IDENTIFICATION OF BIOLOGICAL MATERIAL

6.1 <u>Abstract</u>

Solid phase micorextraction (SPME) use small fibers directly plunged in the solution under investigation to quickly extract and quantify by different techniques the amount of selected dissolved compounds. Biological materials, peptides or proteins are accurately indentified by matrix-assisted laser desorption / ionization mass spectrometry (MALDI-MS). They are difficult to extract by SPME. This work looks for a chemical to be deposited onto fibers and able to act as a good SPME extractant as well as efficient matrix for MALDI detection.

3-Hydroxy-2-naphthoic acid (HNA) and 2-hydroxy-1-(2-hydroxy-4-sulfo-1-naphthylazo)-3-naphtoic acid (HHSNNA) were compared to two classical matrices: α-cyano-4-hydroxycinnamic acid (CHCA) and 2,5-dihydrobenzoic acid (DHB). HNA was found to be a good MALDI matrix comparing well with DHB and CHCA, while HHSNNA did not prove to be effective. Bound to silica particles, DHB and HNA were found to be god MALDI matrices. Only the wide pore silica material gave observable spectra. These particles were then attached in a thin layer onto wires to be used as fiber tips in SPME. Fibers loaded with peptides were introduced into the mass spectrometer to record fiber laser desorption ionization (FILDI) spectra. SPME-FILDI experiments could quikly identify peptides and proteins in solution.

6.2 <u>Introduction</u>

Koichi Tanaka was awarded the 2002 Nobel Prize in chemistry for developing the soft laser ionization process allowing for intact mass spectrometry of biomolecules.[199] Early on it was found that laser beams were able to desorb molecules deposited on a solid surface and ionize them.[199,200] Subsequently it was determined that certain chemicals, referred to as matrices, were able to absorb the laser light energy and transfer it to fragile molecules so that they could be volatilized and ionized without fragmentation and/or destruction.[199,201] Thus, matrix assisted laser desorption ionization (MALDI MS) became a very useful technique for biological molecules.[77]

Usually, the matrix is a relatively low molecular weight chemical that is able to absorb strongly the light energy and ionize the larger fragile molecule. For example, α-cyano-4-hydroxycinnamic acid (CHCA, m.w. 189) or dihydroxybenzoic acid (DHB, m.w. 154) are excellent MALDI matrices. However, they produce a background noise that precludes all MS analyses below m/z 190 (CHCA) or 155 (DHB). To analyze low molecular masses, it was proposed to work with non-volatile matrixes such as silica gel[202] or to bind a proton donor molecule to silica gel to enhance its ionizing power.[94,203] Such approaches have been referred to as "matrix free", however, this is somewhat of a misnomer when the matrix molecule is bonded to a support.

Solid phase micro extraction (SPME) is a solvent-free method that integrates extraction, concentration, and sample clean up in one step.[204] It can be easily coupled with different analytical instruments, especially gas chromatography (GC).[174] SPME devices incorporate an extraction fiber, usually made of a fused silica fiber or metal wire with an extractant coating.[205] The fiber is exposed to the sample using either the head-space in a closed vessel (volatile compounds) or by direct-immersion protocols (compounds in solution). Once the equilibrium between analytes and coating material is

established, desorption from the fiber coating can take place. A laser beam can be used for such desorption.[95]

Having had experience in developing new fibers for SPME extraction,[206,207] we studied the capabilities of different SPME fibers coated with porous silica particle specially grafted with proton donor molecules for laser desorption ionization MS. Different silica particles with different pore sizes were studied. Peptides and proteins were used as representative biological test materials/analytes.

6.3 Experimental

6.3.1 Chemicals

Methanol, acetonitrile, acetone were from VWR, Sugar land, Texas, USA. All peptides and proteins as well as MALDI matrices were obtained from Sigma-Aldrich, St Louis, Missouri, USA. Water was produced by a Millipore Synergy 185 water purification system (Millipore, Molsheim, France). Four different types of silica particles were obtained from Davisil® chromatographic silica of Grace Davison, Deerfield, IL. Table 6.1 lists their physicochemical properties.

6.3.2 Equipment

6.3.2.1Mass spectrometer

All data were collected on a Bruker Autoflex time-of-flight (TOF) mass spectrometer operated in reflector and linear positive ion mode with a 384 plates on a Maldi tray (Bruker Daltonics Inc., Billerica, MA, USA). The Autoflex has a N_2 laser emitting at 337 nm wavelength (pulsed UV light). The non-adjustable 337 nm laser pulse energy was 100 µJ with a pulse duration of 1 ns (pulse average peak power is 100 kW). It was possible to attenuate the laser intensity using the attenuator driven by the Bruker Flexcontrol version 3.0 software acting on the laser fluence (pulse energy combined with spot size). Attenuation is expressed in percentage of the maximum fluence. In addition

122

to attenuation, the software allows the user to adjust the pulse frequency (Hz), the TOF delay (ns), i.e. the waiting time after the laser shot to start the extraction and detection of ionized objects, and the extraction, lens and reflector potentials. The primary extraction potential was set at 19 kV and the secondary ion source at 17 kV for all polar peptide and protein analyses. In reflection mode, the lens voltage was 8.3 kV with 20 kV for the reflector voltage. The reflector gain was set at 7.5 times amplification. In linear mode, the lens voltage was 8.7 kV with a 2.5 amplification setting. Usually, 200 spectra were taken at a 10 Hz frequency in 20 s and averaged. On some occasions (silica bonded matrices essentially), however, 500 spectra were taken at 10 Hz and averaged. The apparatus was calibrated in direct mode using Cytochrome C with peaks at m/z 6181 for $[M+ 2H]^{2+}$ and m/z 12361 for $[M+H]^{+}$ and in reflection mode with Bradykinin and its peak at m/z 1061 for $[M+H]^{+}$. All results obtained with the Autoflex mass spectrometer were processed using the Bruker Daltonics Flex Analysis 3.0 software.

6.3.3 Protocols

6.3.3.1 MALDI experiments

Four different matrices were used: gentisic acid (2,5-dihydrobenzoic acid or DHB, CAS 490-79-9, m.w. 154.1), α-cyano-4-hydroxycinnamic acid or CHCA (CAS 28166-41-8, m.w. 189.2), 3-hydroxy-2-naphthoic acid or HNA (CAS 92-70-6, m.w. 188.2) and calconcarboxylic acid (2-hydroxy-1-(2-hydroxy-4-sulfo-1-naphthylazo)-3-naphthoic acid or HHSNNA, CAS 3737-95-9, m.w. 438.4) (Figure 6.1). The first two matrices are well known and used as MALDI matrices for a broad variety of compounds.[76] They will be used as reference matrices to evaluate the capabilities of the last two proton-donor molecules. The matrices were dissolved up to saturation in acetonitrile/water (1:1 v/v) with 0.1% trifluorocatic acid (TFA). 0.1 mM solutions of the studied peptides (0.1 g/mL protein solution) were prepared in water. A 10:1 mixture of matrix/peptide or 1:1 mixture

of matrix/protein was prepared and vortexed for 10 min to ensure complete mixing. 1 μL of the matrix/analyte mixture was deposited directly on a spot of the Autoflex MALDI tray and let completely dry. The tray was inserted into the Autoflex mass spectrometer and put under high vacuum. The laser was turned on at 50 to 60% power and the selected number of shots was averaged.
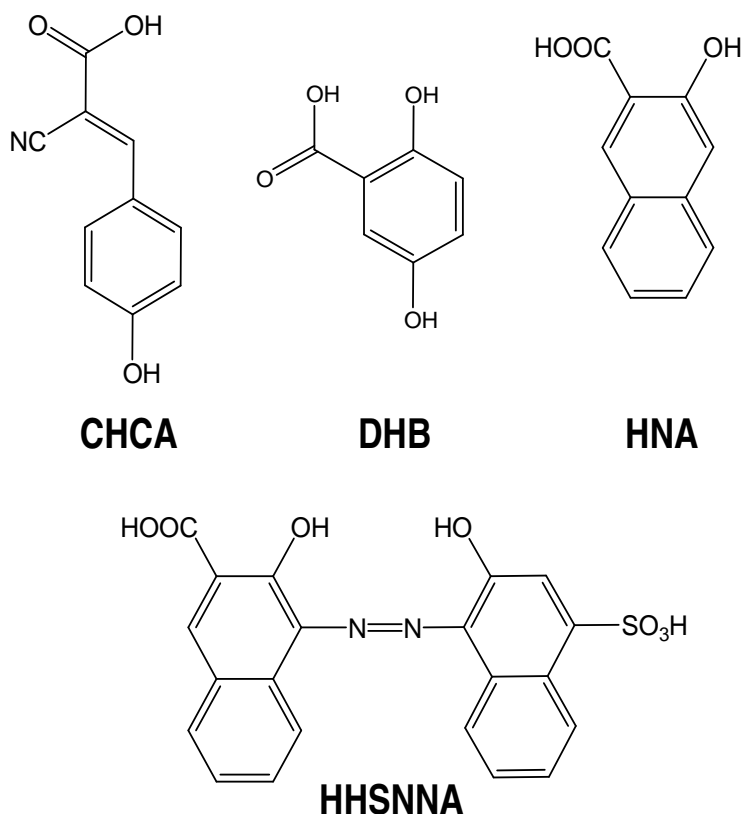
Figure 6.1 The four MALDI matrices evaluated. CHCA = α-cyano-4-hydroxycinnamic acid; DHB = 2,5-dihydroxybenzoic acid; HNA = 3-hydroxy-2-naphthoic acid; HHSNNA = calconcarboxylic acid or 2-hydroxy-1-(2-hydroxy-4-sulfo-1-naphthylazo)-3-naphthoic acid.

6.3.3.2 Silica binding chemistry

The silica surface silanols are used to bind selected proton-donor molecules. The binding procedure follows a protocol previously established.[206] A 100-ml double neck round- bottom flask was filled with 40 mL anhydrous dimethylformamide (DMF) and 4 g (26 mmoles) of DHB were added. The mixture was gently heated at 65°C. 6.4 g (also 26 mmoles) of (3-isocyanatopropyl)triethoxysilane (CAS 24801-88-5, m.w. 247.4) was drop wise added under dry nitrogen. The mixture was kept to 65°C for 12 hours. Next, 1 g of the dry selected silica particles (Table 6.1) was added at once into the DMF solution avoiding moisture entry. The mixture was heated at 110°C and stirred overnight for another 12 h reaction time. The bonded silica product was filtered and washed with DMF, water, methanol and finally acetone. It was dried for 12 h at 60°C in a vacuum oven and analyzed for carbon content. Elemental analysis gave the carbon content of the material allowing to compute the surface coverage in μmol/m^{2}. Considering that DHB has two phenol groups, it was thought that one DHB molecule could react with two isocyanate ethoxysilane bonding agents that would left some DHB molecules unreacted and then reduce the silica surface coverage. A second reaction was similarly done reacting 4 g of DHB (26 mmoles) with 52 mmoles or 12.8 g of triethoxysilane derivative. Table 6.2 lists the results in terms of carbon content and surface coverage for the four silica samples with different porosity and the two bonding conditions. Figure 6.2 illustrates the process. The same procedure was followed to bind HNA and HHSNNA to the same batches of irregular silica particles. All results in term of carbon content and surface coverage are listed in Table 6.2.

Commercial code	Particle size (μm)	Pore diameter (nm)	Pore volume (cm³/g)	Surface area (M²/g)	Bulk density (g/cm³)
LC60A	90-130	6	0.9	550	0.42
LC150A	90-130	15	1.2	320	0.35
XWP500A	90-130	50	1.1	80	0.37
XWP1500A	90-130	150	1.1	25	0.37

Davisil® porous particles are irregular in shape; the MESH size is +140.
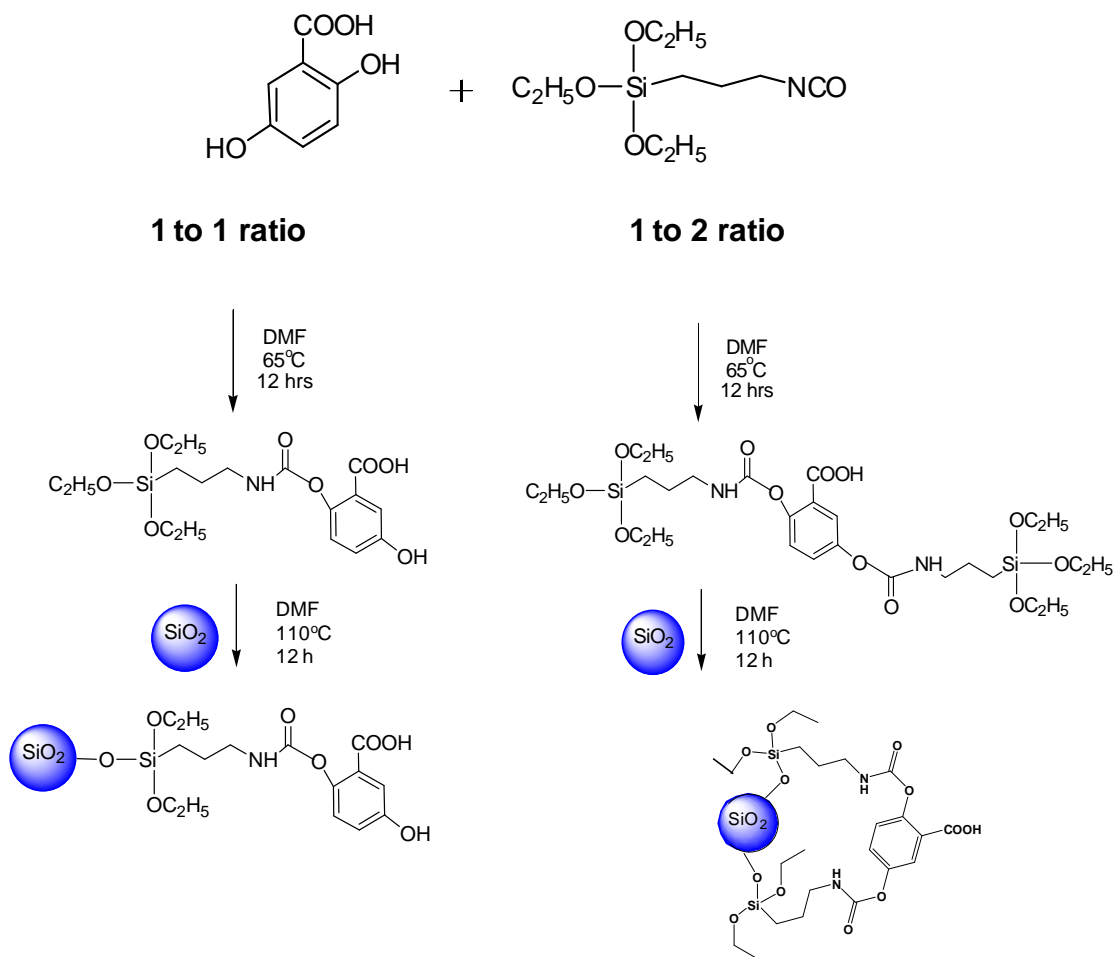
Figure 6.2 Bonding 2,5-dihydroxybenzoic acid to silica particle surface. Left: initial DHB to isocyanate ratio is 1:1; right: initial DHB to isocyanate ratio is 1:2.

126

Table 6.2 Carbon content and surface coverage of different pore size silica particles

Commercial code	Surface area (m^2/g)	DHB bonding 1:1 ratio		DHB bonding 1:2 ratio	
		Carbon load (%C)	Surface coverage[a] $(\mu mol/m^2)$	Carbon load (%C)	Surface coverage[b] $(\mu mol/m^2)$
LC60A	550	10.5	1.34	11.2	0.95
LC150A	320	6.1	1.20	6.3	0.82
XWP500A	80	2.1	1.52	2.3	1.09
XWP1500A	25	0.7	1.58	0.9	1.33
		HHSNNA bonding 1:1 ratio		HHSNNA bonding 1:2 ratio	
LC60A	550	9.1	0.57	9.5	0.49
LC150A	320	7.1	0.73	7.4	0.62
XWP500A	80	2.6	0.98	2.8	0.86
XWP1500A	25	1.0	1.17	1.1	1.04
		HNA bonding 1:1 ratio only			
LC60A	550	10.2	1.00		
LC150A	320	7.4	1.17		
XWP500A	80	1.9	1.09		
XWP1500A	25	0.6	1.10		

Davisil® 90-130 µm porous particles are irregular in shape; the MESH size is +140.
a) surface coverage computed assuming the DHB bonded moiety $SiC_{15}H_{22}O_7N$ with a molecular weight of 356 with 180 for carbon; the HHSNNA bonded moiety $SiC_{29}H_{30}O_{10}N_3S$ with a molecular weight of 640 with 348 for carbon; and the HNA bonded moiety $SiC_{19}H_{24}O_6N$ with a molecular weight of 390 with 228 for carbon.
b) surface coverage computed assuming the bonded moiety $Si_2C_{23}H_{38}O_{10}N_2$ with a molecular weight of 558 with 276 for carbon and the HHSNNA bonded moiety $Si_2C_{36}H_{46}O_{13}N_4S$ with a molecular weight of 830 with 432 for carbon.

6.3.4 Material enhanced laser desorption ionization (MELDI) experiments

Bonded silica (method 1 to 1) (20mg) was first suspended in 1 mL of acetonitrile/water 1:1 v/v mixture. After ultrasonic mixing for 5 min, 1 µL of the top of the mixture was deposited on a spot of the 384 Autoflex tray and let dry as recommended by Zhang et al.[202] Next 1 µL of the Saralasin 0.1 mM aqueous solution was deposited above the thin layer of bonded silica visible after complete dryness on the spot of the 384 Autoflex tray. The spot was again let to dry before putting the tray under high vacuum and starting MS recording. The material enhanced observed signals were very weak. The laser power was increased to 80% and 500 shots at 10Hz were averaged for 50 s. The signal was still very weak (~150 a.u. for the Saralasin sodium adduct for DHB and

HNA and all peaks were barely seen for HHSNNA) for all bonded silicas. The suspension solvent was changed for methanol/water 1:1 v/v giving greatly enhanced signals. Pure methanol was eventually selected as best suspension solvent.

6.3.5 Solid-phase microextraction (SPME)

For all headspace extractions, a Supelco SPME fiber assembly and holder Model 57330 was used with a 57357-U sampling stand, a 57358-U heater block holding eight 15-mm vials of 4.0 mL and a Corning PC420-D heat/stir plate, all provided by Supelco (Sigma-Aldrich). Immersion extractions were done with a home made adapter holding the coated wires used as SPME fibers and plunging in 2 mL mini-vials. The proton-donor chemically-bonded silica particles were sent to Supelco Bellefonte to be attached as an irregular layer onto SPME 200 μm flexible core wire (2 cm long wire coated on 1 cm, Supelco® proprietary protocol). After extraction, the SPME fiber was disconnected from the adapter and attached onto the Autoflex plate using a double sided tape for fiber laser desorption ionization (FILDI) spectrum recording.

6.4 Results and Discussion

6.4.1 MALDI spectra comparing naphthoic acid based matrices with established ones

Table 6.3 lists the average intensity obtained as the main m/z peak (one positive charge unless indicated otherwise) for the test set of peptides and proteins. The peptides cover a mass range from 570 (enkephalin) to 1700 (neurotensin). The three proteins had masses between 12360 (cytochrome C) and 66780 (bovine serum albumin, BSA).

Table 6.3 MALDI response (arbitrary intensity in abundance unit, a.u.) for peptides and proteins associated with different matrices.

Analyte	Peptide sequence	CAS number	m.w.	CHCA	DHB	HNA	HHSNNA
Angiotensin III	RVYVHPF	100900-28-5	920	1000	20,000	11,000	150
Bradykinin	RPPGFSPFR	6846-03-3	1060	3000	3500	9000	250 (+Na$^+$)
Enkephalin	YAGFL	6463-01-5	570	3900	9300	3000	800 (+Na$^+$)
Luteinizing hormone	EHWSYGLRPG	35263-73-1	1183	2000	10,000	9300	150 (+K$^+$)
β-neoandorphin	YGGFLRKYP	77739-21-0	1100	1500	16,000	6700	250 (+Na$^+$)
Neurotensin	GLYGDKPRRPYIL	58889-67-1	1673	900	1500	2000	0
Saralasin	Sar-RVYVHPA	34273-10-4	913	1000	10,000	7000	800 (+Na$^+$)
Protein	**Origin**	**CAS number**	**m.w.**	**CHCA**	**DHB**	**HNA**	**HHSNNA**
Bovin serum albumin	Bovine plasma	9048-46-8	66,776	15,000	30,000 5000 (dimer+)	10,000	noise
Cytochrome C	Bovine heart	9007-43-6	12,360	4500	23,000	3000	1200 (3+)
Myoglobin	Horse heart	100684-32-0	17,200	3500	12,000	900	2000 (3+)

Enkephalin contains the D-form of alanine when all other amino acids belong to the L-form.
Amino acid code: A = alanine; C = cysteine; D = Aspartic acid; E = glutamic acid; F = phenylalanine; G = glycine; H = histidine; I = isoleucine; K = lysine; L = leucine; M = methionine; N = Asparagine; P = proline; Q = Glutamine; R = arginine; S = serine; T = Threonine; V = valine; W = tryptophan; Y = Tyrosine.
CHCA = α-cyano-4-hydroxycinnamic acid; DHB = 2,5-dihydroxybenzoic acid; HNA = 3-hydroxy-2-naphthoic acid; HHSNNA = calconcarboxylic acid or 2-hydroxy-1-(2-hydroxy-4-sulfo-1-naphthylazo)-3-naphthoic acid; Sar = sarcosine.

6.4.2 Peptides spectra

As expected, the well-known DHB matrix performed well and produced good MALDI spectra of peptides. The HNA matrix also was effective being equivalent to DHB for saralasin and luteinizing hormone and even better for bradykinin. The HNA matrix was better than CHCA for all seven tested peptides (Table 6.3). HHSNNA does not appear to be an appropriate molecule for use as a MALDI matrix. Originally, it was thought to be a promising matrix molecule with a molecular structure showing two acid groups, carboxylic and sulfonic acids, and two strongly UV absorbing naphthyl units linked by an azo group (Figure 6.1). However HHSNNA clearly produced sub-standard results. Relatively small signals were obtained even with small and easy-to-analyze peptides such as saralasin or luteinizing hormone. Very weak (bradykinin) or no signals (neurotensin) were obtained with heavier peptides (Table 6.3).

Figure 6.3 shows four MALDI spectra of angiotensin III obtained in the same conditions with the four different matrices. It is interesting to note that HHSNNA forms more sodium and potassium adducts than proton adducts. This was not an isolated case for angiotensin III. In the case of enkephalin and β-neoandorphin and with the HHSNNA matrix, only the sodiated peak at M+23 could be seen. The protonated enkephalin peak was absent and a small peak could be barely seen at M+39 (potassium adduct). In the case of luteinizing hormone only the potassium adduct (mass+39) could be seen with the HHSNNA matrix, the protonated and sodiated ions were barely visible, buried in the background noise.
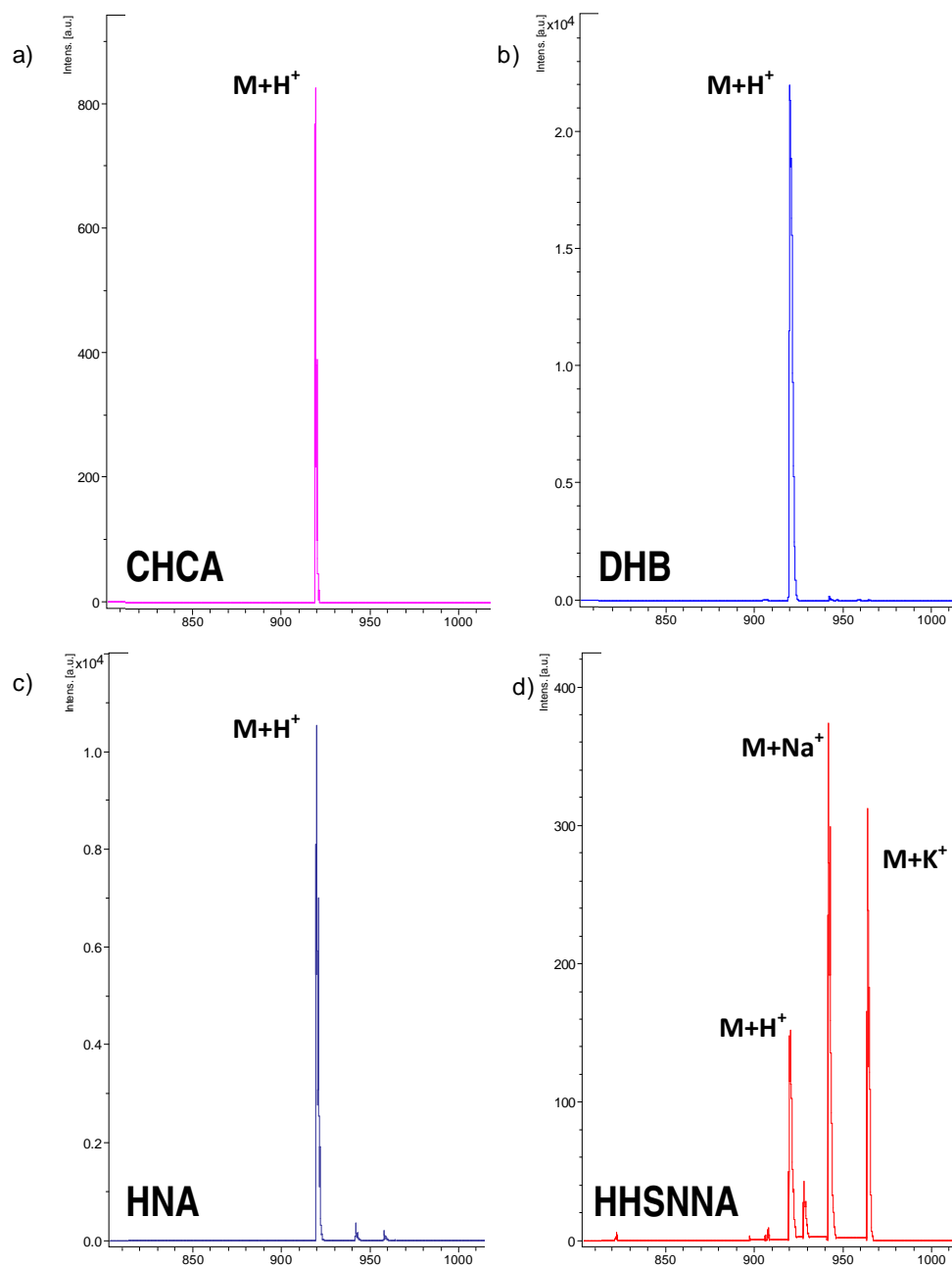
Figure 6.3 MALDI spectra of Angiotensin III obtained with four different matrices. a)CHCA, b) DHB, c) HNA and d) HHSNNA saturated solutions in acetonitrile/water 1:1 with 0.1% TFA were mixed in a 10 to 1 volume ratio with 0.1 mM Angiotensin III solution in water. Peaks are labeled by nature of the flying ion. Abscissas show the m/z value. Protonated Angiotensin III: m/z=921; sodium adduct: m/z = 943; potassium adduct: m/z = 959.

6.4.3 Protein spectra

Similar results were obtained with the higher m/z range proteins. The DHB matrix gave the best results. CHCA and HNA produced reasonable signals, while HHSNNA was ineffective for all proteins. All matrices produced multiple charged ions (2 or 3 charges) as seen at reduced m/z values for cytochrome C (Figure 6.4). However, with the HHSNNA matrix only the ion bearing three charges can be seen at m/3 around 4000. The background noise is so high that some degradation of the protein is suspected.
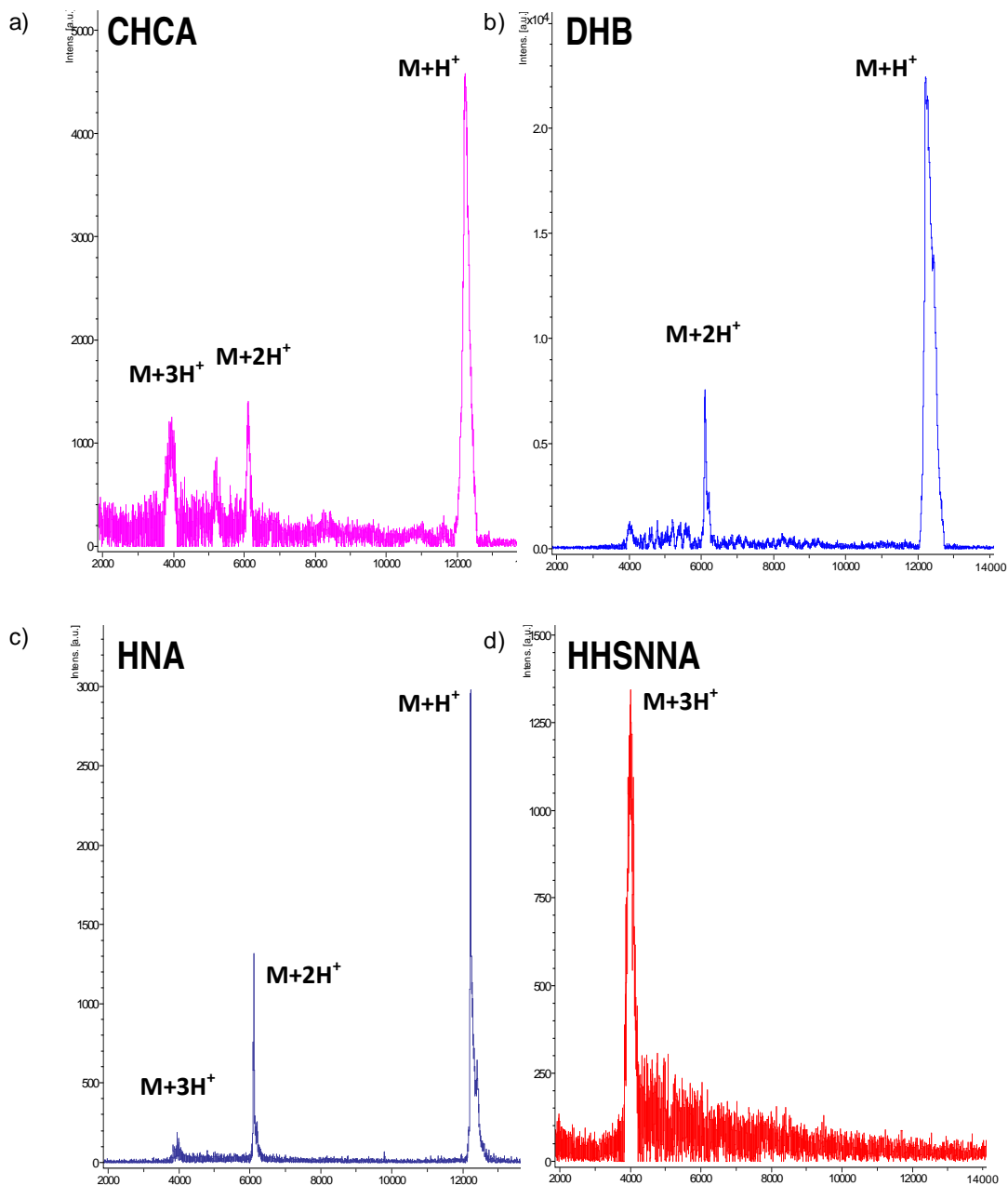
Figure 6.4 MALDI spectra of Cytochrome C obtained with four different matrices. a) CHCA,
b) DHB, c) HNA and d) HHSNNA saturated solutions in acetonitrile/water 1:1 with 0.1% TFA
were mixed in a 10 to 1 volume ratio with 0.1 mM of protein solution in water. Peaks are
labeled by nature of the flying ion. Abscissas show the m/z value. Protonated Cytochrome C:
m/z =12361; dual charge at m/z =6182; triple charge at m/z =4123.

133

6.4.4 Material enhanced laser desorption ionization (MELDI)-MS with bonded silica particles

The idea to use the surface of solid non-volatile materials to enhance the laser desorption-ionization (MELDI) was proposed a decade ago.[202] Mainly it was used to obtain sensitive spectra of low molecular weight molecules such as sugars,[94] metabolites or cholic acids.[203]

6.4.5 Binding matrices to silica surface

The chemistry of silica is well known and used to modify silica particles using the surface silanols always present at an average surface concentration of 8 µmol/m^2.[208-210] The first reaction step (Figure 6.2) couples the matrix with the ethoxysilane compound. The second step is the attachment onto the silica surface, an ethoxysilane group reacting with a silanol group to make the silica-matrix binding. Since the reaction is very sensitive too moisture, it is performed under dry nitrogen minimizing all vessel openings. The intermediate matrix-ethoxysilane compound (Figure 6.2) is not purified nor checked because of its moisture sensitivity. The procedure allowed obtaining bonding densities between 0.5 and 1.6 µmol/m^2. The highest coverage was obtained with DHB giving surface coverages higher than 1.2 µmol/m^2 for all four silica particle batches. The small pore particles had a DHB coverage similar to that of the wide pore particles. This means that the bonding chemistry is not sensitive to silica pore size within the tested pore size limits 6 nm – 150 nm. The procedure worked well with HNA and HHSNNA producing the bonded silica materials listed in Table 6.2. However, the HNA surface coverage is 20% lower than the DHB coverage, being between 1 and 1.2 µmol/m^2. The HHSNNA coverage is even lower showing a pore size effect. The large pore particles show a 1-1.2 µmol/m^2 coverage, similar to the HNA coverage, but the small pore particles show a significantly reduced coverage: 0.57 µmol/m^2 and 0.73 µmol/m^2 for the 6 and 15 nm pore diameter particles, respectively. Steric exclusion of the larger HHSNNA bonding moiety from the smaller pores may explain the observed reduced bonding densities.

Both of the two DHB and HHSNNA phenolic groups can be carbamoylated producing two points of attachment for the intermediate ethoxysilane. This did not increase the bonding density. On the contrary, it was decreased by about 30% for the DHB matrix silica and 12% for the HHSNNA matrix silica (Table 6.2). The bonding densities obtained after a 1-to-1 DHB/siloxane reaction were in the 1.5 $\mu mol/m^2$ and 1 $\mu mol/m^2$ range for DHB and HHSNNA, respectively (Table 6.2) with a maximum coverage of the large pore (150 nm) silica particles. The 1-to-2 DHB/siloxane reaction did give a small increased carbon load but the calculation of the bonding density actually showed a 30% or 12% decrease of the surface coverage decreasing to only 1 or 0.8 $\mu mol/m^2$ for DHB or HHSNNA, respectively (Table 6.2). It can be speculated that the larger moieties attach on two nearby silanols hindering access to vicinal silanols. The single derivatized moieties attach on a single silanol group forming a "brush type" surface cover leaving surrounding silanols more accessible for a denser grafting.

6.4.6 MELDI experiments

6.4.6.1 Optimizing suspension solvent

The suspension solvent was found to be critical for good MELDI spectra. The effective acetonitrile/water 1:1 v/v mixture used for typical MALDI experiments does not work well with bonded silica particles. Methanol/water and especially pure methanol gave better signals with all matrix bonded silicas (Figure 6.5). Experiments done with materials bonded following the 1-to-2 method produced very similar results.
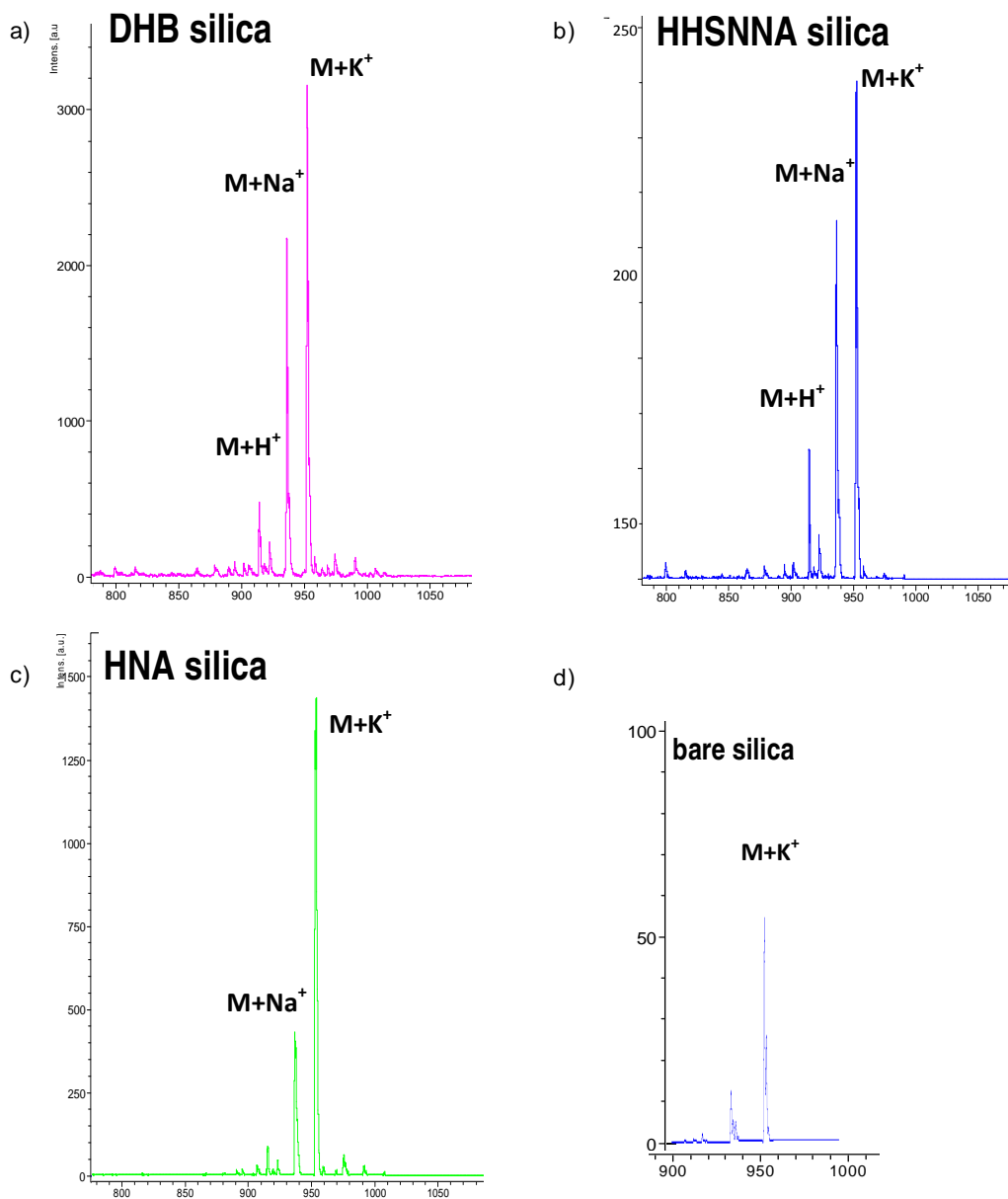
Figure 6.5 MELDI spectra of Saralasin mixed with three different matrix bonded silicas. a) DHB silica, b) HHSNNA silica, c) HNA silica and d) bare silica. Davisil® 150 nm silica bonded with the 1-to-1 procedure (Table 6.3). The fourth Saralasin MELDI spectrum was obtained with underivatized bare 150 nm silica. 20 mg/mL methanol suspension of the bonded silica was deposited and dried on the tray. Next a 0.1 mM Saralasin solution in water was added on the thin silica layer. Abscissas show the m/z value. Protonated Sarasalin: m/z = 914; sodium adduct: m/z = 936; potassium adduct: m/z = 952.

136

6.4.6.2 Alkali adducts due to silica matrix

Figure 6.5 shows the similarity of the saralasin spectra obtained with the DHB, HNA and HHSNNA matrices, all showing three peaks at exactly the same m/z position: m/z 914 for protonated sarasalin; m/z 936 for its sodium adduct, and m/z 952 for the potassium adduct. The alkali earth adducts are favored compared to the protonated ions. Presumably, this is due to the significant sodium and potassium concentrations in the silica gel material obtained by precipitation of alkali silicates.[210] Such disappearance of the protonated ion in MELDI experiment with modified silica particles was previously observed with peptide solutes.[202] These results shows the important effect of the silica material in the laser desorption and ionization. Metal ions are essential chemical agents for ionization of analytes in MELDI with modified silica gel particles as matrices.[94,202,211] Using underivatized 150 nm pore diameter silica particles as support, a spectrum of saralasin was obtained showing only the sodium and potassium adducts with a weak but detectable intensity (lower right spectrum of Figure 6.5). When using neat DHB and HNA, as MALDI matrices, the signals obtained were two orders of magnitude greater in intensity than those obtained with HHSNNA (Table 6.3). The corresponding DHB and HNA bonded material produced peak abundances only two to three times higher than the corresponding values obtained with the HHSNNA bonded silica (Figure 6.5).

6.4.6.3 Silica pore size effect

As soon as the first modified silica gels for MELDI were prepared, it was noted that the silica pore size had a critical effect.[94,211] Figure 6.6 shows four overlaid MELDI spectra obtained with the same peptide, sarasalin 0.1 mM, deposited on a thin layer of the four DHB bonded silica particles of different pore size: 6, 15, 50 and 150 nm (Table 6.2).
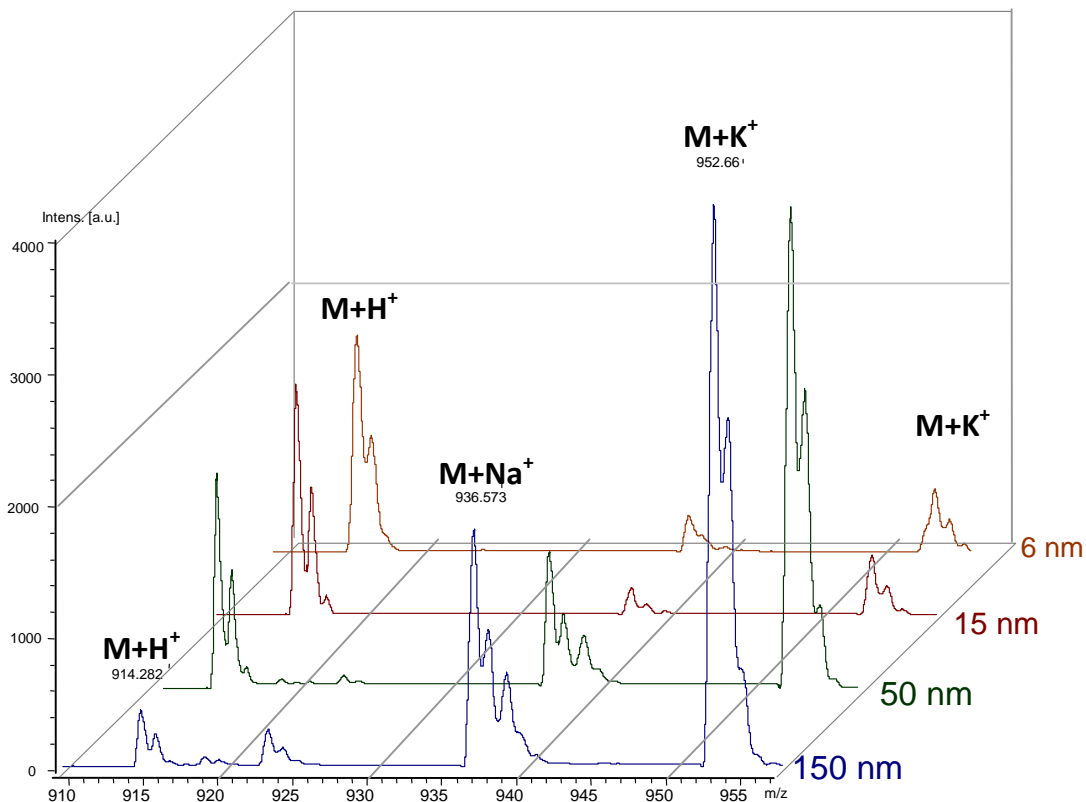
Figure 6.6 Overlaid m/z 909-957 MELDI spectra of Saralasin mixed with DHB bonded silicas of four different pore sizes. Davisil® silica bonded with the 1-to-1 procedure (Table 6.2). 20 mg/mL methanol suspension of the bonded silica was deposited and dried on the tray. Next a 0.1 mM Saralasin solution in water was deposited on the thin silica layer. Protonated Sarasalin: m/z = 914; sodium adduct: m/z = 936; potassium adduct: m/z = 952.

The protonated ion [M+H]$^+$ was clearly seen on 6 and 15 nm small pore DHB bonded silicas and on larger 50 nm silica with a similar intensity around 1500 a.u. The [M+H]$^+$ sarasalin intensity dropped to 400 a.u. on the 150 wide pore DHB bonded silica. Fig. 5 was prepared using mass spectra obtained cumulating the signal of 500 laser shots on the same spot (see experimental section). Absolute intensities varying by more than 50% were obtained with spectra of the same silica taken on different spots, but the trend was always observed: 6, 15

and 50 nm particles have similar [M+H]$^+$ intensities three to five times higher than the larger pore 150 nm particles.

An opposite trend is observed for the two alkali earth adducts [M+Na]$^+$ and [M+K]$^+$. The intensities of the two adducts gradually increase as the silica pore diameters increase (Figure 6.6). The Figure 6.6 sodium adduct intensities were respectively 100, 120, 1060 and 1810 a.u. with the 6, 15, 50 and 150 nm pore diameter silicas. The corresponding values for the potassium adduct were respectively 310, 400, 3450 and 4020 a.u. In a recent study on the effect of silica pore size on MELDI signal it was found that wide pore silica derivatives (30 and 100 nm) produced high signal intensities for oligosaccharides on both protonated and sodium adduct ions. Some differences between ion adducts were also noted.[94] In a study using small (~7000 daltons) proteins, the wide pore modified silica particles produced greatly enhanced signals for all adducts.[211]

Size exclusion effects were first envisaged to explain the low signals obtained on small pore particles with protein solutes: the large molecules may not enter the small pores. Matrix diffusion into the support pores and protein diffusion were thought to be responsible for the effect.[211] It was shown that increasing pore size as well as particle size both improved signal intensity even with small analytes.[94] So it can be thought that large pore particle are well exposed to the laser light when small and tortuous pores may block the laser light quenching analyte desorption. Similarly, considering that the laser spot size is about a square millimeter, smaller 5 µm particles arranged in a multilayer coat may be less irradiated than a monolayer of larger 100 µm particles.[94] Another possible important factor in favor of large pore particles is that the gas phase plume formed by laser heat can escape more easily a large cavernous pore than a small pore where it hit the wall or media surface.

6.4.6.4 Bonded silica coated fibers for Solid Phase Micro Extraction

DHB, HNA and HHSNNA 50 and 150 nm bonded silica (1-to-1 procedure) were attached as an irregular monolayer onto flexible 200 μm metallic wires fitting the home-made SPME holder.[12] The SPME assembly can be directly dipped in a solution to extract its content.
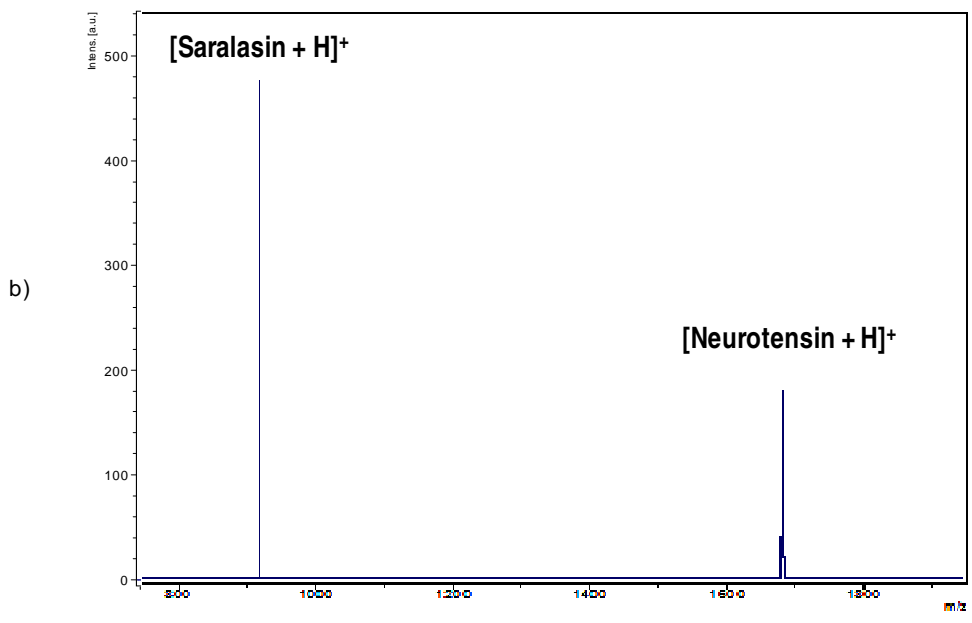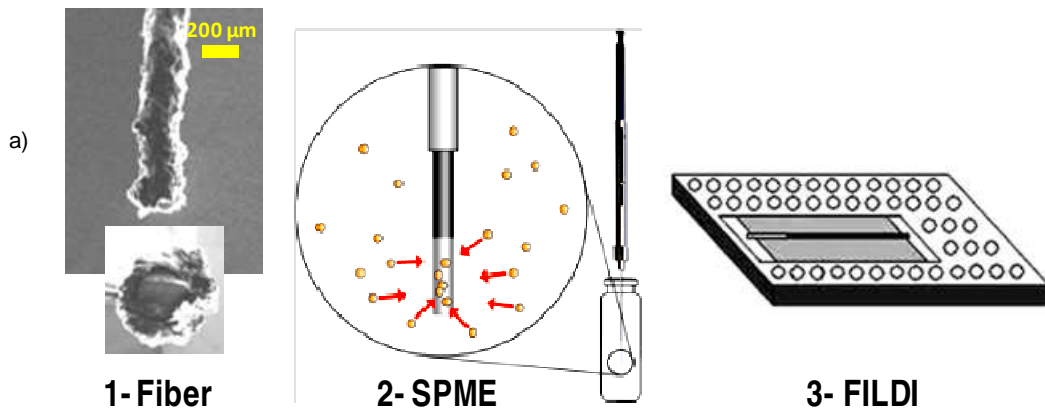
Figure 6.7 Fiber laser desorption ionization (FILDI) mass spectrometry of a mixture of 0.1 mM Saralasin and 0.1 mM Neurotensin in water. The figure a) from left to right: **1-**scanning electron micrograph of the DHB silica (150 nm pore diameter) coated fiber with a cut view showing the 80 μm composite irregular layer attached on the metallic core (fiber diameter ~360 μm, internal metal wire diameter 200 μm), **2-**scheme of the SPME assembly, direct fiber immersion at room temperature for 30 min, and **3-**setting the fiber on the Autoflex tray with a double side tape. The figure b): Mass spectrum showing the Saralasin peak at 914 and the Neurotensin peak at 1674. 80% laser energy, average value of 500 shots at 10 Hz for 50 s.

Figure 6.7 illustrates the process showing a scanning electron micrograph of the cut tip

of a fiber along with the SPME holder extracting components and, after extraction, the

positioning of the tip on the Autoflex MALDI tray. The bottom of the Figure 6.7 shows the fiber laser desorption ionization (FILDI) mass spectra obtained with a mixture of 0.1 mM of both saralasin and neurotensin peptide and a fiber coated with DHB bonded 150 nm silica. The peak intensities are in the few hundredths a.u. range. The saralasin peak shows only the protonated $[M+H]^+$ peak and no alkali adduct as was observed using the same DHB bonded silica (compare Figure 6.7 and Figure 6.5). It seems that the polymer used to attach the silica particles on the fiber wire quenched the silica effect during the laser plume formation responsible for solute ionization. Only the silica bonded DHB protonated the extracted peptides. The observed signals could be weak because the concentration of DHB is limited (Table 6.2).

6.5 Conclusions

The chemistry occurring in the plume formed by the laser light impacting solid matter is still not fully understood.[203] In this study we observed a very different response of the same proton donor molecule (i) used as a classical matrix in MALDI spectra, (ii) bonded to silica in MELDI experiments and (iii) the molecule bonded silica particles being coated on a fiber in SPME-FILDI experiments. DHB, one of the most efficient MALDI matrices, was again found to be effective with peptides and proteins in MALDI experiments. When bound to silica particles, DHB produced efficient material in MELDI experiments. The signals obtained with DHB silica particles coated on a fiber in SPME-FILDI experiments were satisfying. A potentially useful molecule as MALDI matrix, HHSNNA with both a carboxylic acid and a strong sulfonic acid groups, was not as effective as expected in all conditions. HNA seems to be a good candidate as proton donor MALDI matrix. Its behavior when bonded to silica particles is comparable to DHB. Efficient bonded silica particles can be bonded to SPME fibers and used in that mode as well.

CHAPTER 7

GENERAL CONCLUSION

The second and third chapters of this dissertation focus on the development of new chiral stationary phases. Enantiomerically pure Ruthenium (Ru) polypyridyl complexes containing amine groups were attached to the silica gel forming bonded chiral stationary phases. The best Ru-complex CSP was obtained using a reductive amination binding reaction. The Ru complex-bonded CSP provided enantioselectivity toward a wide variety of compounds, in particular, compounds with acidic groups in the polar organic mode and binaphthyl type compounds in the normal phase mode.

Two aromatic-functionalized cyclofrucan chiral stationary phases, R-naphthylethyl-carbamate cyclofructan 6 (RN-CF6) and dimethylphenyl-carbamate cyclofructan 7 (DMP-CF7), were synthesized and evaluated by injecting various classes of chiral analytes including acidic, basic, neutral organic compounds, and metal complexes. In general, better separation of amine containing compounds was obtained on the RN-CF6 stationary phases, while the DMP-CF7 column worked more effectively for acidic compounds in most cases.

Chapter four describes the enantiomeric separation of tetrahydrobenzimidazole intermediates by HPLC and CE. Here, seventeen chiral tetrahydrobenzimidazole compounds were subjected to enantioselective HPLC and CE analyses using cyclodextrin, cyclofructan and its derivatives. In HPLC, the Cyclobond RN and LARIHC CF6-P yielded enantiomeric selectivities for the greatest number of racemates while the Cyclobond DMP phase showed the greatest number of baseline separations towards the analytes. In CE, HP-γ-CD was the most successful chiral additive for the enantiomeric recognition for racemic tetrahydrobenzimidazole analytes. Although IP-CF6 could not provide baseline separation on most of the compounds, it

showed enantiomeric selectivity on a specific compound that was not separated with native or derivatized cyclodextrins.

Chapter five discusses the bonded polymeric ionic liquid materials for solid phase microextraction. It was demonstrated that the polymerized IL bonded silica particles could be coated on SPME fibers to be used for the extraction of small and polar molecules. Headspace as well as immersion SPME protocols were used to quantitate short chain alcohols down to the 10 ppb level. The efficacy of the method was tested checking the ethanol content of a variety of beverages and a NIST standard material. Small amines were extracted using the immersion procedure at pH 11 demonstrating the stability of the polymerized IL coated silica particles.

The last chapter (chapter 6) describes the coupling of solid phase microextraction and laser desorption ionization for rapid identification of biological materials. In this study proton donor molecules were evaluated in several different ways; (i) as a classical matrix in MALDI spectra, (ii) bonded to silica in MELDI experiments and (iii) the molecule bonded silica particles being coated on a fiber in SPME-FILDI experiments. DHB, one of the most efficient MALDI matrices for peptides and proteins. When bound to silica particles, DHB produced efficient material in MELDI experiments. The signals obtained with DHB silica particles coated on a fiber in SPME-FILDI experiments were satisfying. HNA seems to be a good candidate as proton donor MALDI matrix. Its behavior when bonded to silica particles is comparable to DHB.

APPENDIX A

PUBLICATION INFORMATION OF CHAPTER 2 - 7

Chapter 2: A manuscript published in Journal of Liquid Chromatography & Related Technologies. Sun, P; Perera, S; MacDonnell, F.M; Armstrong,D.W, 2006, 29, 1847-1860

Chapter 3: A manuscript published in Analyst. Sun.P; Wang, C; Padivitage, N.L.S; Nanayakkara,Y.S; Perera. S; Qui, H; Zhang.Y; Armstrong,D.W, 2011, 136, 787-800.

Chapter 4: A manuscript in press in Chirality. Perera, S; Na,Yun-Cheol; Doundoulakis, T; Ngo, V.J; Feng, Q; Breitbach, Z.S; Lovely, C.J; Armstrong, D.W.

Chapter 5: A manuscript published in Analytical and Bioanalytical Chemistry. Perera, S; Wanigasekara, E; Crank, J. A; Sidisky, L; Shirey, R; Berthod, A; Armstrong, D. W (2010), 396(1), 511-524.

Chapter 6: A manuscript published in Rapid Communications in Mass Spectrometry Perera, S; Berthod, A; Dodbiba, E; Armstrong, D. W. 2012, 26, 853-862

REFERENCES

(1) Karger, B.; Snyder, L.; Horvath, C. In *An Introduction to separation science;* Wiley: New York, 1973.

(2) Snyder, L.; Glajch, J.; Kirkland, J. In *Practical HPLC method development; W*iley: New York, 1988.

(3) Poole, C.; Poole, S. In *Chromatography Today;* Elsevier: New York, 1991.

(4) Ahuja, S. In *Selectivity and Detectability Optimization in HPLC;* Wiley: New York, 1989.

(5) Ahuja, S. In ACS Symposium Series # 297; American Chemical Society: Washington DC, 1986.

(6) Pasteur, L. *Ann. Chim. Phys.* **1848***, 24*, 442.

(7) Aboul-Enein, H. Y.; Ali, I. In *Chiral separations by liquid chromatography and related technologies;* Marcel Dekker: New York, 2003; pp 1-20.

(8) White, C. A.; Subramanian, G. In *A practical appoach to chiral separatios by liquid chromatography;* VCH Publishers: New York, 1994; pp 1-17.

(9) Pearson, R. M.; Ridgway, E. J.; Johnston, A.; Vadukul, J. *Adv. Contracept.* **1985***, 1*, 103-8.

(10) Chijioke, P. C.; Pearson, R. M. *Contraception* **1986***, 34*, 207-11.

(11) Ahuja, S. In Chiral Separations: Applications and Technology; American Chemical Society: Washington, DC, 1997; pp 1-7.

(12) Food and Drug, A. *Chirality* **1992***, 4*, 338-340.

(13) Poole, C. F. In The Essence of Chromatography; Elsevier Science B. V.: Amsterdam, The Netherlands, 2003; pp 1-78.

(14) Ettre, L. S.; Horvath, C. *Anal. Chem.* **1975***, 47*, 422.

(15) Miller, J. M. In Chromatography: Concepts and Contrasts; John Willey and Sons: Hoboken, NJ, 2005; Vol. 2 nd Edition, pp 35-66.

(16) Lough, W. J. In Lough, W. J., Wainer, I. W., Eds.; Chirality in Natural and Applied Science; Blackwell Science: Oxford, UK, 2002; pp 179-202.

(17) Armstrong, D. W. In Issaq, H. J., Ed.; A Century of Separation Science; Dekker: New York, 2002; pp 555-578.

(18) Armstrong, D. W.; Zhang, L. K.; He, L.; Gross, M. L. *Anal. Chem.* **2001***, 73*, 3679-3686.

(19) Davankov, V. A. *Chromatographia* **1989***, 27*, 475-82.

(20) Davankov, V. A. *Chirality* **1997***, 9*, 99-102.

(21) Mikes, F.; Boshart, G. J.; Gil-Ave, E. *J. Chromatogr.* **1976***, 122*, 205-221.

(22) Mikes, F.; Boshart, G. J. *Chromtogr.* **1978***, 149*, 455-464.

(23) Pirkle, W. H.; Pochapsky, T. C. *J. Am. Chem. Soc.* **1986***, 108*, 352-354.

(24) Pirkle, W. H.; Welch, C. J. *Tetrahedron: Asymmetry* **1994***, 5*, 777-780.

(25) Maier, N. M.; Franco, P.; Lindner, W. *J. Chromatogr. , A* **2001***, 906*, 3-33.

(26) Laemmerhofer, M.; Lindner, W. *J. Chromatogr. A* **1996***, 741*, 33-48.

(27) Hermansson, J. J. *Chromatogr.* **1983***, 269*, 71.

(28) Allenmark, S.; Bomgren, B.; Boren, H. *J. Chromatogr.* **1983***, 269*, 63.

(29) Haginaka, J.; Seyama, C.; Kanasugi, N. *Anal. Chem.* **1995***, 67*, 2579.

(30) Yokoyama, H.; Ikeuchi, H.; Teranishi, Y.; Murayama, H.; Sano, K.; Sawada, K. Japan Patent 2,282,147, 1995.

(31) Okamoto, Y.; Aburatani, R.; Hatano, K.; Hatada, K. *J. Liq. Chromatogr.* **1988***, 11*, 2147-63.

(32) Okamoto, Y.; Kawashima, M.; Yamamoto, K.; Hatada, K. *Chem. Lett.* **1984***, 5*, 739.

(33) Ichida, A.; Shibata, T.; Okamoto, I.; Yuki, Y.; Namikoshi, N.; Toga, Y. *Chromatographia* **1984***, 19*, 280.

(34) Tachibana, K.; Ohnishi, A. *J. Chromatogr. , A* **2001***, 906*, 127-154.

(35) Zhang, T.; Kientzy, C.; Franco, P.; Ohnishi, A.; Kagamihara, Y.; Kurosawa, H. *J. Chromatogr. , A* **2005***, 1075*, 65-75.

(36) Zhang, T.; Nguyen, D.; Franco, P.; Murakami, T.; Ohnishi, A.; Kurosawa, H. *Anal. Chim. Acta* **2006***, 557*, 221.

(37) Gasparrini, F.; Misiti, D.; Rompietti, R.; Villani, C. *J. Chromatogr. , A* **2005***, 1064*, 25-38.

(38) Han, X.; Wang, C.; He, L.; Beesley, T. E.; Armstrong, D. W. *Anal. Bioanal. Chem.* **2007***, 387*, 2681-2697.

(39) Yuki, H.; Okamoto, Y.; Okamoto, I. *J. Am. Chem. Soc.* **1980***, 102*, 6356-6358.

(40) Liu, Y.; Lantz, A. W.; Armstrong, D. W. *J. Liq. Chromatogr. & Rel. Technol.* **2004***, 27*, 1121.

(41) Helgeson, R.; Timko, J.; Moreau, P.; Peacock, S.; Mayer, J.; Cram, D. J. *J. Am. Chem. Soc.* **1974***, 96*, 6762.

(42) Sogah, G. D.; Cram, D. J. *J. Am. Chem. Soc.* **1976***, 98*, 3038.

(43) Newcomb, M.; Toner, J.; Helgeson, R.; Cram, D. J. *J. Am. Chem. Soc.* **1979***, 101*, 4941.

(44) Shinbo, T.; Yamaguchi, T.; Nishimura, K.; Sugiura, M. *J. Chromatogr.* **1987***, 405*, 145-53.

(45) Hilton, L.; Armstrong, D. W. *J. Liq. Chromatogr.* **1991***, 14*, 9.

(46) Armstrong, D. W.; DeMond, W. *J. Chromatogr. Sci.* **1984***, 22*, 411-415.

(47) Armstrong, D. W.; Ward, T. J.; Armstrong, R. D.; Beesley, T. E. *Science* **1986***, 232*, 1132-1135.

(48) Stalcup, A. M.; Chang, S. C.; Armstrong, D. W. *J. Chromatogr.* **1991***, 540*, 113-128.

(49) Armstrong, D. W.; Stalcup, A. M.; Hilton, M. L.; Duncan, J. D.; Faulkner, J. R., Jr.; Chang, S. C. *Anal. Chem.* **1990***, 62*, 1610-15.

(50) Chang, S. C.; Reid, G. L. I.; Chen, S.; Chang, C. C.,; Armstrong, D. W. *Trends Anal. Chem.* **1993***, 12*, 144-153.

(51) Armstrong, D. W.; Tang, Y.; Chen, S.; Zhou, Y.; Bagwill, C.; Chen, J. *Anal. Chem.* **1994***, 66*, 1473-1484.

(52) Peter, A.; Torok, G.; Armstrong, D. W. *J. Chromatogr. , A* **1998***, 793*, 283-296.

(53) Karlsson, C.; Karlsson, L.; Armstrong, D. W.; Owens, P. K. *Anal. Chem.* **2000***, 72*, 4394-4401.

(54) Berthod, A.; Valleix, A.; Tizon, V.; Leonce, E.; Caussignac, C.; Armstrong, D. W. *Anal. Chem.* **2001***, 73*, 5499-5508.

(55) Torok, G.; Peter, A.; Armstrong, D. W.; Tourwe, D.; Toth, G.; Sapi, J. *Chirality* **2001***, 13*, 648-656.

(56) Liu, Y.; Berthod, A.; Mitchell, C. R.; Xiao, T. L.; Zhang, B.; Armstrong, D. W. *J. Chromatogr.* **2002***, 978*, 185-204.

(57) Mitchell, C. R.; Armstrong, D. W.; Berthod, A. *J. Chromatogr. A* **2007***, 1166*, 70-78.

(58) Berthod, A.; Xiao, T. L.; Liu, Y.; Jenks, W. S.; Armstrong, D. W. *J. Chromatogr. A* **2002***, 955*, 53-69.

(59) Berthod, A.; Valleix, A.; Tizon, V.; Leonce, E.; Caussignac, C.; Armstrong, D. W. *Anal. Chem.* **2001***, 73*, 5499-5508.

(60) Kawamura, M.; Uchiyama, K. *Carbohydr. Res.* **1994***, 260*, 297-304.

(61) Kawamura, M.; Uchiyama, K. *Carbohydr. Res.* **1989***, 192*, 83-90.

(62) Mori, H.; Nishioka, M.; Nanjo, F. Japan Patent 2006067896, 2006.

(63) Mori, H.; Nishioka, M.; Nanjo, F. Japan Patent 2006067895, 2006.

(64) Nishioka, M.; Mori, H.; Nanjo, F. Japan Patent 2004337132, 2004, 2004.

(65) Fang, Y.; Ferrie, A. M. US Patent 2005048648, 2005, 2005.

(66) Sun, P.; Armstrong, D. W. *J. Chromatogr. , A* **2010***, 1217*, 4904-4918.

(67) Sun, P.; Wang, C.; Padivitage, N. L. T.; Nanayakkara, Y. S.; Perera, S.; Qiu, H.; Zhang, Y.; Armstrong, D. W. *Analyst (Cambridge, U. K.)* **2011***, 136*, 787-800.

(68) Belardi, R. G.; Pawliszyn, J. *Water Pollut. Res. J. Can.* **1989***, 24*, 179.

(69) Jiang, G.; Huang, M.; Cai, Y.; Lv, J.; Zhao, Z. *J. Chromatogr. Sci.* **2006***, 44*, 324-332.

(70) Pawliszyn, J.; Editor. In *Applications of Solid Phase Microextraction;* Royal Soc. Chem: 1999; pp 655.

(71) Dietz, C.; Sanz, J.; Camara, C. *J. Chromatogr. , A* **2006**, *1103*, 183-192.

(72) Liu, J.; Li, N.; Jiang, G.; Liu, J.; Joensson, J. A.; Wen, M. *J. Chromatogr. , A* **2005**, *1066*, 27-32.

(73) Zhao, F.; Meng, Y.; Anderson, J. L. *J. Chromatogr. , A* **2008**, *1208*, 1-9.

(74) Karas, M.; Hillenkamp, F. *Anal. Chem.* **1988**, *60*, 2299-301.

(75) Juhasz, P.; Costello, C.E.; Biemann, K. *J Am Soc Mass Spectrom* **1993**, *4*, 399-409.

(76) Beavis, R. C.; Chaudhary, T.; Chait, B. T. *Org. Mass Spectrom.* **1992**, *27*, 156-8.

(77) Karas, M.; Bahr, U.; Strupat, K.; Hillenkamp, F.; Tsarbopoulos, A.; Pramanik, B. N. *Anal Chem* **1995**, *67*, 675-679.

(78) Wasserscheid, P.; Keim, W. *Angew Chem Int Ed* **2000**, *39*, 3772-3789.

(79) Armstrong, D.W,: He, L.F,; Liu, Y. S. *Anal Chem* **1999**, *71*, 3873-3876.

(80) Armstrong, D. W.; Zhang, L.; He, L.; Gross, M. L. *Anal. Chem.* **2001**, *73*, 3679-3686.

(81) Crank, J. A.; Armstrong, D. W. *J. Am. Soc. Mass Spectrom.* **2009**, *20*, 1790-1800.

(82) Berthod, A.; Crank, J. A.; Rundlett, K. L.; Armstrong, D. W. *Rapid Commun. Mass Spectrom.* **2009**, *23*, 3409-3422.

(83) Peterson, D. S. *Mass Spectrom. Rev.* **2007**, *26*, 19-34.

(84) Wei, J.; Buriak, J. M.; Siuzdak, G. *Nature* **1999**, *399*, 243-6.

(85) Shen, Z.; Thomas, J. J.; Averbuj, C.; Broo, K. M.; Engelhard, M.; Crowell, J. E.; Finn, M. G.; Siuzdak, G. *Anal. Chem.* **2001**, *73*, 612-9.

(86) Cuiffi, J. D.; Hayes, D. J.; Fonash, S. J.; Brown, K. N.; Jones, A. D. *Anal. Chem* **2001**, *73*, 1292-1295.

(87) Hutchens, T. W.; Yip, T. T. *Rapid. Commun. Mass Spectrom.* **1993**, *7*, 576-580.

(88) Vlahou, A.; Schellhammer, P. F.; Mendrinos, S.; Patel, K.; Kondylis, F. I.; Gong, L.; Nasim, S.; Wright, G. L., Jr. *Am. J. Pathol.* **2001**, *158*, 1491-1502.

(89) Wulfkuhle, J. D.; McLean, K. C.; Paweletz, C. P.; Sgroi, D. C.; Trock, B. J.; Steeg, P. S.; Petricoin, E. F. 3. *Proteomics* **2001**, *1*, 1205-15.

(90) Austen, B. M.; Frears, E. R.; Davies, H. *J. Pept. Sci.* **2000***, 6*, 459-469.

(91) Xu, S. Y.; Li, Y. F.; Zou, H. F.; Qiu, J. S.; Guo, Z.; Guo, B. C. *Anal Chem* **2003***, 75*, 6191-6195.

(92) Go, E. P.; Apon, J. V.; Luo, G.; Saghatelian, A.; Daniels, R. H.; Sahi, V.; Dubrow, R.; Cravatt, B. F.; Vertes, A.; Siuzdak, G. *Anal. Chem.* **2005***, 77*, 1641-1646.

(93) LIn, Y. S.; Chen, Y. C. *Anal. Chem.* **2002***, 74*, 5793-5798.

(94) Hashir, M. A.; Stecher, G.; Bakry, R.; Kasemsook, S.; Blassnig, B.; Feuerstein, I.; Abel, G.; Popp, M.; Bobleter, O.; Bonn, G. K. *Rapid Commun. Mass Spectrom.* **2007***, 21*, 2759-2769.

(95) Teng, C.; Chen, Y. *Rapid Commun. Mass Spectrom.* **2003***, 17*, 1092-1094.

(96) Hinze, W. L.; Riehl, T. E.; Armstrong, D. W.; DeMond, W.; Alak, A.; Ward, T. *Anal. Chem.* **1985***, 57*, 237-42.

(97) Okamoto, Y.; Kawashima, M.; Hatada, K. *J. Am. Chem. Soc.* **1984***, 106*, 5357-9.

(98) Pirkle, W. H.; Pochapsky, T. C. *Adv. Chromatogr. (N. Y.)* **1987***, 27*, 73-127.

(99) Yamagishi, A.; Soma, M. *J. Am. Chem. Soc.* **1981***, 103*, 4640-2.

(100) Yamagishi, A.; Ohnishi, R. *J. Chromatogr.* **1982***, 245*, 213-18.

(101) Yamagishi, A. *J. Chromatogr.* **1983***, 262*, 41-60.

(102) Yamagishi, A. *J. Am. Chem. Soc.* **1985***, 107*, 732-4.

(103) Nakamura, Y.; Yamagishi, A.; Matumoto, S.; Tohkubo, K.; Ohtu, Y.; Yamaguchi, M. *J. Chromatogr.* **1989***, 482*, 165-73.

(104) Smith, G. F.; Cagle, F. W., Jr. *J. Org. Chem.* **1947***, 12*, 781-4.

(105) Sullivan, B. P.; Salmon, D. J.; Meyer, T. J. *Inorg. Chem.* **1978***, 17*, 3334-41.

(106) Goss, C. A.; Abruna, H. D. *Inorg. Chem.* **1985***, 24*, 4263-7.

(107) Sun, P.; Krishnan, A.; Yadav, A.; Singh, S.; MacDonnell, F. M.; Armstrong, D. W. *Inorg. Chem. (Washington, DC, U. S.)* **2007***, 46*, 10312-10320.

(108) Bodige, S.; MacDonnell, F. M. *Tetrahedron Lett.* **1997***, 38*, 8159-8160.

(109) Armstrong, D. W.; Tang, Y.; Chen, S.; Zhou, Y.; Bagwill, C.; Chen, J. *Anal. Chem.* **1994***, 66*, 1473-84.

(110) Nilsson, K.; Larsson, P. O. *Anal. Biochem.* **1983***, 134*, 60-72.

(111) Svensson, L. A.; Karlsson, K. *J. Microcolumn Sep.* **1995***, 7*, 231-7.

(112) Kim, M.; MacDonnell, F. M.; Gimon-Kinsel, M. E.; Du, B., Thomas; Asgharian, N.; Griener, J. C. *Angew. Chem. , Int. Ed.* **2000***, 39*, 615-619.

(113) Gillard, R. D.; Hill, R. E. E. *J. Chem. Soc. , Dalton Trans.* **1974**, 1217-36.

(114) Gillard, R. D.; Hill, R. E. E.; Maskill, R. *J. Chem. Soc. A* **1970**, 707-10.

(115) Yamagishi, A. *J. Chromatogr.* **1985***, 319*, 299-310.

(116) Ekborg-Ott, K. H.; Kullman, J. P.; Wang, X.; Gahm, K.; He, L.; Armstrong, D. W. *Chirality* **1998***, 10*, 627-660.

(117) Ming, Y.; Zhao, L.; Zhang, H.; Shi, Y.; Li, Y. *Chromatographia* **2006***, 64*, 273-280.

(118) Stalcup, A. M. *Annu. Rev. Anal. Chem.* **2010***, 3*, 341-363.

(119) Armstrong, D. W.; Faulkner, J. R., Jr.; Han, S. M. *J. Chromatogr.* **1988***, 452*, 323-30.

(120) Armstrong, D. W.; Chang, C. D.; Lee, S. H. *J. Chromatogr.* **1991***, 539*, 83-90.

(121) Hargitai, T.; Kaida, Y.; Okamoto, Y. *J. Chromatogr.* **1993***, 628*, 11-22.

(122) Zhong, Q.; He, L.; Beesley, T. E.; Trahanovsky, W. S.; Sun, P.; Wang, C.; Armstrong, D. W. *Chromatographia* **2006***, 64*, 147-155.

(123) Okamoto, Y.; Aburatani, R.; Fukumoto, T.; Hatada, K. *Chem. Lett.* **1987**, 1857-60.

(124) Okamoto, Y.; Kaida, Y. *J. Chromatogr. , A* **1994***, 666*, 403-19.

(125) Okamoto, Y.; Yashima, E. *Angew. Chem. , Int. Ed.* **1998***, 37*, 1021-1043.

(126) Okamoto, Y.; Sakamoto, H.; Hatada, K.; Irie, M. *Chem. Lett.* **1986**, 983-6.

(127) Czerwenka, C.; Laemmerhofer, M.; Maier, N. M.; Rissanen, K.; Lindner, W. *Anal. Chem.* **2002***, 74*, 5658-5666.

(128) Gyimesi-Forras, K.; Akasaka, K.; Laemmerhofer, M.; Maier, N. M.; Fujita, T.; Watanabe, M.; Harada, N.; Lindner, W. *Chirality* **2005**, *17*, 134.

(129) Gyimesi-Forras, K.; Leitner, A.; Akasaka, K.; Lindner, W. *J. Chromatogr. , A* **2005**, *1083*, 80-88.

(130) Hoffmann, C. V.; Pell, R.; Laemmerhofer, M.; Lindner, W. *Anal. Chem. (Washington, DC, U. S.)* **2008**, *80*, 8780-8789.

(131) Krawinkler, K. H.; Maier, N. M.; Sajovic, E.; Lindner, W. *J. Chromatogr. , A* **2004**, *1053*, 119-131.

(132) Krawinkler, K. H.; Maier, N. M.; Ungaro, R.; Sansone, F.; Casnati, A.; Lindner, W. *Chirality* **2003**, *15*, 17.

(133) Lammerhofer, M.; Franco, P.; Lindner, W. *J. Sep. Sci.* **2006**, *29*, 1486-1496.

(134) Kawamura, M.; Uchiyama, T. *Denpun Kagaku* **1992**, *39*, 109-16.

(135) Jiang, C.; Tong, M.; Breitbach, Z. S.; Armstrong, D. W. *Electrophoresis* **2009**, *30*, 3897-3909.

(136) Sun, P.; Wang, C.; Breitbach, Z. S.; Zhang, Y.; Armstrong, D. W. *Anal. Chem.* **2009**, *81*, 10215-10226.

(137) Zhang, Y.; Breitbach, Z. S.; Wang, C.; Armstrong, D. W. *Analyst (Cambridge, U. K.)* **2010**, *135*, 1076-1083.

(138) Sawada, M.; Tanaka, T.; Takai, Y.; Hanafusa, T.; Hirotsu, K.; Higuchi, T.; Kawamura, M.; Uchiyama, T. *Chem. Lett.* **1990**, 2011-14.

(139) Sawada, M.; Tanaka, T.; Takai, Y.; Hanafusa, T.; Taniguchi, T.; Kawamura, M.; Uchiyama, T. *Carbohydr. Res.* **1991**, *217*, 7-17.

(140) Wang, C.; Breitbach, Z. S.; Armstrong, D. W. *Sep. Sci. Technol.* **2010**, *45*, 447-452.

(141) Hyun, M. H. In Wiley-VCH Verlag GmbH & Co. KGaA: 2007; , pp 275-299.

(142) Hyun, M.,H; Jin, S. N.; Lee, W. *J. Chromatogr. A* **1998**, *822*, 155-161.

(143) Hyun, M. H.; Han, S. C.; Lipshutz, B. H.; Shin, Y.; Welch, C. J. *J. Chromatogr. , A* **2002**, *959*, 75-83.

(144) Kersten, B. S. *J. Liq. Chromatogr.* **1994**, *17*, 33-48.

(145) Immel, S.; Schmitt, G. E.; Lichtenthaler, F. W. *Carbohydr. Res.* **1998***, 313*, 91-105.

(146) Armstrong, D. W.; Ward, T. J.; Armstrong, R. D.; Beesley, T. E. *Science (Washington, D. C. , 1883-)* **1986***, 232*, 1132-5.

(147) Okamoto, Y.; Yashima, E. In American Chemical Society: 1996; , pp CELL-100.

(148) Yashima, E.; Fukaya, H.; Okamoto, Y. *J. Chromatogr. , A* **1994***, 677*, 11-19.

(149) Yashima, E.; Sahavattanapong, P.; Okamoto, Y. *Chirality* **1996***, 8*, 446-451.

(150) Zhang, T.; Nguyen, D.; Franco, P. *J. Chromatogr. , A* **2010***, 1217*, 1048-1055.

(151) Zhao, Y.; Pritts, W. A. *J. Chromatogr. , A* **2007***, 1156*, 228-235.

(152) Beesley, T. E.; Lee, J. *J. Liq. Chromatogr. Relat. Technol.* **2009***, 32*, 1733-1767.

(153) Han, X.; Huang, Q.; Ding, J.; Larock, R.; Armstrong, D. *Sep. Sci. Technol.* **2005***, 40*, 2745-2759.

(154) Zhang, D.; Li, F.; Hyun, M. H. *J. Liq. Chromatogr. Relat. Technol.* **2005***, 28*, 187-198.

(155) Pirkle, W. H.; Welch, C. J. *Tetrahedron: Asymmetry* **1994***, 5*, 777-80.

(156) Sun, P.; Perera, S.; MacDonnell, F. M.; Armstrong, D. W. *J. Liq. Chromatogr. Relat. Technol.* **2009***, 32*, 1979-2000.

(157) Armstrong, D. W.; DeMond, W.; Czech, B. P. *Anal. Chem.* **1985***, 57*, 481-4.

(158) Sun, P.; Wang, C.; Armstrong, D. W.; Peter, A.; Forro, E. *J. Liq. Chromatogr. Relat. Technol.* **2006***, 29*, 1847-1860.

(159) Nishi, H.; Kuwahara, Y. *J. Biochem. Biophys. Methods* **2001***, 48*, 89-102.

(160) Blaschke, G.; Kraft, H. P.; Marrkgraf, H. *Chem. ber.* **1980***, 113*, 2318-2322.

(161) Wan, H.; Blomberg, L. G. *J. Chromatogr. , A* **2000***, 875*, 43-88.

(162) Tong, M.; Payagala, T.; Perera, S.; MacDonnell, F. M.; Armstrong, D. W. *J. Chromatogr. , A* **2010***, 1217*, 1139-1148.

(163) Forte, B.; Malgesini, B.; Piutti, C.; Quartieri, F.; Scolaro, A.; Papeo, G. *Mar. Drugs* **2009***, 7*, 705-753.

(164) Stien, D.; Anderson, G. T.; Chase, C. E.; Koh, Y.; Weinreb, S. M. *J. Am. Chem. Soc.* **1999**, *121*, 9574-9579.

(165) Domostoj, M. M.; Irving, E.; Scheinmann, F.; Hale, K. J. *Org. Lett.* **2004**, *6*, 2615-2618.

(166) Du, H.; He, Y.; Rasapalli, S.; Lovely, C. J. *Synlett* **2006**, 965-992.

(167) Lovely, C. J.; Du, H.; He, Y.; Dias, H. V. R. *Org. Lett.* **2004**, *6*, 735-738.

(168) Sivappa, R.; Mukherjee, S.; Dias, H. V. R.; Lovely, C. J. *Org. Biomol. Chem.* **2009**, *7*, 3215-3218.

(169)Doundoulakis,T.Evaluation of an oxidative bd-ring formation en route to Palau'amine, and the synthesis of natural products functionalized with tethers suitable for marine coatings, University of Texas at Arlington, Arlington, 2012.

(170) Sivappa, R.; Hernandez, N. M.; He, Y.; Lovely, C. J. *Org. Lett.* **2007**, *9*, 3861-3864.

(171) He, Y.; Chen, Y.; Wu, H.; Lovely, C. J. *Org. Lett.* **2003**, *5*, 3623-3626.

(172) Breitbach, Z. S.; Feng, Q.; Koswatta, P. B.; Dodbiba, E.; Lovely, C. J.; Armstrong, D. W. *Supramol. Chem.* **2010**, *22*, 758-767.

(173) Advanced Separation Technologies Inc, USA, Ed.; In *Cyclobond* *TM* *Handbook. Bonded Cyclodextrin Phase for Liquid Chromatography.* Advanced Separation Technologies Inc: USA, 2005; , pp 66.

(174) Arthur, C. L.; Pawliszyn, J. *Anal. Chem.* **1990**, *62*, 2145-8.

(175) Pawliszyn, J. In *Solid phase microextraction theory and practice;* Pawliszyn, J., Ed.; Wiley: New Youk, NY. USA, 1997.

(176) Scheppers W S In *Solid phase microextractio. A practical guide;* Scheppers Wercinsky S, Ed.; CRC Press: Boca Raton, FL,USA, 1999.

(177) Hinshaw, J. V. *LC-GC Eur.* **2003**, *16*, 803.

(178) Majors, R. E. *LCGC North Am.* **2008**, *26*, 1074.

(179) Venkatachalam M In *Properties of commercial SPME coatings;* Pawliszyn, J., Ed.; Application of SPME. RSC Chromatography Monographs: 1999; pp 57-72.

(180) Anonymous In *SPME: Theory and optimization of conditions;* Supelco Bulletin 923, Ed.; Supelco: Bellefonte, PA,USA, 1998.

(181) Mullett V, M.; Pawliszyn, J. *J. Sep. Sci.* **2003***, 26*, 251-260.

(182) Earle, M. J.; Seddon, K. R. *Pure Appl. Chem.* **2000***, 72*, 1391-1398.

(183) Olivier-Bourbigou, H.; Magna, L. *J. Mol. Catal. A: Chem.* **2002***, 182-183*, 419-437.

(184) Carda-Broch, S.; Berthod, A.; Armstrong, D. W. *Anal. Bioanal. Chem.* **2003***, 375*, 191-199.

(185) Koel, M. In *Ionic liquids in synthesis;* Koel, M., Ed.; CRC: Boca Raton, FL,USA, 2009.

(186) Anderson, J. L.; Armstrong, D. W.; Wei, G. *Anal. Chem.* **2006***, 78*, 2893-2902.

(187) Berthod, A.; Ruiz-Angel, M. J.; Carda-Broch, S. *J. Chromatogr. , A* **2008***, 1184*, 6-18.

(188) Poole, C. F.; Kollie, T. O. *Anal. Chim. Acta* **1993***, 282*, 1-17.

(189) Anderson, J. L.; Armstrong, D. W. *Anal. Chem.* **2003***, 75*, 4851-4858.

(190) Anderson, J. L.; Armstrong, D. W. *Anal. Chem.* **2005***, 77*, 6453-6462.

(191) Vidal, J.; Psillakis, E.; Domini, C. E.; Grane, N.; Marken, F, Canals, A *Anal. Chim. Acta* **2007***, 584*, 188-195.

(192) Hsieh, Y.; Huang, P.; Sun, I.; Whang, T.; Hsu, C.; Huang, H.; Kuei, C. *Anal. Chim. Acta* **2006***, 557*, 321-328.

(193) He, Y.; Pohl, J.; Engel, R.; Rothman, L.; Thomas, M. *J. Chromatogr. , A* **2009***, 1216*, 4824-4830.

(194) Huang, K.; Han, X.; Zhang, X.; Armstrong, D. W. *Anal. Bioanal. Chem.* **2007***, 389*, 2265-2275.

(195) Wu, C.; Chen, C.; Huang, C.; Lee, M.; Huang, C. *Anal. Lett.* **2004***, 37*, 1373-1384.

(196) Anderson, J. L.; Ding, J.; Welton, T.; Armstrong, D. W. *J. Am. Chem. Soc.* **2002***, 124*, 14247-14254.

(197) Berthod, A.; Ruiz-Angel, M. J.; Huguet, S. *Anal. Chem.* **2005***, 77*, 4071-4080.

(198) Sprunger, L. M.; Gibbs, J.; Proctor, A.; Acree, W. E., Jr.; Abraham, M. H.; Meng, Y.; Yao, C.; Anderson, J. L. *Ind Eng Chem Res* **2009***, 48*, 4145-4154.

(199) Tanaka, K.; Waki, H.; Ido, Y.; Akita, S.; Yoshida, Y.; Yohida, T. *Rapid Commun. Mass Spectrom.* **1988***, 2*, 151-3.

(200) Carnevale, J.; Cole, E. R.; Nelson, D.; Shannon, J. S. *Biomed. Mass Spectrom.* **1978***, 5*, 641-6.

(201) Liu, L. K.; Busch, K. L.; Cooks, R. G. *Anal. Chem.* **1981***, 53*, 109-13.

(202) Zhang, Q.; Zou, H.; Guo, Z.; Zhang, Q.; Chen, X.; Ni, J. *Rapid Commun. Mass Spectrom.* **2001***, 15*, 217-223.

(203) Rainer, M.; Qureshi, M. N.; Bonn, G. K. *Anal. Bioanal. Chem.* **2011***, 400*, 2281-2288.

(204) Belardi, R. P.; Pawliszyn, J. B. *Water Pollut. Res. J. Can.* **1989***, 24*, 179-91.

(205) Zhang, Z.; Pawliszyn, J. *Anal. Chem.* **1993***, 65*, 1843-52.

(206) Wanigasekara, E.; Perera, S.; Crank, J. A.; Sidisky, L.; Shirey, R.; Berthod, A.; Armstrong, D. W. *Anal. Bioanal. Chem.* **2010***, 396*, 511-524.

(207) Carda-Broch, S.; Ruiz-Angel, M. J.; Armstrong, D. W.; Berthod, A. *Sep. Sci. Technol.* **2010***, 45*, 2322-2328.

(208) Iler, R. K. In *The chemistry of silica* John Wiley: New York, USA, 1979.

(209) Unger, K. K., Ed.; In *Porous silica;* Elsevier: Amsterdam, 1979; Vol. 16.

(210) Berthod, A. *J. Chromatogr.* **1991***, 549*, 1-28.

(211) Trojer, L.; Stecher, G.; Feuerstein, I.; Bonn, G. K. *Rapid Commun. Mass Spectrom.* **2005***, 19*, 3398-3404.

BIOGRAPHICAL INFORMATION

Sirantha Perera is an alumnus of Mahanama Collage-Colombo, Sri Lanka. He obtained his Bachelor of Science honors degree in Chemistry from the University of Peradeniya, Sri Lanka. After working as a teaching assistant in the Department of Chemistry at University of Peradeniya and University of Kelaniya, he joined the Textile Industry as an assistant compliance manager. In 2006, Sirantha came to the United States of America to pursue his Ph.D. in chemistry under the supervision of Dr. Daniel W. Armstrong. His research mainly focuses on chiral and achiral separations in HPLC and GC. He also has developed new chiral selectors for HPLC and new stationary phases for SPME for rapid detection of proteins. He obtained his Ph.D degree in Chemistry in November 2012.